3-1992

A Response Surface Methodology Study of Ferroelectric Memory Devices

Kevin C. Smith

A Response Surface Methodology Study of Ferroelectric Memory Devices

Thesis

Kevin C. Smith, Captain, USAF

AFIT/GST/ENS/92M-7

DEPARTMENT OF THE AIR FORCE
AIR UNIVERSITY
AIR FORCE INSTITUTE OF TECHNOLOGY

Wright-Patterson Air Force Base, Ohio

AFIT/GST/ENS/92M-7

A Response Surface Methodology Study of Ferroelectric Memory Devices

Thesis

Kevin C. Smith, Captain, USAF

AFIT/GST/ENS/92M-7

AFIT/GST/ENS/92M-7

A Response Surface Methodology Study of Ferroelectric Memory Devices

Thesis

Presented to the Faculty of the School of Engineering

of the Air Force Institute of Technology

Air University

In Partial Fulfillment of the

Requirements for the Degree of

Master of Science in Operations Research

Kevin C. Smith, Captain, USAF

March 1992

THESIS APPROVAL

STUDENT: Capt Kevin C. Smith CLASS: GST-92M

THESIS TITLE: A Response Surface Methodology Study of Ferroelectric Memory Devices

DEFENSE DATE: 4 March 1992

COMMITTEE:	NAME/DEPARTMENT	SIGNATURE
Advisor	Maj Paul F. Auclair	Paul F. Auclair
Co-Advisor	Capt Mark A. Mehalic	Mark A. Mehalic

Acknowledgements

I must thank numerous individuals for their support throughout the course of this thesis. My committee, Major Paul Auclair and Captain Mark Mehalic were an invaluable sounding board when I was first trying to formulate my thoughts on this entire project. They also kept me on the right track when I found myself distracted by interesting results which were not pertinent to the objectives of the thesis. Next, I would like to thank Captain Robert Pugh for his aid in the laboratory. This project would have been severely limited without his tutorials on the operation of the RT-66 and his insights regarding ferroelectric behavior. Finally, I would like to thank Victoria Fraider, my parents, and my sister for tolerating my behavior during the last six months.

Table of Contents

Abstract

This study examined fatigue in ferroelectric memory devices. The application of fatigue pulses to a ferroelectric sample was controlled by the RT-66 Ferroelectric Tester, a variation of the Sawyer-Tower circuit. The RT-66 also controlled data collection following the fatiguing process. Initial poling voltage, aging, cycling voltage, frequency, time, ferroelectric material, and electrode material were evaluated for their affect on fatigue. A sequence of fatigue tests, which varied the settings of these variables, was developed using Response Surface Methodology experimental designs. Least-squares regression models were developed once a particular set of experiments was completed. Analysis of these models provided the basis for new designs. First-order models failed to fit the data for any of the designs. The final model developed fit the observations well with two pure quadratic terms and three first-order terms. However, this design only involved one type of ferroelectric. Further testing is necessary before the findings of this study can be extended to modeling fatigue in other ferroelectric materials. Within the experimental operating region aging and initial poling voltage did not affect fatigue, and differences in ferroelectric materials and electrode materials were the most important factors in determining fatigue.

List of Figures

List of Tables

A Response Surface Methodology Study of Ferroelectric Memory Devices

I. Introduction

1 Background

Certain nonferrous materials display spontaneous polarization characteristics when an electric field is applied to the specimen, a phenomena analogous to ferromagnetism. The term ferroelectric (FE) was coined to describe nonferrous materials exhibiting this type of polarization (18:212).

> Spontaneous polarization means that electrical dipoles in the material align themselves along electrical field lines when an electric field is applied to a specimen and remain in the aligned position even if the field is subsequently removed (i.e., nonvolatile). Applying the opposite polarity causes the dipoles to switch and align in the opposite direction. Because ferroelectric materials exhibit at least two stable states that can be switched back and forth, it [is] feasible to build a ferroelectric device that can store information in digital form [i.e., memory]. (18:212)

What this really means is that a FE device can "store binary data in the state of the material itself" (40:1). The advantage of FE nonvolatility is that a system can suffer a power failure, but when power is restored the system starts at the same point as when power was interrupted (21:97).

There are a number of reasons designers have been interested in developing FE memories rather than relying on silicon-based

technology. A problem with silicon-based technology is that the designer must make tradeoffs between "features such as nonvolatility, low power, high speed, low cost per byte, and number of accesses. The designer must therefore build a hierarchy of memory types into a system" in order to satisfy all system requirements (30:29). FE devices may provide the opportunity to combine all the above features on a single chip (30:29).

FE materials may alleviate some of the fabrication difficulties of current high-density silicon devices. The FE layer stores "a much greater charge per unit area than can silicon" (59:36). Therefore it may be possible to construct tiny planar memory cells, thereby avoiding the need to perform exotic geometric design changes in device designs. For instance, 4 Megabyte Dynamic Random Access Memories (4MB DRAMs) (and other high-density memory devices) require trenching of the silicon material in order to fit the device on a chip (52:175). Trenching essentially creates a "well" in the silicon surface and increases fabrication difficulties in the manufacture of memory devices. FE device architectures appear to bypass this undesirable increase in the complexity of fabricating memory devices (52:175, 24:83, 16:1). Another useful byproduct of FE architectures is that FE read-only memory (ROM) devices do not require a high-intensity electric field (41:1661).

Inadequate technology prevented the use of ferroelectrics as computer memory devices until the 1970s. The predominant barrier

was that the materials used were "bulk" ferroelectrics. Their "switching thresholds of tens or hundreds of volts and switching speeds in the range of microseconds or milliseconds render[ed] the technology incompatible with integrated circuit technology" (18:212). In the 1970s, improved deposition techniques, the process by which a ferroelectric film is applied to a substrate, made ferroelectric memory devices feasible. Thin films could then be deposited on silicon wafers "without losing either the properties of the ferroelectric or the silicon wafers" (30:29). Because the film was thin, lower switching thresholds and higher switching speeds were achieved than in bulk FE materials. Research then concentrated on optimizing deposition techniques and choosing the best doping materials. Doping materials are trace elements added to a chemical mixture with the idea that the doping material will either enhance some desirable property or diminish some undesirable property. Basic research has continued, in parallel with improved manufacturing techniques, to determine the physical mechanisms that control the stability of the polarized state (44:325).

In the 1990s, the two key engineering questions which limit FE applications are the aging and fatigue characteristics of a given ferroelectric (31:217). Aging is the "loss of switchable polarization with time in a poled capacitor", while fatigue is the "loss of switchable polarization as a result of repeated polarization reversals, i.e., voltage cycling" (53:279). The emphasis of this study is an examination of fatigue in FE

devices. A poled FE capacitor is a FE which has been polarized in a certain direction. Frequent mention will also be made of a poling voltage, a voltage which orients the FE in a particular direction. This direction may be described as up or down, or it may be described as a "0" or "1" state.

When a ferroelectric memory device is sufficiently fatigued, it effectively fails because the polarization state can no longer be determined. Fatigue is important commercially because reliability rates must be established, and compared with existing memory devices, before a new type of memory is marketable. At least one device has already been reported to have a write cycle "10,000 times faster than the write cycle for standard EEPROMs" (erasable electronic programmable read only memories) and an endurance that is "more than one billion times greater than the one million write-cycle lifetime for the industry's best EEPROMs" (26:17). Unfortunately, this is only one case, and the question of what mechanisms drive fatigue rates remain unsolved.

FE research has been designated a high-leverage technology and is monitored by the Assistant Secretary of the Air Force for Acquisition (47:3). There is significant military interest in ferroelectrics because they are radiation-hard and nonvolatile. In fact, Radiation hardness is a significant issue in space technology, and ferroelectric devices are less responsive than silicon semiconductors to radiation encountered during space flights (28:189). FE capacitors are also "impervious to the total dose, transient, and single-event upset effects of

electromagnetic pulse" (19:33). Current nonvolatile, radiation-hard memories used by the military are primarily magnetic core and plated-wire technologies. The high cost and limited density of these mediums limit their military use in areas such as the Strategic Defense Initiative (SDI) (19:33, 43:1, 25:88).

In the 1970s non-volatile ferromagnetic bubble memories appeared to fill the military niche. Unfortunately bubble memories require special processing that is incompatible with standard semiconductor processes. "They are also more expensive and have not kept up with standard processes in either speed or density" (25:89).

2 Problem Statement

The mechanisms that determine the fatigue characteristics of ferroelectrics are not well defined. In fact, there is no theoretical model which predicts the effects of the fatiguing of FE materials as a function of a number of explanatory variables.

3 Objective

This study has two objectives. The first objective is to develop an empirical model, using Response Surface Methodology, that provides estimates of parameters for predicting fatigue in a FE sample. The second objective is to demonstrate the validity of using RSM tools in conducting ferroelectrics research.

4 Methodology

The methodology describes the steps that will be taken to achieve the objectives.

1. Select a set of parameters for investigation, and construct a design based upon these parameters. The parameter settings selected will simulate possible FE memory device operating environments.

2. Perform appropriate transformations of the parameters to simplify the design.

3. Perform the experiments and collect the data, using the RT-66 Ferroelectric Tester.

4. Use least-squares regression techniques to estimate the coefficients of the model parameters.

a) Screen out parameters which are not statistically or empirically significant.

b) Evaluate the models for explanatory power, parsimony, and predictive power.

c) Iteratively repeat steps one through four as required.

5. Record temperature and humidity data in the laboratory during experimentation because these two factors affect FE devices. This data will allow experimenters in other locations to include temperature and humidity as parameters in designs which seek to replicate the results of this work.

6. Some initial data gathered will not be used in the model fitting phase. Instead, predicted results for each fitted model will be generated using the input parameters of the withheld tests. The model results will be compared with the actual system response as a check of the predictive power of the model. This

step verifies that the RSM designs generated reproducible predictions.

7. To validate the usefulness of RSM, experimental findings will be compared with the results of other researchers.

5 Limitations of the Study

Four wafer sections, each containing several thousand ferroelectric memory devices, were provided by Radiant Technology, 1009 Bradbury Drive SE, Albuquerque, NM, 87106. The specific point of contact was Mr. Joe Evans, whose telephone number is (505) 842-8007. The depth and cross-sectional area of the ferroelectric devices were assumed constant for all practical purposes; that is, the manufacturing technique was assumed to exhibit negligible variance. No testing was performed to verify the validity of this assumption. Since complete wafers were not provided, it is possible that the sections received were not representative of a cross-section of devices normally produced on a complete wafer.

Only seven variables will be considered in this thesis. A variety of other variables bear examination as contributors to fatigue rates, but including more variables would have extended this work beyond the time limits available. In addition, tests on certain parameters require laboratory facilities beyond the capabilities of the equipment available during the course of this study. For instance, a temperature and humidity controlled environment would allow two important parameters to be modeled rather than simply recorded.

6 Summary

Using RSM designs, this study will develop empirical models which attempt to predict the fatigue rate of FE memory devices. Controlling the fatigue rate of FE devices is important as a reliability issue. Until fatigue rates and the effects of aging can be controlled, existing technologies with higher reliability rates will continue to be preferred to ferroelectrics. If fatigue and aging can be controlled, then the other advantages of ferroelectrics may, for instance, lead to the replacement of technologies currently used to construct memory devices such as disc drives.

The empirical models of fatigue rate developed will be compared with the efforts of other researchers. If RSM can generate similar findings with fewer experiments, in less time, or at a lower cost, then the utility of RSM will have been demonstrated.

II. Ferroelectrics Background

1 Introduction

As stated in the introduction, the primary impediments to the expanded use of ferroelectric memory devices are limitations due to the effects of fatigue and aging on data retention. Controlling fatigue and aging is the primary focus of study among those currently trying to market ferroelectric (FE) devices. This chapter will provide a framework within which FE research can be explained. In doing so, it will review some of the parameters that researchers have studied in attempting to explain fatigue or aging in ferroelectrics.

The discussion begins by examining the molecular structure of ferroelectrics and some of the physical mechanisms that control their behavior. Within this section, the concept of a hysteresis curve will be presented. A hysteresis curve is a loop which can be used to describe the behavior of a FE as it moves between its two binary states. The movement along the hysteresis curve is measured in terms of changes in polarization. The most commonly measured polarized states will also be defined. Polarization can be studied in terms of the switching of molecule domains parallel to the direction of polarization. This domain effect can be viewed as placing a master switch in a particular direction, and all the slaved switches within its domain move in

the same direction as the master switch. The properties of domain structure will be briefly examined, but this topic is not directly pertinent to the study objectives. The section concludes with a brief discussion of how to electrically determine the state of a FE device. Throughout this section explanations of how a FE memory device works will be provided.

The next major section of this chapter discusses the manufacturing variables that affect the fabrication of a particular FE device. The fatigue characteristics of a FE material are affected by the manufacturing process, the types of material used in a particular device's manufacture, and the interactions between the materials in a particular device. Several measures used to evaluate different FE manufacturing devices will be introduced. The specific measures do not apply directly to the study objectives, but the results provide a means of validating this study's findings.

The next section contains expanded definitions of fatigue and aging, along with some criteria for evaluating FE devices. Although a study of aging is not one of the objectives of this study, the effect of aging upon fatigue is one of the parameters which will be examined. Fatigue in FE materials has not been the focus of extensive research, but a few attempts have been made to control fatigue, and a few research efforts have attempted to model fatigue. These research efforts will be discussed, and the criteria for measuring fatigue in this study will be introduced. At that point the objectives of this chapter will have been met,

and a brief summary will close out the background material on ferroelectrics.

2 Ferroelectric Physical Mechanisms

Although the physical mechanisms which control fatigue rates of FE devices are not understood, the mechanisms which allow a FE thin film to be used as a binary memory element have been studied quite extensively. This section examines the molecular characteristics which make ferroelectrics suitable as memory devices, and provides means for characterizing the difference between binary states.

2.1 Molecular Structure. The phrase regular perovskite crystal is frequently used to describe the structure of ferroelectric thin films. Figure 1 is an example of the molecular structure of a FE.

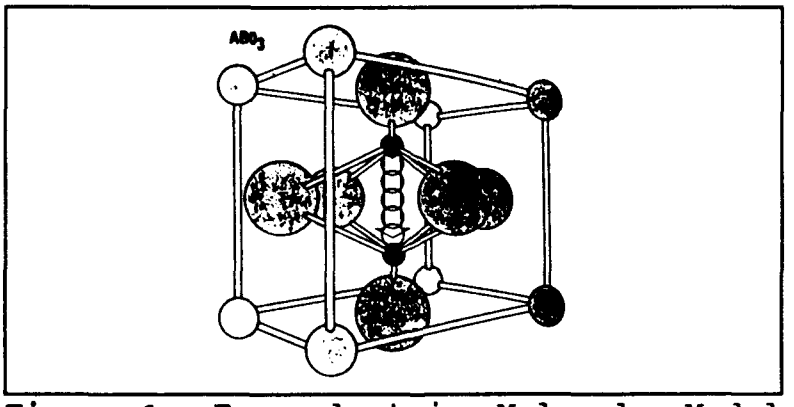

Figure 1. Ferroelectric Molecule Model (17:42)

A regular perovskite crystal "is a crystal that allows a central metallic ion to be displaced into one of two positions along the axis of the applied electric field to create an electric dipole" (19:30). This electric dipole is a measurable

state difference, and since there are only two states, a binary relationship can be formed. This binary relationship is the basis for a two-state memory device.

2.2 Curie Temperature. Thin-film FE devices are created by applying a FE film atop a substrate. Curie Temperature, T_c, is analogous to the Curie Point in ferromagnetic materials (58:F-74). T_c is the transition temperature at which the FE phenomena of polarization disappears. Since polarization is the FE property which allows them to be used as binary memory elements, a ferroelectric device must have a T_c that is higher than the device operating temperature or the memory characteristics (polarizability) will be destroyed.

2.3 Dielectrics, and Capacitance. The term dielectric (or nonconductor) refers to "a class of bodies supporting an electric strain. A charge on one part of a nonconductor is not communicated to any other part" (58:F-75). A dielectrics key characteristic is the ability to store electric energy (35:145). Placing a dielectric between two conductors increases capacitance, which is the ability to store charge. "It is found experimentally that if the dielectric fills the space between the two conductors, it increases the capacitance by a factor K which is called the dielectric constant" (34:573, 43:7). K is defined:

$$K = 1 + P/\epsilon_o E$$

where,

K: dielectric constant
P: polarization ($\mu C/cm^2$)
ϵ_o: *permittivity of free space*
E: field that produces polarization (*mV/cm*)

FE devices operate in a manner analogous to capacitors. Capacitance can be viewed as stored charge. If a capacitor had only two states, charged or not charged, it would emulate a basic binary memory element. Similarly, polarizing a ferroelectric memory device to one of two states effectively creates a binary memory element. Continuing the analogy with capacitance, polarization can be viewed as stored memory.

2.4 Hysteresis Loop. In iron (Fe) samples, hysteresis is a process in which "the magnetization of a sample of iron or steel, due to a magnetic field which is made to vary through a cycle of values, lags behind the field" (58:F-83). The following discussion by Giancoli, with reference to Figure 2, should clarify the definition of hysteresis. Though the discussion is based on ferromagnetic materials (i.e., the material includes Fe), the analogy to ferroelectrics is good in terms of what the hysteresis loop looks like, even if the physics are not necessarily the same.

> Suppose the iron core is initially unmagnetized and there is no current in the windings of the torus. Then the current I is slowly increased, and B_0 [field due to the current in the wire] increases linearly with I. The total field B [sum of the field due to the current and due to the magnetism, B_M] also increases, but follows the curved line shown in the graph of [Figure 2]. (Note the different scales: $B >> B_0$.) Initially (point a), no domains are aligned. As B_0 increases, the domains become more and more aligned until at point b, nearly all are aligned. The iron is said to be approaching saturation. (Point b typically is 70 percent of full saturation; the curve continues to rise very slowly, and reaches 98 percent saturation only when B_0 is increased by about a thousandfold above that at point b; the last few domains are very difficult to align.) Now suppose the external field B_0 is reduced by decreasing the current in the torus. As the current

is reduced to zero, point c in [Figure 2], the domains do not become completely unaligned. If the current is then reversed in direction, enough domains can be turned around so B = 0 (point d). As the reverse current is increased further, the iron approaches saturation in the opposite direction (point e). Finally, if the current is again reduced to zero and then increased in the original direction, the total field follows the path efgb, again approaching saturation at point b. (34:663)

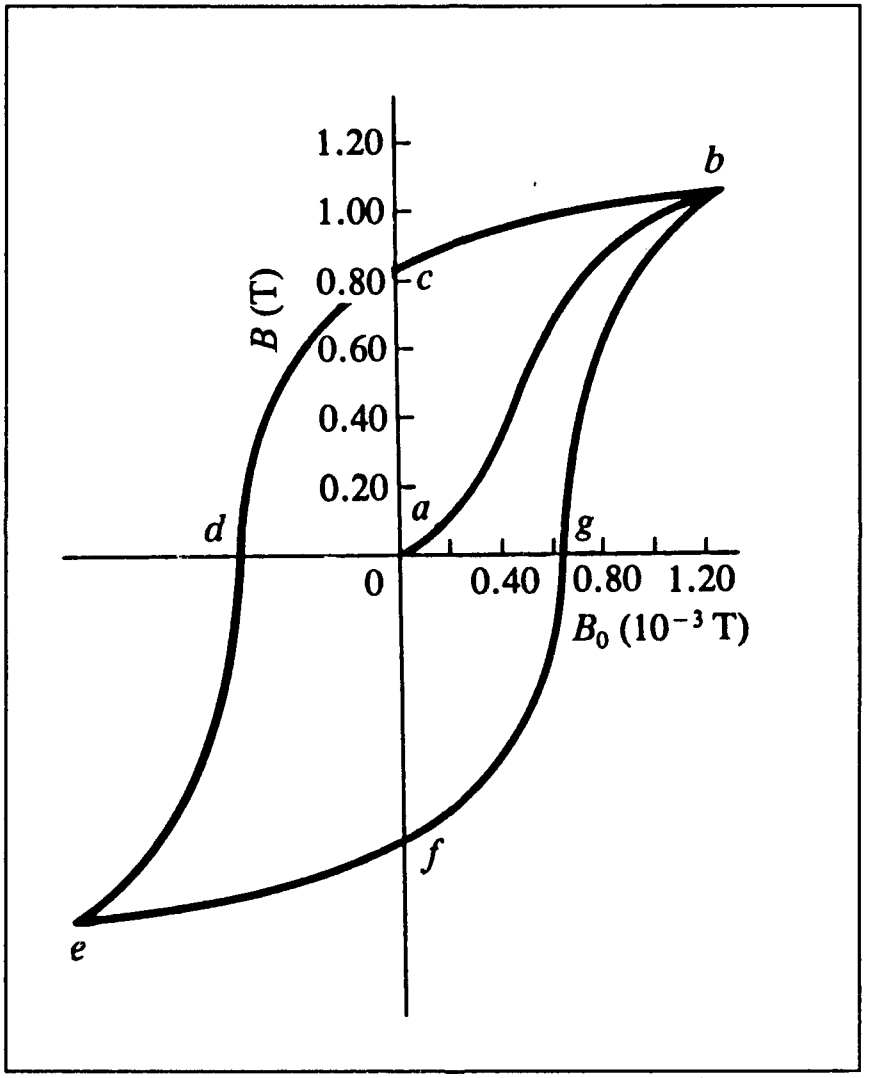

Figure 2. Ferromagnetic Hysteresis Loop (33:663)

FE hysteresis loops differ from ferromagnetic loops in several key ways. First, the tops and bottoms of the FE loop are

not as horizontal as in the ferromagnetic case. Second, the ferromagnetic material retraces the same loop, while FE loops change with every cycle. That is, the present FE loop is biased by its previous states. Finally, a FE loop is not symmetric about the x and y axes (22:185).

2.5 Polarization. Based on the discussion of hysteresis loops, several analogous ferroelectric terms can be defined. From a system standpoint, the hysteresis curve "describes the amount of charge the device stores as a function of the applied voltage" (19:30). Polarization is technically the "dipole moment per unit volume", where a ferroelectric dipole is the molecular arrangement that aligns itself with an applied electric field (35:145). In other words, the ferroelectric material is polarized.

FE thin films not only align themselves with an applied field, part of this alignment is maintained after the field is removed. The property of assuming and maintaining a polarized state makes ferroelectrics desirable as nonvolatile memory devices. The problem with FE devices is that the difference between polarized states diminishes to indistinguishable with aging or cycling of the FE device. Eventually, the application of a coercive field has no measurable effect on the polarization state of a given FE device. The relationship between polarization and the coercive field "is not only nonlinear, but also shows hysteresis effects; that is, the polarization produced

by a given electric field intensity depends on the past history of the sample" (35:149).

Saturation polarization, P_s, is equivalent to point b on Figure 2 (43:5). Polarization is typically measured along the vertical axis and the coercive electric field applied, E_c, is measured along the horizontal axis. After initially driving the ferroelectric thin film to P_s, and then removing E_c, the polarization of the film moves to point c. This is the remanent polarization P_r (31:223, 19:33). Points e and f are $-P_s$ and $-P_r$ respectively. Figure 3 is a FE hysteresis loop which depicts the various polarization values discussed. "Polarization is measured in units of charge/cm^2 and the field across the capacitor [ferroelectric memory device] is measured in volts/cm" (42:243).

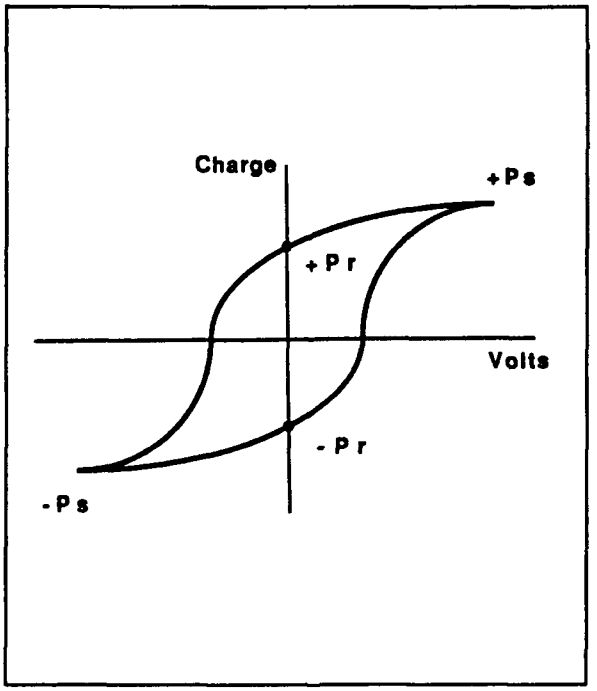

Figure 3. Hysteresis Loop (31:223)

2.6 Domains. A domain structure is an area of a material that displays a common characteristic. Any given material may exhibit several domains of different characteristics. Similarly, a single dominant characteristic may define domains in noncontiguous portions of a material, as seen in Figure 4.

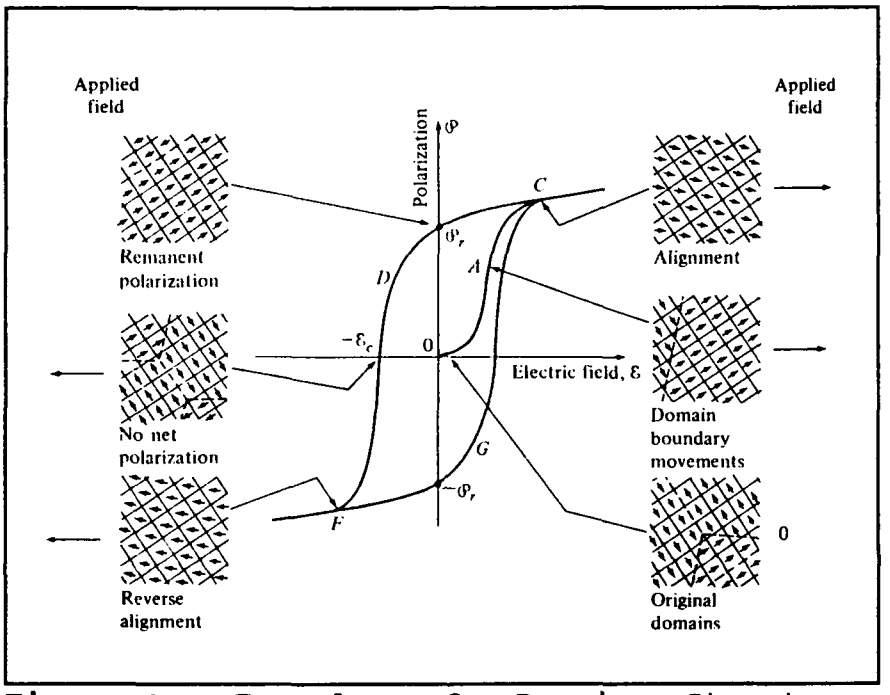

Figure 4. Example of Domain Structures (32:476)

Domain structure is important because it

> gives rise to a complex nonlinear state which is very sensitive to the quality of the sample and its crystal defects, as well as to external boundary conditions and other influences. The properties of multidomain crystals - and more especially polycrystalline materials like ceramics and composites - are usually poorly defined; thus they often change with time, making it difficult to obtain reproducible effects. . . It [domain structure] causes degradation and aging effects in ceramic capacitors and transducers, and has frustrated the development of ferroelectric memory devices. (54:xi)

2.7 Determining FE state (0/1).

> The capacitor's state cannot be determined without applying a voltage to drive the capacitor to a known condition, and then verifying if it switches state. If little charge comes out, the capacitor was already in that state. If more charge comes out, then the capacitor switched and must have been in the other state. After the "read", which is destructive, the capacitor must be returned to its original state. (30:29)

3 Manufacture of Ferroelectric Memory Devices

The manufacture of FE memory devices involves three basic components. The three components are the substrate, the FE capacitor, and the electrodes. Each of these components consists of essentially different materials. For instance, the substrate might be silicon, the FE might be lead titanate ($PbTiO_3$), and the electrode might be gold. Intercomponent adhesion, electronic compatibility, and ease of manufacture are just some of the variables to consider in determining the manufacturing viability of a given FE device.

The following sections will discuss the manufacture of FE memory devices and the effects of manufacturing processes. The choice of FE material, deposition techniques, and substrate materials affect the characteristics of manufactured FE thin film devices. The topic of electrode materials will receive minimal attention since minimal references were found in the literature. An exception was a model for fatigue and aging that considered "the influence of electrical-contact materials" (20:201). This model found that the interaction between the electrode and material near the electrode surfaces had a significant effect on

the fatigue rate by causing losses in the electronic signals applied to the ferroelectric (20:203).

3.1 Manufacturing Processes. Techniques devised and refined in the development of silicon semiconductor technology are used to process FE devices. Essentially the FE material is "sandwiched between two metal electrodes" as in Figure 5 (19:30).

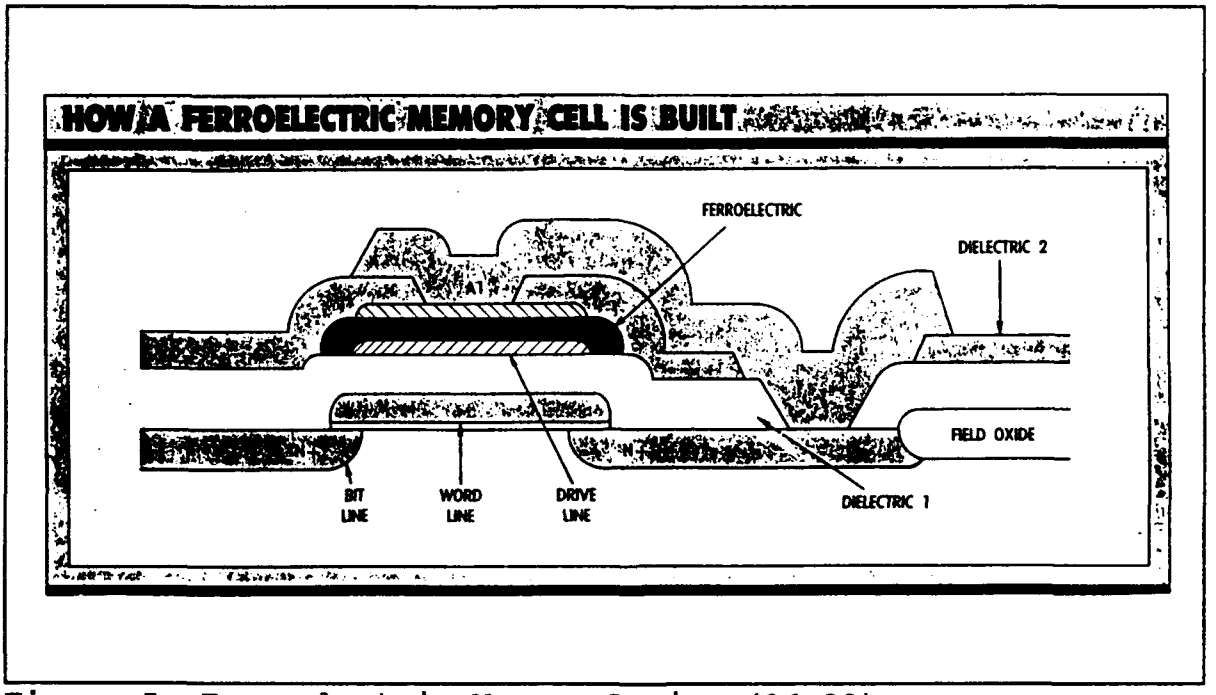

Figure 5. Ferroelectric Memory Device (26:88)

The first step in constructing a FE memory device is depositing the FE thin film. Different deposition methods will be discussed in a following section. The thickness of the FE material deposited may be a factor in determining the ferroelectric properties of a given material. A minimum thickness of 0.308μm has been established as the lower limit for a FE to retain a poled state (20:204).

Interestingly, there is disagreement on what constitutes a thin film versus a bulk material. The question is important since there is disagreement in the ferroelectric community as to whether thin films display significantly different characteristics from bulk films. However, it is acknowledged that the development of techniques for applying thin films has spurred advances in FE semiconductor technology which were infeasible with bulk ferroelectrics. In bulk materials, the

> operating voltages of 10-100 volts were high, control of the switching threshold of the thick-film capacitors was poor, and there were no active devices at the crosspoints to isolate the capacitors from voltage disturbances. (19:30)

Once the FE thin film is deposited on a substrate, other processes can affect the characteristics of a FE device. For instance, after the FE is deposited, the film must be annealed. The annealing consists of a heat treatment to achieve a crystalline structure. By changing the annealing temperature or the length of time a film is annealed, the characteristics of the device are changed in unpredictable ways. In fact, applying different annealing processes to two identical materials may result in ferroelectrics that have such completely different characteristics that they constitute essentially different materials. It is possible that the change in properties is due to a change in the defect density of the film brought about by different annealing procedures.

After annealing, the material must be etched. Essentially, this is a procedure for removing portions of the FE film to allow

connections to be made to the substrate. The etching process will not be discussed in detail since it is not pertinent to this study. In the process of etching the film, it is possible that ionic contaminates or electro-chemical reactions may degrade the ferroelectric device (20:204).

During the etching process, the FE material which remains has a manufacturer-specified area (within some tolerance). The area helps determine the charge capacity of a given FE device. This relationship is given by (35:160)

$$q = CV$$

$$C = \epsilon A/d$$

$$q = V\epsilon A/d$$

where,

q: *charge on the capacitor* (μC)

C: *capacitance of the capacitor* ($\mu farads$)

V: *voltage applied* (*volts*)

ϵ: *permittivity* ($\mu farads/cm$)

d: *capacitor plate separation* (cm)

A: *area of capacitor plates* (cm^2)

Unlike thickness, there appears to have been no research to determine if there is a critical value for capacitor area below which ferroelectric properties degrade significantly or disappear completely.

3.2 Material Composition of Thin Films. The primary elements and doping elements in a ferroelectric sample determine the material composition. Investigations have centered on

several combinations of primary elements as the basis for ferroelectric memory devices, with various dopants added. Doping elements are essentially contaminants added to change the ferroelectric characteristics of a given film (60:5). Doping elements constitute a small percentage of the ferroelectric material.

Numerous combinations of elements have been used as the primary elements in ferroelectric thin films. Examples are $PbTiO_3$ and PbZrTi. The former is known as lead titanate, while the latter, lead zirconate titanate, usually goes under the acronym of PZT (60:5, 62:91). Experimentation has also been performed on materials such as lithium niobate ($LiNbO_3$), barium titanate ($BaTiO_3$), strontium titanate ($SrTiO_3$), and PbLiZrTi, also written as PLZT (36:13, 37:57, 42:243, 20:202). Clark and Scott did some work with potassium nitrate, KNO_3, because manufacturing high quality films of KNO_3 was simple. They found switching times on the order of 10ns or less at voltages of about five volts. Unfortunately, KNO_3 is presently an unacceptable material because it is extremely sensitive to water "at every step of fabrication" (23:4).

For the purposes of memory devices, most manufacturers have concentrated on PZT and PLZT (49:293). The advantages of PZT include "a wide temperature range (+350°C Curie Temperature), low coercive voltage, high specific polarization charge (10-20$\mu C/cm^2$), good retention, and good endurance" (18:212).

3.3 Doping. Doping is one way to change the characteristics of a ferroelectric. For instance, Wojcik examined how Lanthanum (La) doping of $PbTiO_3$ decreased the Curie Temperature, decreased the maximum permittivity (ϵ_{max}), and increased ϵ_{max} (60:5). The effect of a change in T_C and ϵ_{max} is to alter the hysteresis loop of a given FE. The hysteresis loop is examined when trying to ascertain the polarizability of a given ferroelectric material. Wojcik found that relatively small amounts of doping had marked effects on T_C and ϵ_{max}, but the changes in P_S and E_C were insignificant (60:12). In other words, the polarizability was not markedly enhanced. Similar experimental doping of PZT with Niobium (Nb) gave only a slight increase in the ferroelectric properties, but an addition of excess PbO generated superior ferroelectric properties (57:1458). This study will use undoped PZT as the basis for all experiments.

3.4 Thin Film Deposition Techniques. Several deposition methods of PZT thin films have been

> reported, including rf-magnetron sputtering, sol-gel processing, electron-beam evaporation, rf-diode sputtering, and ion-beam deposition. However, there were some deficiencies in these fabrication techniques, such as high substrate temperature above 500° C (or past thermal annealing temperature), or low deposition rate, which precludes applications to possible devices and processes. (38:560)

Other techniques for applying films to a substrate include chemical vapor deposition of $PbTiO_3$ and pulsed laser ablation of $Pb(Zr,Ti)O_3$ (38:560, 63:336). Deposition methods impact several important characteristics examined in ferroelectric thin films. Some factors that impact film characteristics are substrate

temperature, nucleation rate, deposition time, Pb content deposited, O_2 partial pressure during application of the film, and type of electrodes (e.g., aluminum, silver, or gold). One experiment found "deposition efficiency is a decreasing function of the substrate temperature" when using the spray method for applying a thin film (15:145). The effects of these factors can be measured in the films homogeneity, crystalline quality, adherence to the substrate, and grain size (38:560). The composition and electrical properties of the films are also indicators of the efficiency of the application process. Usually the electrical properties are evaluated in terms of the dielectric constant, dc conductivity, P_r, and the hysteresis loop (63:336).

3.5 Substrate Materials. The ferroelectric film is applied to a substrate, a material that acts as a foundation. Although primarily a foundation, the characteristics of the substrate may alter the FE device characteristics, such as its polarizability (50:1636). "The substrate for a particular film is usually chosen because of specific properties (e.g. it may have a coefficient of thermal expansion similar to that of the thin film)" (50:1635).

Tests have been performed with substrates such as sapphire, magnesium oxide, and aluminum nitride, but most of the interest has centered on less exotic materials such as doped silicon and gallium arsenide (GaAs) (22:185, 50:1635, 61:13). The reasoning behind the emphasis on less exotic materials is that they are

semiconductors that are well understood in the engineering community. Investigations of more exotic materials, such as sapphire, generally focus on the electro-optic qualities of ferroelectrics.

4 Aging and Fatigue Characteristics

4.1 Aging. For the purposes of this paper, aging is defined as the loss in polarizability of a capacitor since it was initially poled (31:218). The effect of aging is to translate the hysteresis loop along the x-axis, accentuating any asymmetries which existed prior to aging (20:202). The direction of movement along the x-axis is "in the direction opposite to the direction of the field used to pole the material" (46:2). That is, if the device is poled in the negative direction ($-V_s$) then the direction of movement will be in the positive x direction, as shown in Figure 6.

"The most significant consequence of aging in memory devices is the reported reduction in the difference between two remanent polarization values" (46:3). Figure 6 provides visual indicators that if aging is accepted as movement along the x-axis, then the differences in $\pm P_r$ will eventually be undetectable. At that time, the prior state of a memory device can no longer be determined. It is possible, however, to de-age a material and then use the material again. "De-aging, or relaxation of the domain stabilization, can be accomplished by either repeatedly cycling the polarization or by heating the material above its Curie temperature" (46:2). Note that de-aging is itself

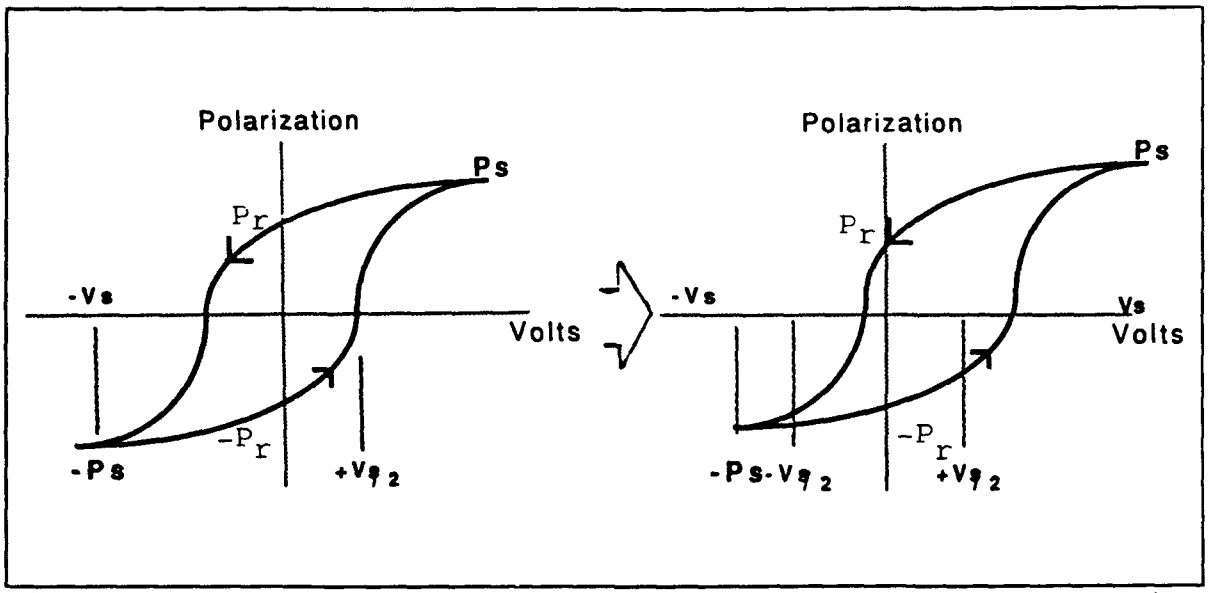

Figure 6. Ideal Hysteresis Loop and Loop Shifted Right by Aging (20:206)

destructive of the state of the material which existed before de-aging began.

4.2 Fatigue. Fatigue is the result of cycling a FE material. "Since memory operation involves a reversal every time a "1" is read, fatigue is a fundamental issue" (53:279). Fatigue causes the hysteresis loop to shrink, reducing the difference between the remnant polarization states as seen in Figure 7 (20:202).

For this study DP, the difference between remnant polarization states, will be used to investigate the fatigue rate of FE samples. DP is measured in units of $\mu C/cm^2$, and when DP decreases below 1 $\mu C/cm^2$ the device is considered to have failed, according to Radiant Technology (32). It is critical to note that DP is not referring to a derivative. The correct viewpoint is to picture DP as the change in polarization when transitioning

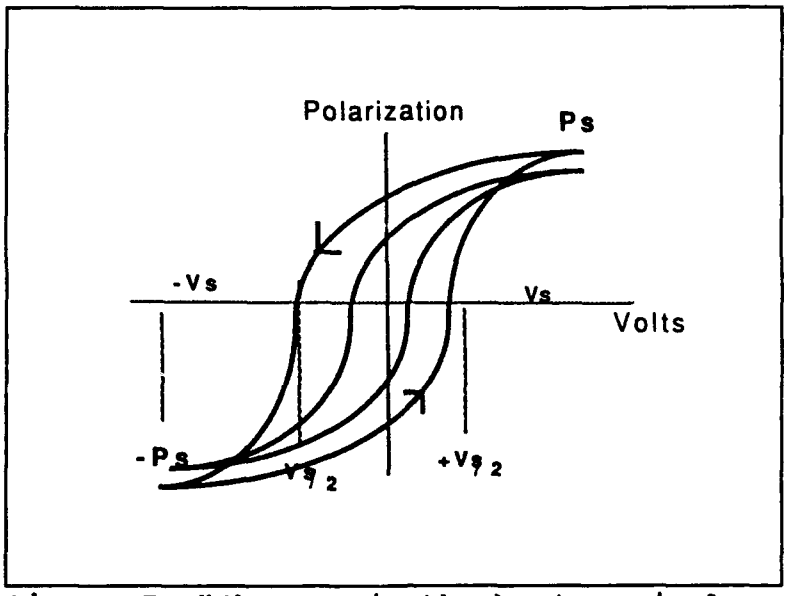

Figure 7. "Changes in the hysteresis loop shape resulting from fatigue" (20:206)

from the "0" state to the "1" state at a particular moment in time, using a specific voltage. The equation for calculating DP will be deferred to the chapter on equipment used in this study.

Despite the fact that fatigue has been described as a fundamental issue, little research has been done on the topic of fatigue in thin-film FE materials (53:285). The key concerns with fatigue are how increased cycling causes the hysteresis loop parameters, P_r and E_c, to vary (39:289). A study by Shepherd describes the fatigue process in FE thin films. Shepherd begins by defining the value ΔPr as the variation of switched remanent polarization and then describes the fatigue process in two phases.

> There is an initial induction period during which ΔPr remains constant (lower [applied] voltages) or rises (higher [applied] voltages) which is then followed by a final decay period. The decay, when it is clearly defined, seems to proceed linearly with the logarithm of cycles. Increasing the cycling voltage hastens the

onset of the decay and this is the reason for the reduced endurance at higher voltages. (53:281)

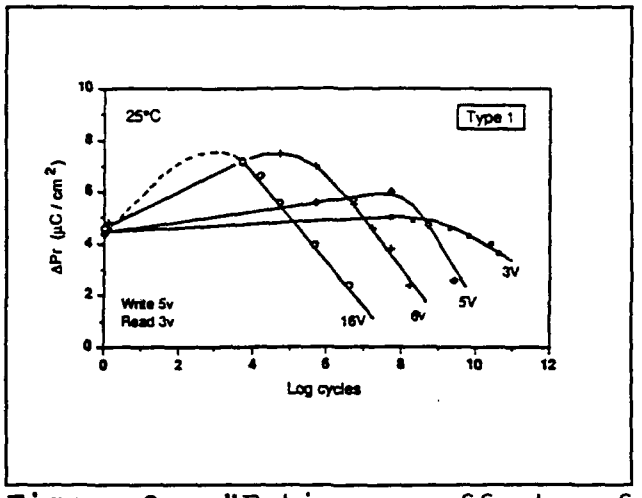

Figure 8. "Fatigue: effect of cycling voltage" (52:281)

The fatigue process described is seen in Figure 8. Shepherd also examined

- normalized ΔPr as a function of operating temperature
- ΔPr as a function of film thickness
- ΔPr as a function of applied switching field
- ΔPr as a function of temperature during cycling
- ΔPr as a function of the area of the capacitor (53:280).

Fatigue differs in the opposite polarized states. Suppose the capacitor is poled negatively to set a "1" state. A read, which consists of a positive pulse, will then take the capacitor through a hysteresis loop because the read destroys the data and a write must follow any read. Reading a "0" simply goes back and forth along the top of the loop (14:306). Figure 9 is a typical FE memory circuit element.

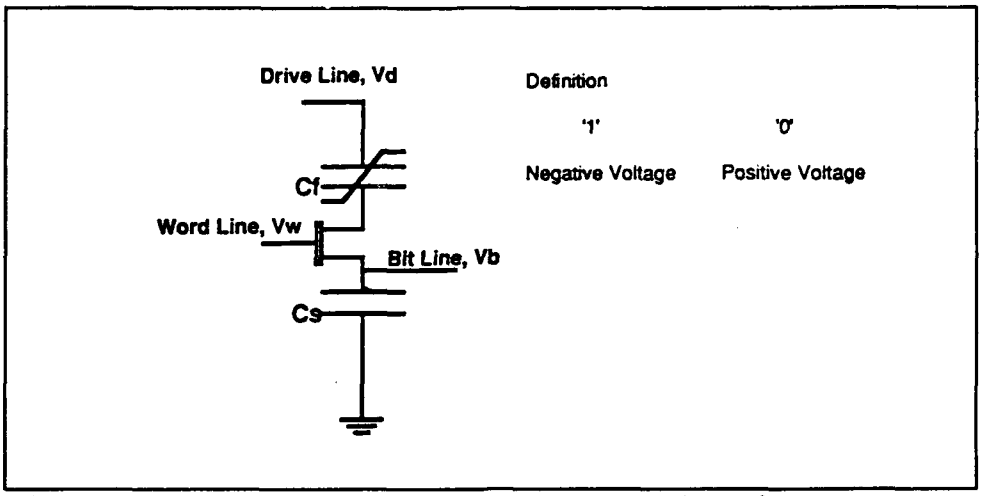

Figure 9. "Ferroelectric memory circuit element" (14:305)

4.3 Coercive Field (E_c) and Fatigue. The Ramtron Corporation attempted to solve the issue of FE fatigue in 1989. They first defined the critical variables as E_c and fatigue. Of these two they felt the major problem was the

> lack of a well-defined and stable coercive field, which resulted in the eventual loss of data due to half-select pulses applied to unselected cells in the crosspoint array structure. Fatigue or wear out was also a problem in that the amount of available signal depended upon the number of polarization reversals ... The lack of a well-defined coercive field was overcome with a DRAM like circuit architecture [Figure 10], which provides for transistor switches in series with each ferroelectric element preventing disturb pulses from affecting the unselected cells. (18:212)

The problem with such half-pulses is that they fatigue unselected cells, so by defining E_c the fatigue problem was also partially remedied. While this technique may allow Ramtron to develop FE RAM technologies it does not fully address the issue of determining what parameters control the optimum FE characteristics. For instance, "E_c is thickness and possibly

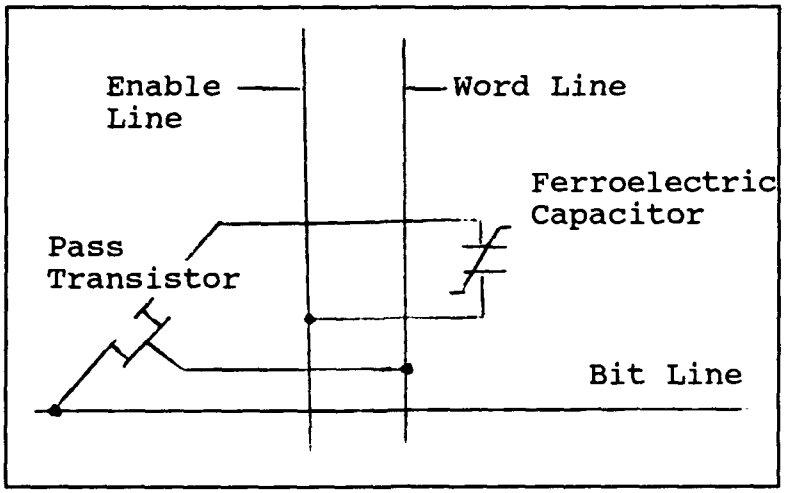

Figure 10. DRAM-like circuit architecture (19:33)

grain-size dependent" (28:191). In particular "the E_c was significantly enhanced in the finer-grained ceramics" (28:191).

4.4 Commercial Operational Parameters Ramtron does, however, establish some desirable, commercially viable, properties that a FE memory device should exhibit. The material should have

> good retention and endurance, adequate dielectric breakdown for submicron layers, a coercive field compatible with five volt operation and a signal charge of at least $5\mu c/cm^2$ [recent developments have lowered this figure to $1\mu C/cm^2$]. The Curie temperature should be sufficiently above the highest storage temperature and inherent switching speeds in the nanosecond range. (18:213)

Other important properties that have been mentioned are the "tradeoffs among product life, noise immunity, [and] circuit speed" (14:310). The pulse shape and pulse durations are important considerations in assessing these tradeoffs (14:307). Ramtron has developed specific minimum criteria that any FE device must meet before being commercially viable. While not the

final word on what constitutes acceptable performance criteria for FE devices, at least a standard is created. The Ramtron criteria are:

- Polarization retention > 10 years
- Endurance > 10^{15} read/write cycles
- Breakdown > 7V
- Coercive voltage ≈2.5 V and stable
- Polarization charge from 1-20 $\mu C\ cm^{-2}$
- Switched charge of $0.1\mu C\ cm^{-2}$ per 10 ns
- Full polarization switched in < 100ns
- Transition temperature > 200° C
- No significant waiting time effects
- Compatible with existing semiconductor processing
- Radiation hard to strategic levels (49:293)

Work in the FE device community has also looked at the "charge storage density (Q_c'), leakage current density (J_L), unipolar switching time to 10% decay (t_s), time dependent dielectric breakdown (TDDB), and electrical fatigue" (55:331). It was found that Q_c' was constant at a given electrical field, but J_L and TDDB degrade with decreasing film thickness. An equation which approximates t_s has been suggested by Dey (28:191):

$$t_s \sim P_s A/I$$

The experiments regarding Q_c', etc., used films of 200 nm, 400 nm, and 600 nm. It should be noted that thin films are generally considered to be from 30 to 300 nm thick, although some

$$I = V/R_L$$

where,

t_s: *switching time*

P_s: *saturation polarization*

A: area of electrodes

I: current through load resistor (amps)

V: voltage

R_L: *load resistor (ohms)*

researchers have defined a thin film as 0.1-20 μm thick (27:319, 52:175). These disparities in terminology contribute to the problem of determining optimal FE parameters because the basic working assumptions researchers use are different. Films thicker than 600nm thick are described as bulk materials for this thesis.

The question of TDDB degradation with increasing film thickness merits further research. A paper, submitted at the same time as Sudhama's research cited above, stated that TDDB was not a problem in FE devices. The contention was that "when the capacitor is not being written or read there is no voltage across the ferroelectric capacitor", therefore TDDB cannot occur (14:306). TDDB issues matter because it is a problem in present DRAM technologies. If ferroelectrics do not suffer from TDDB, it is another reason to pursue the use of ferroelectrics in memory architectures as a replacement for existing DRAM technology.

5 Summary

The primary concerns about ferroelectrics center on the problems of fatigue and aging. The FE response was then

explained in terms of the variable which was allowed to vary. For the purpose of evaluating the fatigue rate of FE samples the value DP will be used in this study.

III. Equipment

1 Introduction to the RT-66 Ferroelectric Tester

Numerous instruments have been used to investigate the properties of thin-film ferroelectrics (FE). Optical measurements using laser Raman spectroscopy were used in an attempt to understand the kinetics of FE materials as fast switching devices, and scanning electron micrographs have been used to investigate the quality of the manufacture of FE devices (23:4, 43:12). Because FE devices are pyroelectric, experiments have been conducted to determine device response to illumination at various wavelengths. For instance, a UV-light source was used to generate a space-charge effect. The sample was then optically probed and data was acquired on the ceramic polarization as a function of varying voltage (20:202). Perhaps the most frequently used devices in FE research are derivations of the Sawyer-Tower (S-T) circuit seen in Figure 11. The hysteresis generated by the S-T circuit is usually sampled using an oscilloscope while the spontaneous polarization, applied voltage, and coercive field can be read on a voltmeter (29:30). Readers interested in the development of the S-T circuit and its derivatives are referred to Diamant, Sawyer, Josefson, Evans, and Tsui (29, 51, 40, 31, 56).

The RT-66 used in this study constitutes a modification of the basic Sawyer-Tower circuit. The RT-66 takes advantage of computer technology, using four software programs, to control

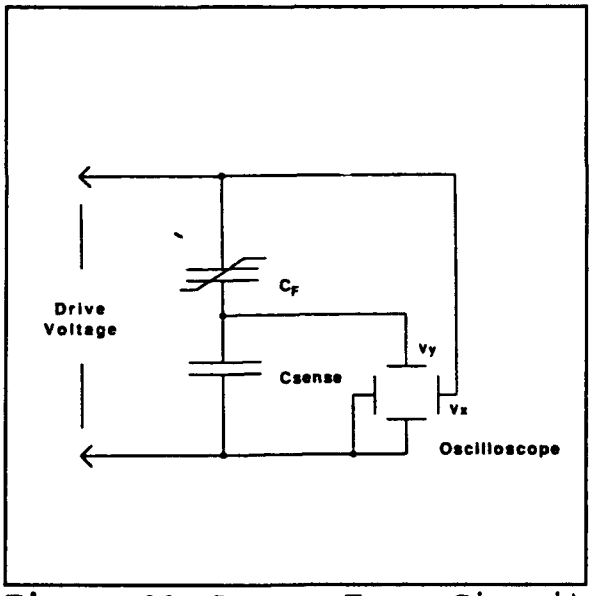

Figure 11. Sawyer-Tower Circuit (31:222)

signal application and collect output data (48:18). Four basic programs (CHARGE, FATIGUE, RETAIN, and RESIST) for testing a device are provided and, once a test begins, no operator input is required.

2 RT-66 Specifications

Figure 12 shows a block diagram of the RT-66 configuration. The DT2811 is a digital and analog input/output board which translates between the software packages and the S-T circuitry. All components are selected to have tolerances of 0.1%, and that tolerance is constant as long as ambient temperature does not change more than 12°F during program execution. Polarization measurements are accurate to within 0.5%, according to Radiant Technology (32). Note that no hardware compensation is included

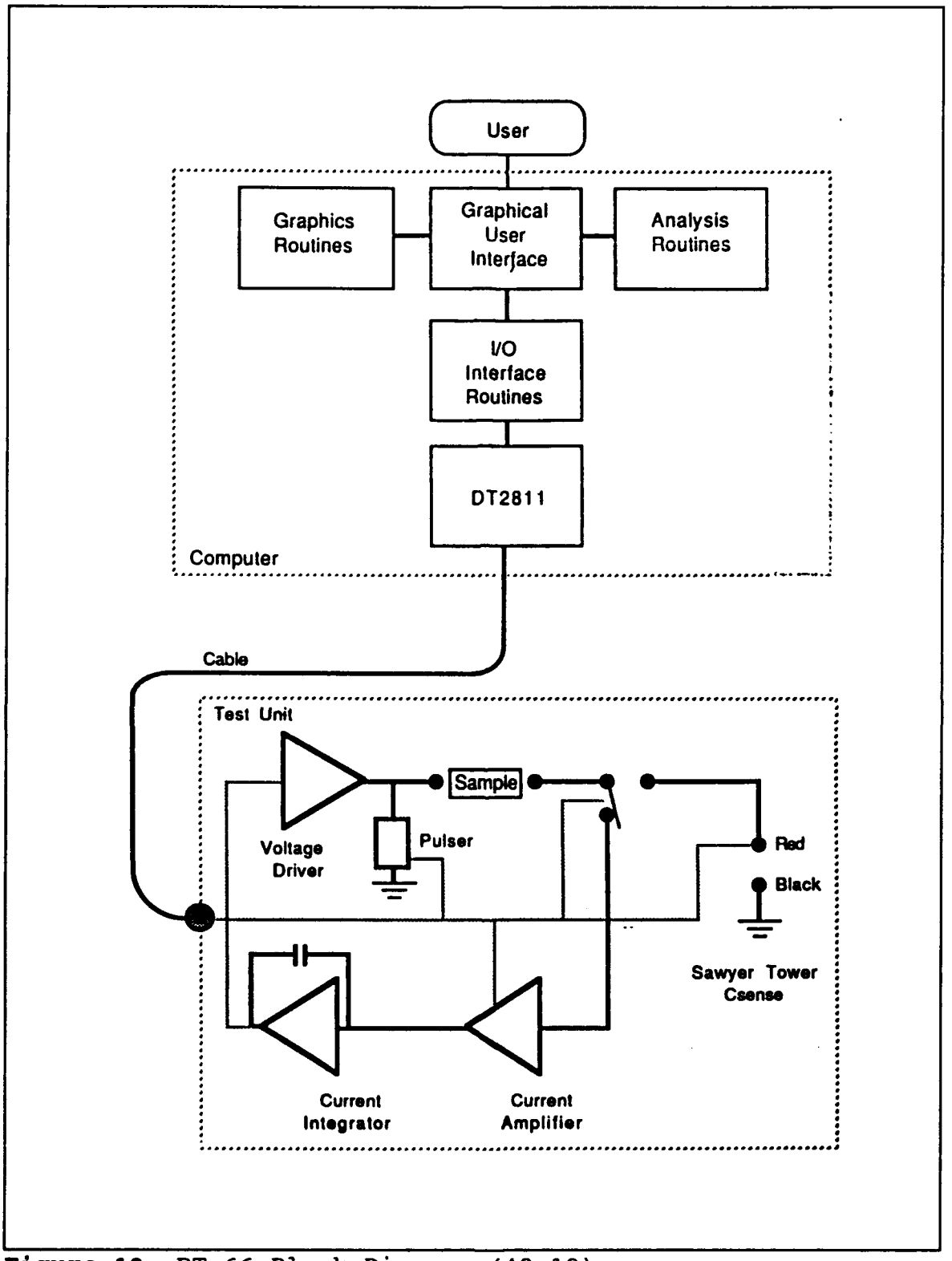

Figure 12. RT-66 Block Diagram (48:19)

since software provides the necessary compensation (31:220). The RT-66 can be configured to emulate a traditional S-T circuit, but that configuration will not be used in this study (48:18). A recent modification allows an external signal to be applied to the FE device through the RT-66 (48:21). That modification has not been completed on the RT-66 used for this research.

3 RT-66 Software

The RT-66 has four software programs. The programs are designated as CHARGE, RETAIN, RESIST, and FATIGUE. The FATIGUE program was the primary software package used in this study. Some preliminary work, described in Appendix A, used the CHARGE program, but only the FATIGUE program will be discussed in detail.

3.1 CHARGE Program. The CHARGE program output consists of hysteresis, pulse response, and resistivity measurements. Either a hysteresis loop ($\mu C/cm^2$ vs. voltage) or capacitance versus voltage may be displayed, as seen in Figure 13 (48:25). Only the hysteresis loop function was used in this thesis.

3.2 RETAIN Program. The RETAIN program provides a measure of retention loss in the sample FE material (48:47). The problem of retention can be viewed in terms of aging, that is, what are the decay characteristics of a given state over time. The presumption is that, for example, the user may wish to gain insight into how long it will take for a sample's poled state to deteriorate to the point where the original poled state can no longer be determined. The data display various polarization

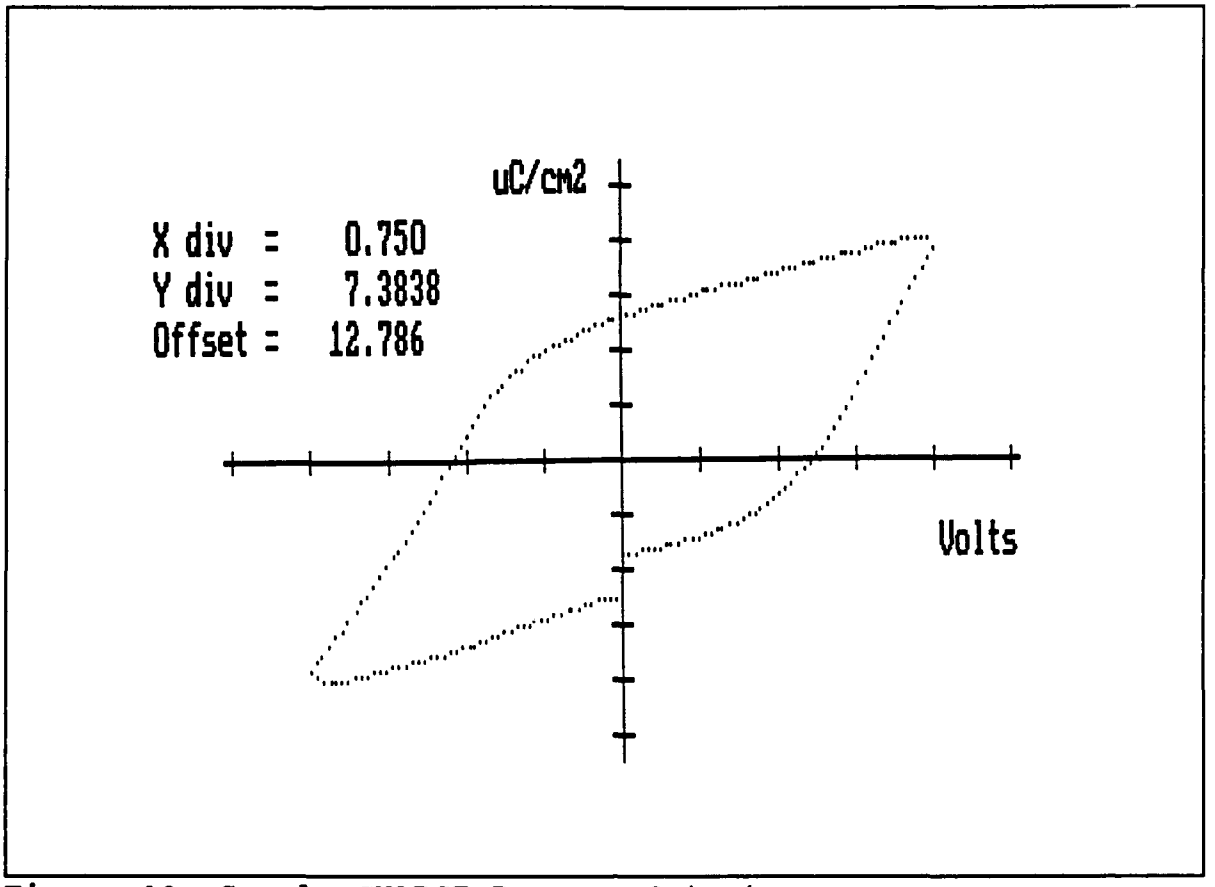

Figure 13. Sample CHARGE Program Output

measures vs. time ($\mu C/cm^2$ vs. seconds) (48:50). Since this study did not use RETAIN, no example is provided.

3.3 RESIST Program. The RESIST program measures "changes in resistivity of a thin film ferroelectric capacitor due to long term DC bias" (48:55). The data plotted have units of amps, ohms, or ohm-cm vs. seconds (48:57). No example is provided since RESIST was not used.

3.4 FATIGUE Program. The FATIGUE program was the primary means of collecting data. The program fatigues a sample by subjecting it to a series of pulses for a given period. A fixed pulse width is used "regardless of the pulse frequency. This

capability more closely simulates the operation of the sample capacitor in a memory type environment than fatigue with a square wave or sine wave" (48:37). The fatigue pulsewidth is approximately .0086 msec for the RT-66 Version 2.0 (48:38). The maximum frequency is a function of the computer system. For instance, on a 8 MHz 8088, the maximum frequency the system can support is 14 KHz. The system used for this research is an 8 MHz 80286 with a minimum fatigue period of .000044 sec, equivalent to a maximum frequency of about 23 KHz.

Once the fatigue period is completed, the pulse response of the sample is measured. Each pulse measurement is two milliseconds in duration. "Pulse measurements are checked for out-of-range values. If they are out of range, the amplification is adjusted and the test repeated" (48:21). Any cycling of the sample while range-finding is insignificant compared with the number of cycles applied to the sample during testing.

Figure 14 shows the train of pulses applied during measurements of the sample response. Figure 15 depicts the same information using hysteresis loops. The pulse measurements are converted to polarizations, and up to eight different polarizations can be plotted against time ($\mu c/cm^2$ vs. log seconds). Figure 16 is a sample FATIGUE program run. Only $+P^*$ and $-P^*$ are plotted in Figure 16, a user-controlled feature.

4 DP: A Value for Measuring the Change in Polarization

Pulse measurements do not provide a means of evaluating the fatigue rate, nor do they provide a direct measure of the change

Fixed Values: Pulse rise and fall times are 1ms each.

Signal Description: The pulse polarization test applies a series of five 2 millisecond pulses to the sample with 100ms delay between each pulse. The pulse profile is as follows:

Pulse #1:	-Vmax
Pulse #2:	Vmax
Pulse #3:	Vmax
Pulse#4:	-Vmax
Pulse#5:	-Vmax

Measurement: The first pulse presets the sample capacitor to Pr(-Vmax). For the next four pulses, the integrating capacitor is zeroed out prior to each pulse. A measure of the voltage across the integrating capacitor is made at the top and bottom of each pulse. The parameter measured at each point is shown below.

Pulse #	Voltage Applied	Parameter Measured
1	-Vmax	-
1	0	-
2	Vmax	P*
2	0	P*r
3	Vmax	P^
3	0	P^r
4	-Vmax	-P*
4	0	-P*r
5	-Vmax	-P^
5	0	-P^r

Signal Plot:

Vmax = 5.00 Volts

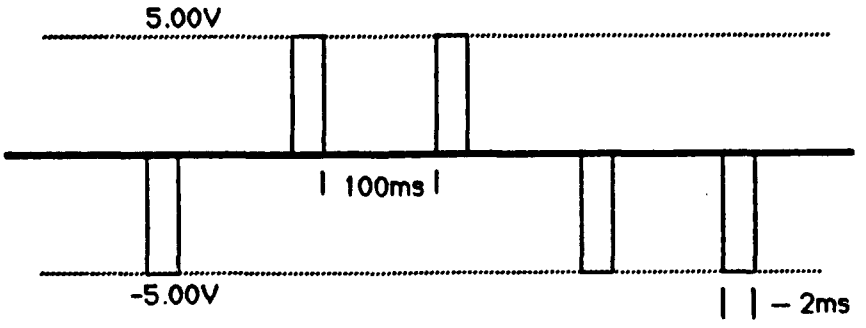

Figure 14. Pulse Polarization Measurements (48:80)

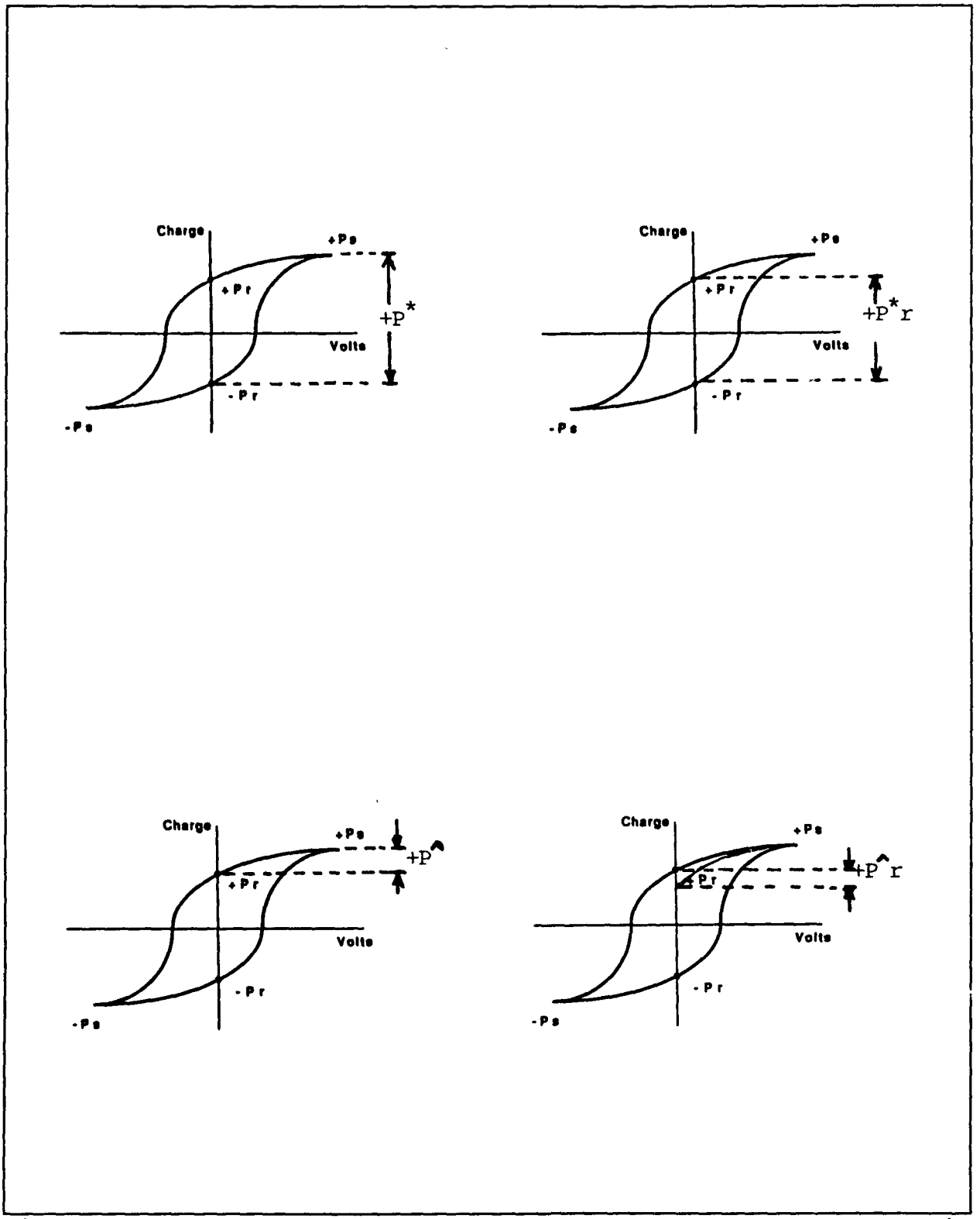

Figure 15. Pulse Polarization Measurements Related to Hysteresis Loop

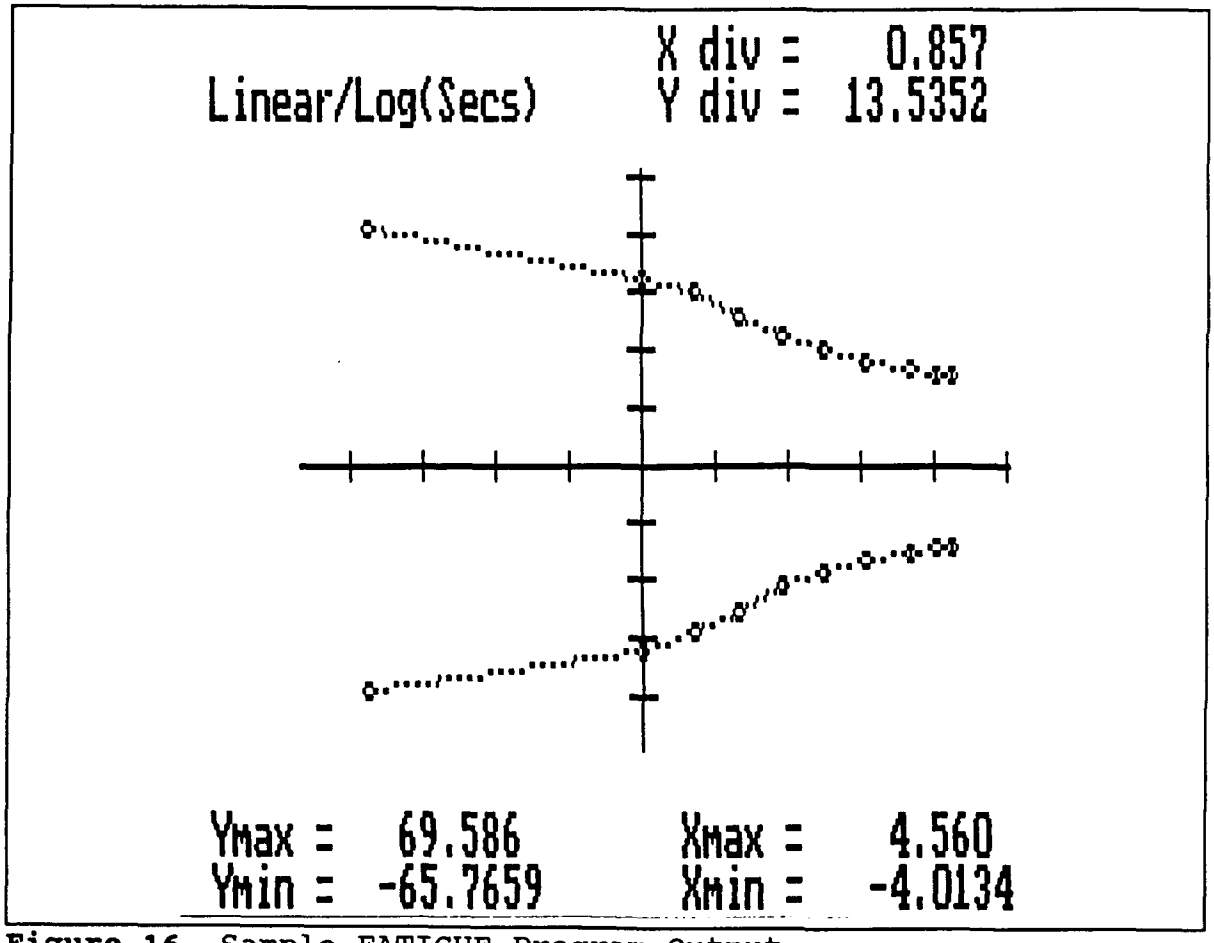

Figure 16. Sample FATIGUE Program Output

in polarization. A value which measures the change in polarization can be found by manipulating the pulse measurements. This change in polarization will be denoted by DP = P* - P^, the difference between two pulse measurements, as shown in Figure 17.

Note that DP is <u>not</u> a derivative. DP is a measure of the change in polarization when the device transitions from the "0" state to the "1" state at a particular moment in time using a specific voltage. DP is measured in $\mu C/cm^2$. A value related to DP, DPr, also measures the change in polarization by DPr = P*r - P^r. The difference between DP and DPr is caused by parasitic capacitance. DPr is also measured in $\mu C/cm^2$.

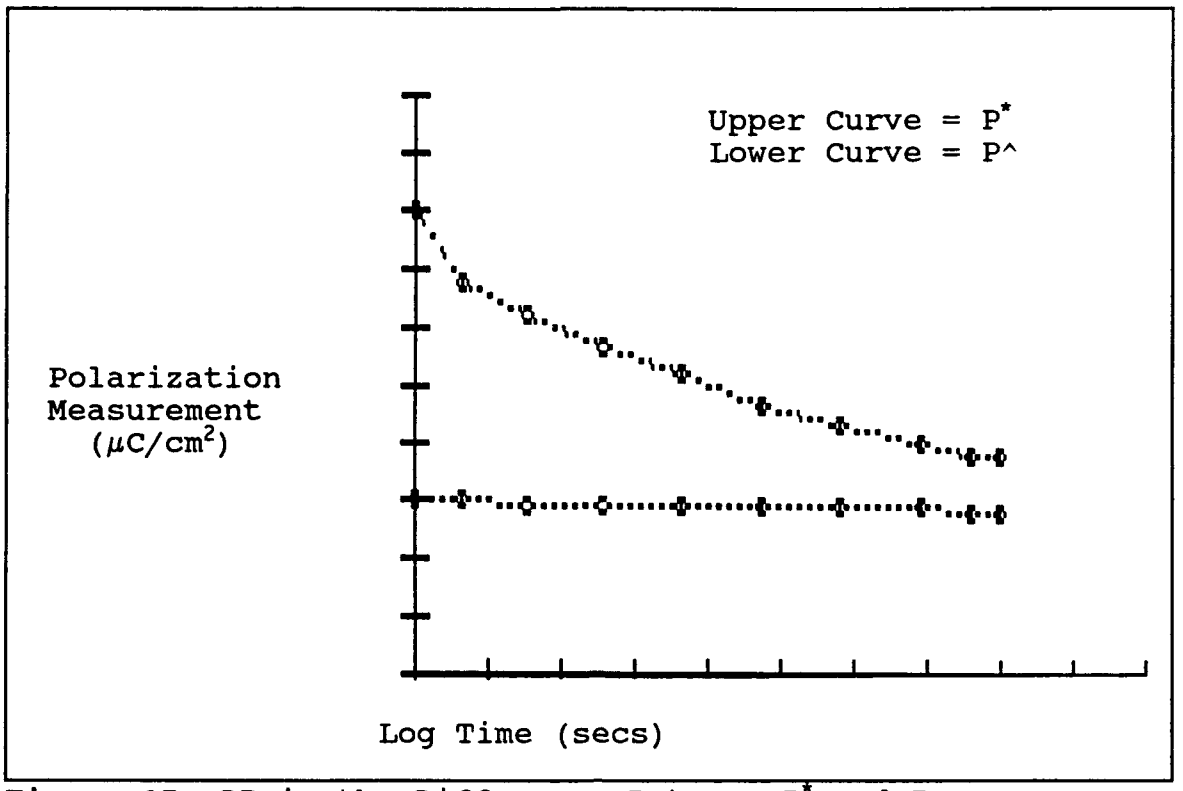

Figure 17. DP is the Difference Between P* and P^

An important feature of the FATIGUE output is that the x-axis is a logarithmic scale in time (seconds), while the y-axis is in $\mu C/cm^2$. An interesting feature of the profile section is that the times are cumulative. That is, if the user sets up a profile with 4 periods and selects 5 seconds for each period, then when the process is complete a total of 20 seconds will have elapsed. At the end of each 5 second period a pulse measurement will have been taken. The reason for explaining this is that an alternate interpretation would be that the RT-66 performs 4 pulse measurements at the end of 5 seconds.

5 RT-66 Limitations

1. The RT-66 can only measure ferroelectric capacitors limited to 40 nanofarads in the virtual ground mode and 120 nanofarads in the S-T mode (48:11).

2. The connector cable and front face of the RT-66 should be kept clear of power cables "to minimize the coupling of 60 Hz noise into the data" (48:11).

3. Due to software drivers and hardware limitations, the RT-66 commonly modifies the user input for the period at which the device is to be cycled. For instance, on one experiment a period of .000736281 seconds (approximately 1358 Hz) was entered, but the RT-66 used a value of .00073776 seconds instead (approximately 1355 Hz). This less than one-half of one percent difference is unlikely to affect any results. In a subsequent experiment the computer-generated period was 0.000735225 seconds (approximately 1360 Hz) when 0.000736281 seconds was entered. The maximum difference observed in this study was approximately 2% greater than the actual frequency.

4. Another software "error" which the RT-66 generates occurs in the Profile section of the FATIGUE program. The user-input time values occasionally increase by one second. For instance, instead of a profile pulse measurement being taken at time zero, it will take place one second later. Since the region of operability initially had a lower operating end of 1444 seconds, the addition of 3 or 4 seconds causes less than one-half of a

percentage point difference in the total time an experiment is run.

6 RT-66 Testing Procedures and Test Limitations

1. Each time a test is performed, the test itself affects the characteristics of the sample (31:219). However, the test can be viewed as two cycles of the sample. A single test has an insignificant effect unless fewer than one or two hundred total cycles are applied to a FE device.

2. Samples should be disconnected during computer startup to insure proper system calibration and avoid affecting the samples. Once the first application has been executed, it should be possible to leave one application and enter "another without fear of a spurious voltage application to the sample" (48:23).

3. Power should be removed from the entire system before connecting the RT-66 to, or disconnecting from, the computer. Otherwise the DT2811 board may be damaged (48:10).

4. Because FE devices are pyroelectric, ambient light will affect the results. However, the tests performed in this thesis are relative measurements. Therefore, as long as each device is exposed to a constant amount of light, the data should not be affected. In particular, a light on the probe station must be used in order to position the probes. Switching the light on and off might be more detrimental to results than choosing to leave the light on (45:7).

5. FE devices are piezoelectric. Therefore, the application force of the probe on the devices could have an effect on the

results. No mechanism was available for either measuring or controlling this variable. Since one experimenter performed all tests for this thesis there may have been some unintended experimental error induced due to probe manipulation technique.

7 Summary

In Chapter III, the RT-66 Ferroelectric Tester was introduced. Four software programs control the RT-66 and the pulse measurement data collected is based on changes in the state of polarization. The FATIGUE program was the primary software tool used to collect data during this study. Some preliminary work was also done with the CHARGE program, as seen in Appendix A. The value used in this study for measuring fatigue, DP, is based on the pulse measurement data, and these measurements are accurate to within 0.5%. Four limitations of the RT-66 were also discussed, along with five operating procedures.

IV. Response Surface Methodology (RSM)

1 Response Surface Methodology Overview

Response surface methodology comprises a group of statistical techniques for empirical model building and model exploitation. By careful design and analysis of experiments, it seeks to relate a response, or output variable to the levels of a number of predictors, or input variables, that affect it. (5:1)

A response surface is an n-dimensional shape which represents the output of a system with n-1 inputs. If only one input exists, the response surface can be represented by a curve in two-dimensional space (see Figure 18).

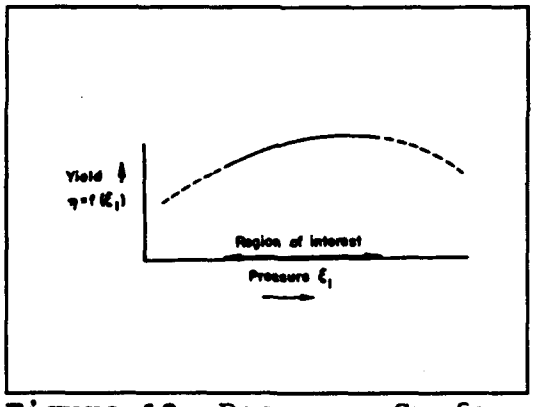

Figure 18. Response Surface in Two Dimensions (5:2)

Similarly, a system response with two inputs can be plotted in three-dimensional space (see Figure 19).

When more than two inputs exist it is no longer possible to represent the entire response surface visually. While the graphical depiction of a response surface is limited to 3

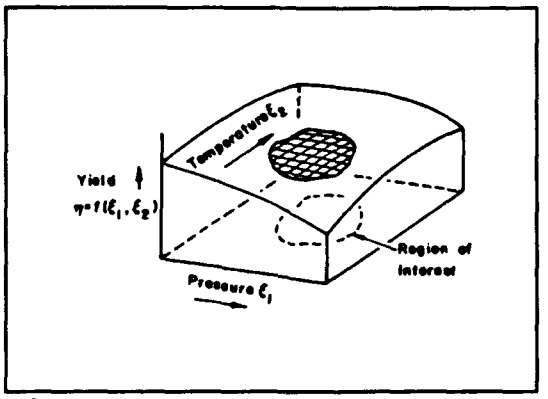

Figure 19. Response Surface in Three Dimensions (5:2)

dimensions, the mathematical representation is not limited at all by dimension. Thus, the mathematical representation of a response surface provides an empirical model of a system response regardless of the number of predictor variables (5:3). Frequently, more than one system response can be measured as the result of changing system inputs. Although it is possible to conduct a multi-response system analysis, tools in this area are generally poor (12:145).

1.1 Characteristics of Response Surfaces. A characteristic feature of response surfaces is that the system response can typically be modeled in local regions by a low-order polynomial, even if the system-wide response is widely irregular (5:3). Experience has shown that a second-order model will generally be sufficient to adequately model a system response within a given region of interest. Where higher-order models are required it is frequently possible to perform transformations which will allow first or second-order models to be generated (7:205). Some of

the general classes of second-order models are displayed in Figure 20.

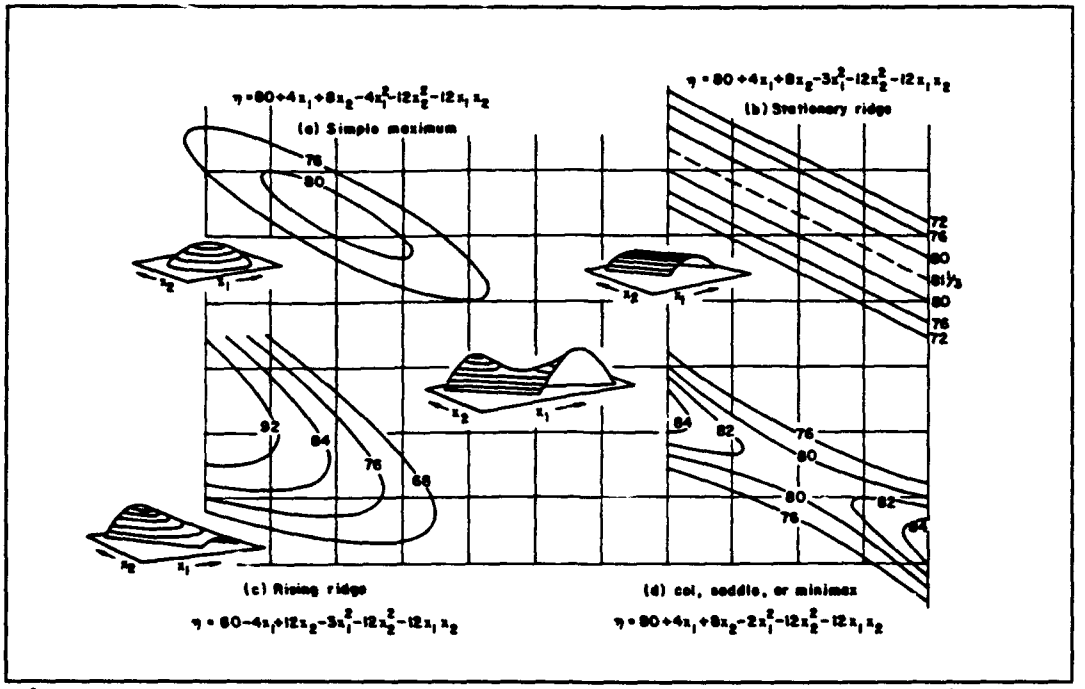

Figure 20. "Some examples of types of surfaces defined by second-order polynomials in two predictor variables x_1 and x_2" (5:24)

1.2 Goals of RSM. The essential goal of RSM is to fit a model to a localized surface. After fitting a model, the next step may be to move to a new region of interest, or to more thoroughly explore the localized surface. RSM is also used to screen out unimportant variables, or to develop empirical models for prediction when no complete physical and mathematical descriptions of a system exist.

A typical RSM goal is to fit a localized surface to represent the limited operating range of a manufacturing process. This type of analysis has typically taken place in mixture problems. If an RSM model can be fitted for the operating range,

RSM tools can be employed to seek improvements in the system response or to find critical points in the process. Optimality is not always the goal of RSM as it may not be feasible or economically justified. However, some improvement in the system or process is usually possible through the use of RSM techniques (12:37).

1.3 RSM Tools. RSM is an iterative process of experimental design, experimentation, and analysis of the data. The experimental designs are usually of first or second-order, in accordance with the idea that local phenomena can usually be approximated by functions of less than third order. Once the data is collected, data analysis is typically performed by computer software packages using least-squares regression techniques. Statistical tests are then performed to measure the validity and predictability of the model. For first-order models, a gradient search might be used to determine the next region of interest in the iterative design process (5:4). The next two sections will discuss some basic model-building tools.

2 Experimental Designs

RSM designs are usually described as being of order 1, 2, or 3, where order refers to the highest power polynomial model that can be fit to the data. In practice, third-order designs are usually avoided, if suitable transformations can be made, because the resulting model may involve an unreasonably large increase in the number of parameters (9:573). For instance, a third-order

model with four parameters $x_1,\ldots,x_4$ can involve up to 14 third-order terms: $\{x_1x_2x_3,\ x_1x_2x_4,\ x_1x_3x_4,\ x_1^2x_2,\ \ldots\ x_1^3,\ x_2x_3x_4,\ \ldots,\ x_4^3\}$.

2.1 Two-level Factorial Designs. Two-level factorial designs are very useful designs in which each variable is observed at only two levels. A two-level factorial design in k variables is designated by 2^k. The 2^k design is particularly useful in the early stages of experimentation (5:107). A complete factorial design in k factors is obtained

> by choosing n_1 levels of factor 1, n_2 levels of factor 2, ... ,n_k levels of factor k, and then selecting the $n = n_1 \times n_2 \times \ldots \times n_k$ runs obtained by taking all possible combinations of the levels selected. (5:105)

As an illustration, Table I presents a complete two-level factorial design in three parameters.

Table I. Two-Level 2^3 Complete Factorial Design

x_1	x_2	x_3	x_1x_2	x_1x_3	x_2x_3	$x_1x_2x_3$
-1	-1	-1	1	1	1	-1
1	-1	-1	-1	-1	1	1
-1	1	-1	-1	1	-1	1
1	1	-1	1	-1	-1	-1
-1	-1	1	1	-1	-1	1
1	-1	1	-1	1	-1	-1
-1	1	1	-1	-1	1	-1
1	1	1	1	1	1	1

Table I may give the mistaken impression that input parameters must equal ±1. Typically, parameters are coded to ±1

to simplify calculations and enhance the analysis process, particularly graphical analysis.

2.2 Saturated Two-Level Factorial Designs. A saturated design is a design in which the levels of additional factors are set equivalent to the levels of interaction terms in a full factorial design. For instance a 2^3 (i.e., three factors) design has four interaction terms: {12, 13, 23, 123}. This design is saturated if four new factors are introduced and the equivalences 4=12, 5=13, 6=23, and 7=123 are made as in Table II.

Table II. Two-Level 2^{7-4} Fractional Factorial Design

x_1	x_2	x_3	x_4	x_5	x_6	x_7
-1	-1	-1	1	1	1	-1
1	-1	-1	-1	-1	1	1
-1	1	-1	-1	1	-1	1
1	1	-1	1	-1	-1	-1
-1	-1	1	1	-1	-1	1
1	-1	1	-1	1	-1	-1
-1	1	1	-1	-1	1	-1
1	1	1	1	1	1	1

The resulting design is designated 2^{7-4} and constitutes a fractional factorial design (5:154). The advantage of such a design is that the seven main effects can be estimated with 2^{7-4} = 8 design points, rather than 2^7 = 128 observations. The primary problem with saturated designs is aliasing (12:140). Aliasing occurs when an effect is attributed to more than one factor or

interaction term, although certain terms may be dealiased through carefully selected additional observations. In Table II, all seven main effects may be estimated free of aliasing with each other, but they are aliased with two-factor interaction terms. The 2^{7-4} design has Resolution III, which means that the main effects are aliased with two-factor or higher order interactions.

2.3 Central Composite Designs. A composite design is created by using several basic designs as building blocks, generally in order to create designs which can estimate higher-order coefficients (5:163). An example is the second-order central composite design (CCD). Typically CCDs use a blend of a two-level fractional factorial design augmented with other design points referred to as center points and star points. The advantage of this design is that all first order, two factor interaction, and quadratic terms can be estimated.

In the simple three-variable CCD of Figure 21 the corners of the cube constitute the two-level factorial or fractional factorial of the composite design. The coordinates of the corners of the cube are the coded values (±1,±1,±1), while the center point is the origin (0,0,0). The star, or axial, point coordinates selected in this study were at ±1.668 along each axis. The criteria for selecting the coordinates of the star points can be found in Box and Draper (5:510). The factorial portion of the design is used to estimate the first-order and two factor interaction terms. The remaining portion of the CCD consists of a point at the center of the cube and symmetric axial

points along the three axes. These points allow the estimation of pure quadratic effects (5:305-306). Other second-order designs exist, and the interested reader can refer to any RSM textbook for details.

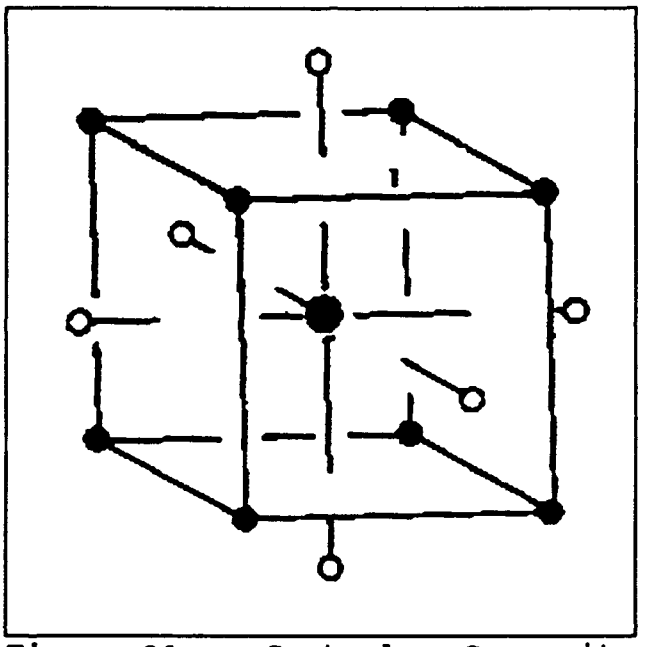

Figure 21. Central Composite Design (5:306)

3 Regression Models

Once the experiments in an RSM design have been performed, the coefficients of the model are usually estimated using least-squares regression tools. Given that **X** represents the matrix of input parameters, and **Y** the vector of responses, then the coefficients are estimated by

$$b = (X^T X)^{-1} X^T Y$$

The statistical significance of these coefficients is then examined, and an attempt made to fit a parsimonious model to the data observations. If the model is sufficient to meet the needs

of the researcher, the design process terminates. Otherwise, additional steps are taken in an attempt to attain the research objectives. If the fitted model is in a region where first-order effects predominate, a gradient search may be an appropriate means to determine a new design location where the response is either higher or lower, as desired (5:184). When a first-order model is inadequate, data transformations or more sophisticated second-order models such as the CCD may be appropriate.

3.1 Gradient Search. A gradient search allows the experimenter to move in the direction of the greatest localized increase or decrease in system response. The gradient points in the direction of steepest ascent/descent. Movement along the gradient yields the greatest change in system response until the response surface changes shape. Once the response surface changes, a new equation describing the surface must be found. The new equation models a system with a gradient different from the gradient which pointed to this new surface. The purpose of the gradient search is to provide a procedure for moving from one area of localized interest to a new localized area where the system response is either higher or lower than in the previous area (5:190).

4 RSM Background

Box and Wilson have been identified by some as the founders of RSM, in 1951 (9:571). Other authors have traced the origins back to the 1930s when response curves first gained frequent usage in the literature. In general, the motivation behind the

development of RSM was the problem of "planning and analyzing experiments in a search for desirable conditions on a set of controllable (or design) variables" (12:37). Traditionally, experiments proceeded along a sequence of design points, examining the system response at each point. RSM was developed to accelerate the experimental process by examining several points simultaneously.

Chemical mixture problems are one area where response surface methodologies are frequently used to solve research problems. The problems might include improving compounds by changing the proportion of catalysts, or saving money by changing the temperature and pressure conditions under which the compound is formed.

> A typical RSM study begins with a definition of the problem (which response is to be measured, how it is to be measured, which variables are to be studied, over what ranges they are to be explored, etc.) and includes, (9:576)
>
> (a) performing a statistically designed experiment
> (b) estimating the coefficients in the response surface equation
> (c) checking on the adequacy of the equation (via a lack-of-fit test), and
> (d) studying the response surface in the region of interest. (12:144)

Several rules of thumb have been established for developing successful RSM models. First, the model should be kept as simple as possible. The first rule of thumb is known as the <u>principle of parsimony</u>, that is, use as few variables as necessary to build an acceptable model (9:573). It should be noted that the most parsimonious model is not always the best model, but the best

model should be as parsimonious as possible. While two models may both be acceptable, a model with more variables may exhibit much more predictive power (10:3).

The next rule of thumb is that the practical implications of the results must be understood by the experimenter (9:573). In a simple case, this may mean that the experimenter recognizes it is not economically feasible to operate at certain "optimal" conditions. In a more complex instance a critical point might be found,but the experimenter must determine whether he has "simply a true maximum or minimum or, on the contrary, a minimax or a rising ridge" (9:581).

Finally, the model should include "as much of the currently available theoretical knowledge of the system" as possible, up to the point where the model becomes too cumbersome (9:573). The models created with RSM very rarely give a theoretically valid description of the relationship between independent parameters and the response. Instead, an empirical relation is usually generated. There are then two purposes this relation can serve. First, it can "replace an elaborate table of numbers by a "formula" " or, second, the relation can serve as a tool for prediction (10:2).

RSM has been used to gain insight into the underlying physical mechanisms of a process being investigated (9:572). This insight may be a simple matter of comparing theoretical and RSM-generated empirical models (9:582). In chemical mixture problems "the discovery of factor dependence of a particular type

may, in conjunction with the experimenter's theoretical knowledge [,] lead to a better understanding of the basic mechanism of the reaction" (2:23). In particular "the canonical variables of the empirical surface can relate to the basic physical laws controlling the system" (3:287). The nature of a ridge system might provide similar insight (3:288). Despite this approach in search of fundamental mechanisms, the resulting empirical equations would properly be described as empirical models, not theoretical models (9:573).

One alternate modeling approach which merits a brief glance is the Taguchi approach, now being used by many companies. An advantage of RSM, as compared to the Taguchi approach is that RSM can target interactions among factors while Taguchi targets only main effects. RSM seeks to eliminate much of the labor involved in sequential experimentation by creating efficient experimental designs, designs which account for factor interactions (12:144). An analyst may be able to more accurately predict how changing factors will impact system response by including interaction terms in an empirical model.

5 An Iterative Design Process for a New System

Different design considerations apply based on the maturity of the system under investigation. A system which is already well developed presumably operates "in the vicinity of the currently known best process" (5:183). In this case a user might seek incremental improvements in the system; that is, changes which occur within the operating regime of the equipment.

For a new system there may be few guidelines to suggest where to begin the investigation. There may also be much broader allowable operating regimes pursuant to investigation. One approach to initially sounding out the "best" operating environment is the one-factor-at-a-time method (5:182). A procedure which may be more effective and economical is the gradient search procedure (5:183).

A typical stepping-stone procedure when investigating a new system is to first perform experiments in a response area which can be described by a linear equation (5:183). For an investigation of a system with seven variables, a 2^{7-3} fractional factorial design requiring 16 design points might be constructed. This particular design has resolution IV, which refers to the aliasing, or confounding, inherent in the design. For instance, in a resolution IV model all first-order coefficients can be estimated free of aliasing with second-order and higher order coefficients.

Presuming the linear model is appropriate, a gradient search procedure can be used to find the next design point. Even if a surface has some curvature it may be possible to maintain a linear model through appropriate transformations of the response or the variables. Transformations are particularly valuable "if, over the region of interest considered, the observed response is curved but smoothly monotonic in each of the" variables (5:304). However, to approximate the response surface in a region with substantial curvature requires an equation of at least second

degree (5:305). At this point the gradient search procedure can be put aside and powerful second-order techniques can be used to analyze the surface. A typical second-order design is the CCD. As stated previously, a CCD allows the least-squares estimation of all first-order, two factor interaction, and quadratic terms.

Once a suitable model has been developed, it must be interpreted. An important aspect of interpreting an RSM model is to consider its assumptions. A major assumption was that the true response could be reasonably approximated by a low order polynomial in a restricted region of the parameter spaces. Thus, the fitted model only applies to the region which has been explored. Therefore, optimal solutions generated by RSM techniques must be considered local minima or maxima. Use of RSM techniques does not guarantee a global maximum or minimum.

6 Key Terms

This section may be skipped without loss of continuity by those familiar with the jargon of RSM. Others should find that this section provides definition of terms as well as a reinforcement of many of the key concepts involved in RSM.

6.1 Variance, Bias, Residuals, and Mean Square Error. All three of these terms are used "to characterize the goodness of a point estimator" (11:338). The variance provides a measure of how much sample values differ from their mean. Other conditions being equal a small variance is preferable. The sample variance is calculated as

$$s^2 = \frac{1}{n}\sum_{i=1}^{n} [y_i - mean(y)]^2$$

Bias (B) measures how well the sampling distribution of an estimator is centered about the target parameter (11:337). Occasionally the bias criterion for judging a model has led to compromising the variance criterion. A slight bias might be acceptable if the variation in the biased case is significantly less than for the unbiased estimator (12:141, 13:412). Figure 22 depicts a situation where a biased estimator with a small variance might be preferable to an unbiased estimator with a large variance.

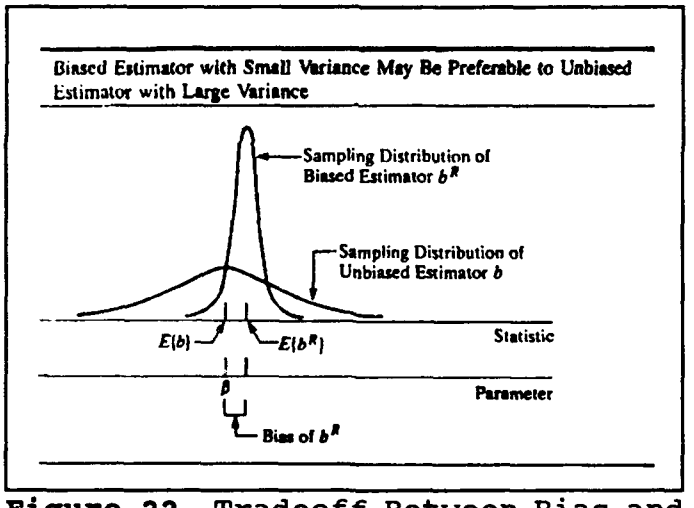

Figure 22. Tradeoff Between Bias and Variance (13:412)

6.2 Lack of Fit. Fit is a general term to describe how well a model predicts the observations. The utility of the concept of fit is seen in Mandel's observation that in "the current literature, it is clear that the omission of regressors is always based on goodness-of-fit considerations" (10:2). However, Mandel

cautions that a fitting procedure is only justified when the principle of parsimony is invoked (10:3). Another caution is that a model which fits may not necessarily be a good model. For instance, a seventh order model can always be designed which will fit exactly through eight data points, but fluctuations between the data points might eliminate the model's usefulness except for predicting what is already known.

A fitted, or estimated, value is the response predicted by a model for a particular level of the parameters. This fitted value usually differs from the observed response at those parameter settings (13:45). The residual (e) is the difference between the fitted value and the observed value (13:115). Mean square error (MSE) measures the square of the distance between an estimator and its target parameter (11:338). It is calculated by

$$MSE = \frac{e^T e}{n - p}$$

where,

n: number of observations

p: number of parameters

MSE is a function of both variance and bias, therefore it should be a better check of the goodness of a particular estimator than variance or bias alone (11:339).

Several other criteria have been suggested for measuring the fit of a particular model, that is whether the model's predictions approximate the observed values within some tolerance. The goodness (or lack) of fit test is one way of statistically measuring how well a proposed model fits the data.

The lack of fit test requires replicated observations in the data set for at least one data point. The test statistic, (F^*), and the decision rule are

$$F^* = \frac{MSLF}{MSPE}$$

If $F^* \leq F(1 - \alpha; c - p, n - c)$, *good fit*

where,

α: *determines risk level of Type I err*

c: *number of replicate groups*

p: *number of parameters*

n: *number of observations*

MSLF: *mean of the squares of lack of fit*

MSPE: *mean of the squares of pure e*

The lack of fit test assumes that the response observations (Y) for given parameter settings (X) are independent, normally distributed, and that the distributions of Y have the same variance σ^2 (13:131). The details for developing MSLF and MSPE can be found in Appendix B.

Another tool for assessing fit is Mallow's C_p criteria. Essentially C_p "is concerned with the total mean squared error of the n fitted values for each subset regression model" (13:447). Models which exhibit little bias tend to have a C_p value close to or less than the total number of input parameters, n. Models with substantial bias will tend to have values much higher than n (13:448).

A final tool for measuring the overall fit of a model is the R^2 statistic. R^2 "represents the faction of the variation about

the mean that is explained by the fitted model" (5:74). More information on R^2 can be found in Neter's textbook (13:444-447).

6.3 Rotatability. Box and Hunter felt that a key to a useful experimental design was to develop a variance function which was spherical, or nearly spherical, in nature. "Such designs insure that the estimated response has a constant variance at all points which are the same distance from the center of the design. Designs having this property are called rotatable" (4:195). The intent of rotatability is to stabilize prediction variance.

Rotatability is desirable in an RSM study because "it is not usually known in advance which direction from the center point will be of later interest" (13:335). If the direction of interest was known it might instead make sense to find some design which minimized variance along the lobe of interest. In general, rotatability is a function of the design points chosen. Factors which might hinder choosing design points which maximize rotatability include: robustness to model misspecification, quality estimation of the slope, and robustness to outliers (12:139). For any design, rotatable or not, there are regions within the design space where responses are estimated well, and where they are not (6:161).

6.4 Orthogonality. Orthogonality is a desirable design property because it results in joint confidence regions and confidence intervals that are much smaller than those of non-

orthogonal designs. In the simplest case, two vectors are said to be orthogonal if

$$a^T b = 0$$

This property is used profitably when performing linear least-squares regressions. For a linear system, minimizing the diagonal elements of the variance-covariance matrix $[\sigma^2(X^TX)^{-1}]$ generates much smaller joint confidence regions and much smaller confidence intervals for the individual coefficients (5:79). This minimization can be achieved with an orthogonal design (1:50). A necessary and sufficient condition for a linear design to be orthogonal is a diagonal X^TX matrix. Note that as a result of orthogonality in a linear design, all off-diagonal entries in the variance-covariance matrix are zero.

For higher-order designs the X^TX will not be diagonal. In the second order RSM design case, orthogonality is defined by the absence of correlation between the quadratic terms. More information on orthogonality may be found in Box and Draper's textbook (5:512).

6.5 Time Trends. Data which is collected over time may exhibit autocorrelation, an undesirable characteristic indicating that errors in measurement are dependent on previous measurements. An example is a reaction which exhibits "a change in the activity of the catalyst with time" (8:67). "Traditionally, the elimination of time trends has been accomplished by the use of blocking - Latin squares and randomized blocks - or by the use of covariance analysis in which

the covariate is a time trend" (8:67). Autocorrelation can also be eliminated if the vector used to estimate the time trend is orthogonal to other vectors in the design (8:71).

V. Experimental Variables and Designs

1 Introduction

This chapter describes the framework within which the experiments in this study were performed. The variables used limited the operating area, or parameter space, over which response were observed. The experimental procedures explain how the ferroelectric (FE) devices were tested, and the designs define the variable settings for individual experiments. In this chapter, the discussion of procedures is limited to the criteria for choosing a particular FE device to test. All other experimental procedures have been described in chapter three of this thesis and the pertinent sections of the RT-66 manual (49).

The starting point of this study was the initial selection of the variables of interest. The final selection of seven variables was based on several factors. The length of time available for testing was limited, the variables chosen were easily controlled, and other studies involving these variables had been performed, thereby allowing comparisons of research findings.

The data collection process proceeded in three distinct phases, one phase for each Response Surface Methodology (RSM) design. Throughout these three phases additional tests were performed to secure replicant data, investigate possible outliers, and develop data for testing the prediction capabilities of proposed empirical models. After completing each

of the three phases various statistical tests were performed to determine if a sufficient empirical model could be proposed. An α value of 0.05 was required before any statistical test would be considered significant.

2 Initial Experimental Parameters

Initially seven parameters were selected for study:

- type of FE material
- type of electrode
- poling pulse voltage
- aging
- fatigue applied voltage
- frequency of applied fatigue voltage pulses
- time duration of the FATIGUE program

Each parameter will be discussed in the following sections.

2.1 Material and Electrode Characteristics

Four PZT samples were provided for this study. Each sample will be discussed in terms of the material composition of the FE and the types of electrodes used. The FE material is designated with three numbers which, in series, represent the respective percentages of lanthanum/zirconium/titanium used in the mixture. The FE materials were 0/60/40 and 0/20/80. The electrodes are designated as bottom electrode/top electrode. Two configurations were used for each FE material: Platinum/Platinum (Pt/Pt) and Platinum/Palladium (Pt/Pd).

The samples received were incomplete wafers. Each sample contained more than 20 mask sets, and each mask set contained 9

arrays as seen in Figure 23. The decision was made to test devices with an area of 4×10^{-6} cm^2. Arrays 1 and 3 on each mask set were the only arrays with devices of that area. As shown in Figure 24, each array provided up to 16 devices, since device 3 is not connected and device 12 is the contact for the bottom electrode of the devices.

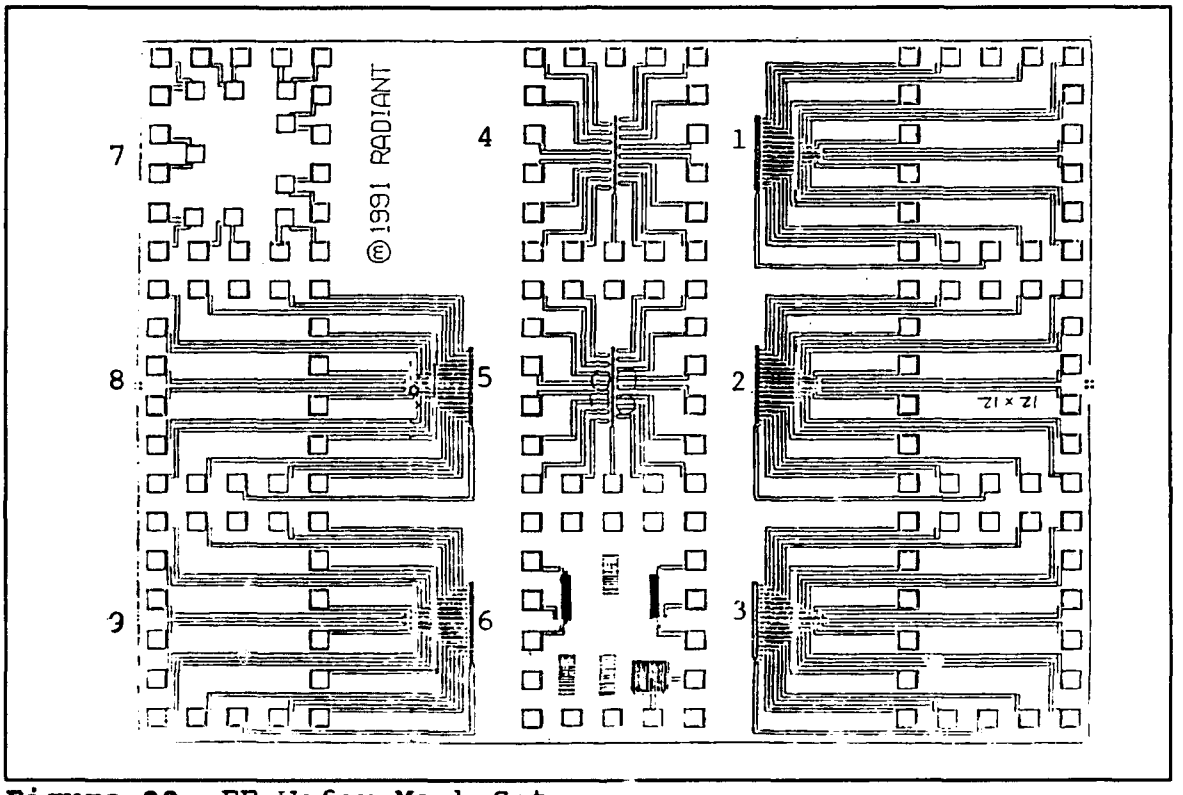

Figure 23. FE Wafer Mask Set

2.1.1 Selecting a Device for Testing. A system of randomly selecting devices was implemented. First a specific mask set and array were selected, then a specific device was randomly chosen. If this device failed, another device on the same mask set and array was selected for testing. This process continued until a test completed as scheduled or until no more devices were left on an array. If an array was exhausted, the

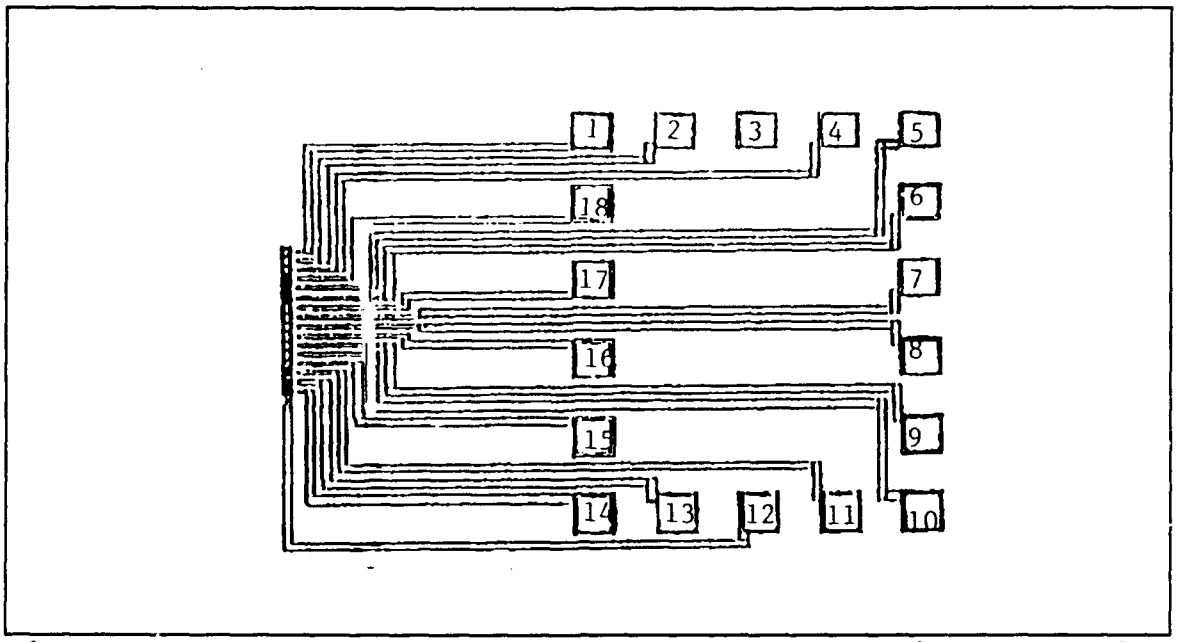

Figure 24. Array Structure (1 and 3) and Device Numbering Scheme

device selection procedure restarted at the mask set selection step.

2.1.2 Establishing $V_{100\%}$ for each Sample. Upon receipt of the samples, preliminary investigation of the devices was used to determine a relative voltage scheme. This study defined $V_{100\%}$ as the applied voltage at which a particular sample began to exhibit undesirable characteristics. A discussion of the criteria for judging $V_{100\%}$ is given in Appendix A. The values for $V_{100\%}$ are shown in Table III.

During the experimental phase, relative voltages were used as one of the variables in the experimental designs. For the two-level factorial designs, the relative voltage occurred at only two levels: $V_{70\%}$ or $V_{80\%}$. If a specific experiment for 0/60/40 Pt/Pt called for an applied voltage of $V_{80\%}$, then the applied voltage used was 8.0 volts. Had the sample called for

Table III. $V_{100\%}$ Values for the Samples

Material	Electrode	$V_{100\%}$
0/60/40	Pt/Pt	10.0
0/60/40	Pt/Pd	7.0
0/20/80	Pt/Pt	5.0
0/20/80	Pt/Pd	3.5

testing 0/20/80 Pt/Pt, then $V_{80\%}$ would have corresponded to an applied voltage of 4.0 volts. The central composite design used additional relative voltages, but the process of transformation from $V_{\%}$ to an absolute voltage does not change.

2.2 Poling Pulse Voltage and Aging. The purpose of the poling pulse voltage is to pole the device under test (DUT) in a positive or negative direction. For this study the device was poled with either a positive or negative $V_{80\%}$. The DUT was then tested with the FATIGUE program at one of two times. Some devices were tested immediately, while others were aged for 24 hours prior to testing. Thus, it was possible to determine if 24 hours of aging nad any statistically significant effect on fatigue rates.

Some previous studies have indicated that aging can be reduced or eliminated by cycling the material between its positive and negative states. This cycling process is referred to as de-aging. Thus, fatiguing a FE material has an affect upon the aging process of that material. This study reversed that

issue to assess whether aging has an affect upon the fatigue rate.

2.3 Applied Fatigue Voltage. The applied fatigue voltage is entered as an input to the FATIGUE program. The relative voltages used ranged from approximately $V_{67\%}$ to $V_{98\%}$. The DUT was fatigued by alternately pulsing the DUT with a positive or negative V_x.

2.4 Frequency of Pulses. Frequency can be multiplied by time to determine the total number of cycles applied to a particular device, a two-factor interaction term. Much of the literature states that the fatigue rate of FE materials is linear in the log of the number of cycles applied to a device. Appropriate RSM designs allow statistical testing of this proposed linear in log of cycles relationship.

2.5 Time Duration of FATIGUE Program. Another mechanism for controlling the total number of cycles applied to the DUT was to vary the length of time the FATIGUE program ran. The inclusion of any time-related variable inevitably raises the question of autocorrelation. Chapter 4 indicated that autocorrelation could be avoided by insuring that the time parameter is orthogonal to other parameters. That orthogonality was insured in all designs used in this study.

3 Three RSM Designs

Three RSM designs were used in this study. The first two designs were fractional factorial designs. The third design was

a central composite design (CCD). Each design will be presented, along with the motivation for using each design.

3.1 RSM Design One: Estimates Main Effects

The first design was a two-level, 1/8 fractional factorial with Resolution IV, as shown in Figure 25. The primary purpose of this design was to determine if any of the original seven variables could be eliminated from future consideration within the selected operating region. All first-order terms could be estimated without fear of confounding with terms of second order. The design called for sixteen combinations of parameter settings, with replicants collected at six of the settings.

Replicants permitted better analysis of the variance of the devices and allowed a lack of fit test to be performed. The operating region for this phase included voltages of $V_{70\%}$ to $V_{80\%}$, frequencies from 200 Hz to 1 kHz, time of experiment from 1444 to 4444 seconds, and aging of 0 hours or 24 hours.

3.2 RSM Design Two: Includes Two-Factor Interactions.

Following the variable screening exercise of the first design, an analysis of two-factor interactions appeared to have some potential. In order to estimate all two-factor interaction terms without aliasing among themselves, the orthogonal design shown in Figure 26 was adopted.

Design two was a 1/2 fractional factorial design of resolution V. The design called for sixteen combinations of parameter settings, with replicants collected at six of the settings. The design served a twofold purpose. First, the same

RUN	A	B	C	D	E	F	G	I	Nbr Cycles
1	-	-	-	-	-	-	-	2	4.44 E6
2	+	-	-	-	-	+	+	1	0.29 E6
3	-	+	-	-	+	-	+	2	2.94 E6
4	+	+	-	-	+	+	-	1	0.89 E6
5	-	-	+	-	+	+	+	2	0.29 E6
6	+	-	+	-	+	-	-	1	4.44 E6
7	-	+	+	-	-	+	-	1	0.89 E6
8	+	+	+	-	-	-	+	1	2.94 E6
9	-	-	-	+	+	+	-	1	0.89 E6
10	+	-	-	+	+	-	+	2	2.94 E6
11	-	+	-	+	-	+	+	1	0.29 E6
12	+	+	-	+	-	-	-	2	4.44 E6
13	-	-	+	+	-	-	+	1	2.94 E6
14	+	-	+	+	-	+	-	1	0.89 E6
15	-	+	+	+	+	-	-	2	4.44 E6
16	+	+	+	+	+	+	+	1	0.29 E6

DESCRIPTION OF VARIABLES

**A: Fatigue voltage. +=80%, -=70%
**B: Poling Voltage +=80%, -=neg(80%)
C: Aging (hrs). +=0, -=24
D: FE Material. +=0/60/40, -=0/20/80
E: Electrode Material. +=Pt/Pt, -=Pt/Pd
F: Frequency (Hz) +=200, -=1000
G: Time (sec). +=1444, -=4444
I: Number of times to run this experiment
* Temperature and humidity measured
** Variables A and B depend on D and E
0/60/40...Pt/Pt...Pr:10V....80%=8V.....70%=7V
0/60/40...Pt/Pd...Pr:7V.....80%=5.6V...70%=4.9V
0/20/80...Pt/Pt...Pr:5.....80%=4V.....70%=3.5V
0/20/80...Pt/Pd...Pr:3.5V...80%=2.8V...70%=2.45V

Figure 25. Design One: 2^{7-3}_{IV} (Two-Level Fractional Factorial of Resolution IV)

operating region was used as in design one. If design two produced the same statistically significant first-order coefficients as a parsimonious model fitted to design one, this would constitute further evidence that the screening process used in design one was appropriate. Second, a resolution V design allows first-order coefficients to be estimated free from aliasing with terms of less than fourth order, and second-order coefficients to be estimated free from aliasing with terms of less than third order. Pure quadratic terms could not be estimated with this model, but a resolution V model can be used as the basis for a composite model such as a CCD.

3.3 RSM Design Three: Central Composite Design (CCD). For reasons discussed in Chapter VI, the CCD shown in Figure 27 was adopted. The third design has 3 parameters, $n_c = 8$ cube data points, $n_s = 6$ star data points, and $n_o = 9$ center points. The rotatability condition requires $\alpha = 1.682$, but using this value of α requires $n_o = 9.3$. Since the number of center points must be integer (9 were used), both rotatability or orthogonality could not be achieved. Orthogonality was chosen as the more important criteria, particularly in light of potential autocorrelations. Near rotatability was still achieved with $\alpha = 1.668$.

The frequency range was changed significantly for the CCD. Instead of operating from 200 Hz to 1 kHz, the frequencies ranged from 1 kHz to 19 kHz. 1 kHz was chosen as the lower bound to allow comparisons with results from the two factorial designs.

RUN	A	B	C	D	E	F	Nbr Cycles
1	-	-	-	-	+	2	4.44 E6
2	+	-	-	-	-	1	4.44 E6
3	-	+	-	-	-	1	0.89 E6
4	+	+	-	-	+	2	0.89 E6
5	-	-	+	-	-	1	2.94 E6
6	+	-	+	-	+	1	2.94 E6
7	-	+	+	-	+	2	0.29 E6
8	+	+	+	-	-	1	0.29 E6
9	-	-	-	+	-	2	4.44 E6
10	+	-	-	+	+	1	4.44 E6
11	-	+	-	+	+	1	0.89 E6
12	+	+	-	+	-	1	0.89 E6
13	-	-	+	+	+	2	2.94 E6
14	+	-	+	+	-	1	2.94 E6
15	-	+	+	+	-	2	0.29 E6
16	+	+	+	+	+	1	0.29 E6

DESCRIPTION OF VARIABLES

**A: Fatigue voltage. + = 80%, - = 70%

B: Frequency (Hz) + = 200, - = 1000

C: Time (secs) + = 1444, - = 4444

D: FE Material. +=0/60/40, -=0/20/80

E: Electrode Material. +=Pt/Pt, -=Pt/Pd

F: Number of times to run this experiment

* Temperature and humidity measured

** Variable A depends on D and E

0/60/40...Pt/Pt...Pr:10V....80%=8V.....70%=7V

0/60/40...Pt/Pd...Pr:7V.....80%=5.6V...70%=4.9V

0/20/80...Pt/Pt...Pr:5.....80%=4V.....70%=3.5V

0/20/80...Pt/Pd...Pr:3.5V...80%=2.8V...70%=2.45V

Figure 26. Design Two - 2^{5-1}_{V} (Two-Level Fractional Factorial of Resolution V)

RUN	VLT	TIM	FREQ	V*T	V*F	T*F	V*T*	Nbr Cycles
1	-1	-1	-1	1	1	1	-1	6.65 E6
2	1	-1	-1	-1	-1	1	1	6.65 E6
3	-1	1	-1	-1	1	-1	1	20.5 E6
4	1	1	-1	1	-1	-1	-1	20.5 E6
5	-1	-1	1	1	-1	-1	1	22.2 E6
6	1	-1	1	-1	1	-1	-1	22.2 E6
7	-1	1	1	-1	-1	1	-1	68.4 E6
8	1	1	1	1	1	1	1	68.4 E6
9	0	0	0					29.4 E6
10	0	0	0					29.4 E6
11	0	0	0					29.4 E6
12	0	0	0					29.4 E6
13	0	0	0					29.4 E6
14	0	0	0					29.4 E6
15	0	0	0					29.4 E6
16	0	0	0					29.4 E6
17	0	0	0					29.4 E6
18	1.668	0	0					29.4 E6
19	-1.668	0	0					29.4 E6
20	0	1.668	0					54.4 E6
21	0	-1.668	0					4.42 E6
22	0	0	1.668					55.9 E6
23	0	0	-1.668					2.94 E6

VLT: -1.668=3.33V, -1=3.5V, 0=3.75V, 1=4.0V, 1.668=4.167V
TIM: -1.668=442, -1=1444, 0=2944, 1=4444, 1.668=5446
FREQ: -1.668=1000, -1=4604, 0=10000, 1=15396, 1.668=19000

Figure 27. Design Three - Central Composite Design (CCD)

The upper bound of 19 kHz allowed the center of the frequency range to occur at 10 kHz, thereby simplifying several calculations.

0/20/80 Pt/Pt was selected as the material to use in the CCD. Its $V_{100\%}$ approximates the maximum voltages experienced in a typical semiconductor environment, and the devices did not fail as frequently as 0/20/80 Pt/Pd. By reducing parameters to voltage, frequency, and time all main effects, two-factor interactions, and three-factor interactions could be estimated free of aliasing with higher-order terms. This estimation could be performed using only the cube points of the CCD. The star and axial points allow the estimation of pure quadratic terms.

4 Summary

This chapter presented the two material and two electrode combinations which formed the four FE samples used to examine FE fatigue rate. For each of the four samples, $V_{100\%}$ was determined in a preliminary study so that a relative voltage scheme could be used to evaluate the four samples at equal relative applied voltages. Finally, a sequence of three RSM designs described the parameter settings to be used in the experiments.

VI. Analysis of Experimental Results

1 Introduction

Chapter five discussed the three distinct data collection phases, one phase for each Response Surface Methodology (RSM) design. This chapter presents and analyzes the results of the experiments for each of these designs. At the end of the chapter, three anomalous results are reported. Further research is needed to determine if these anomalies affected the findings made during this research.

Throughout the three RSM design phases, additional tests were performed to secure replicant data, investigate possible outliers, and develop data for testing the prediction capabilities of proposed empirical models. After completing each of the three phases, various statistical tests were performed to determine if a sufficient empirical model could be proposed. A 0.05 level of significance was applied to all statistical tests in this research.

The coefficients for each model were calculated by several different commercial software packages using least-squares regression techniques: SAS, Statistix 3.5, and MathCAD 3.0. Various tests, such as the Durbin-Watson test for autocorrelation and the Kolmogorov test for normality were performed to analyze the data. SAS and Statistix 3.5 were used to determine parsimonious models because of their data manipulation characteristics. Appendix B contains a sample MathCAD template

which was used to perform calculations for the Central Composite Design (CCD) used in this study. Similar templates were used to analyze the two-level factorial designs. The MathCAD templates include the lack of fit test.

2 RSM Design One: Estimates Main Effects

The primary purpose of this design was to determine which, if any, of the seven original variables did not have statistical significance when constructing a model for DP. The values of DP and DPr for each experimental run are given in Tables IV - VII. The tables are broken down by material/electrode combination so that each sample can be studied separately. The variable settings corresponding to the run numbers are listed in Figure 25 of Chapter V.

Table IV. 0/60/40 Pt/Pt

Run	DP	DPr	DPr - DP
9	18.240 19.310	19.577 20.065	1.337 0.775
10	23.410	25.680	2.207
15	19.480 18.830	16.980 20.210	-2.500 1.380
16	20.880	23.550	2.670

As explained in Chapter III, the difference between DP and DPr is caused by parasitic capacitance. Examining Table VII reveals that the difference between DP and DPr of 0/20/80 Pt/Pd sometimes approaches the same magnitude as the value of DP. In

Table V. 0/60/40 Pt/Pd

Run	DP	DPr	DPr - DP
11	14.910	16.891	1.981
12	12.910	15.330	2.420
13	11.790 10.260	13.439 11.418	1.649 1.158
14	14.290	16.062	1.772

Table VI. 0/20/80 Pt/Pt

Run	DP	DPr	DPr - DP
3	7.120	7.438	0.318
4	6.920 7.210	7.643 8.074	0.723 0.864
5	9.080	9.309	0.229
6	4.300	4.497	0.197

Table VII. 0/20/80 Pt/Pd

Run	DP	DPr	DPr - DP
1	1.960 1.441	2.940 2.162	0.98 0.721
2	3.800	7.440	3.64
7	2.277 1.504	3.633 3.056	1.356 1.552
8	4.210	7.491	3.281

Tables IV, V, and VI no instances occur where the difference between DP and DPr approaches the value of DP. Furthermore, the differences measured for runs 2 and 8 in Table VII, 0/20/80

Pt/Pd, are larger than the difference between DP and DPr measured for any other sample. Had the DPr - DP values for 0/20/80 Pt/Pd been comparable to those of the other samples, then experimental technique might have been suspected as the source of the difference between DP and DPr. Instead, the data points to some intrinsic difference in the characteristic response of 0/20/80 Pt/Pd. The specific reason for the different behavior of 0/20/80 Pt/Pd is not known, and time did not permit further research into this area. Possible explanations include a material/electrode interaction, manufacturing technique, or an incorrectly estimated value of $V_{100\%}$ for this sample.

2.1 Analysis of Main Effects. An Analysis of Variance (ANOVA) table indicated that, for a p-value of 0.05, only the material and electrode were statistically significant when all seven parameters were included in the model for DP, as seen in Table VIII. The model for DPr indicated that time, material, and electrode were statistically significant at the 0.025 level when all seven variables were included. However, when the model for DPr was fitted using only time, material, and electrode, the level of significance for time dropped to 0.046. This three-parameter model for DPr failed the lack of fit test.

At the conclusion of this section of analysis, it was decided to defer further model fitting to DPr due to time constraints.

2.2 Developing a Parsimonious Model. A software program determined that the best subset of parameters for developing an

Table VIII. Key Statistical Terms for Seven Parameter Model of DP

	significant	coefficient	p-value
intercept	Y	10.9	*
$volt_{applied}$	N	.31	.44
$volt_{poling}$	N	.29	.47
aging (hrs)	N	.43	.30
material	Y	5.9	.00
electrode	Y	2.9	.00
frequency (Hz)	N	.33	.39
time (secs)	N	.76	.07
Sum Squares Model	999.8	*	*
Sum Squares Total	1056.5	*	*
F-test (H_o:coeff = 0)	Y F^*=50.53	F(.95;7,13) 2.83	.00
Autocorrelation (Durbin-Watson)	N	1.9040	*
Error Terms Normal (Wilke-Shapiro)	Y	0.9751	*
Does the model fit (H_o: Model fits)	N F^* = 12.2	F(.95;8,6) 4.15	*

empirical model would include applied fatigue voltage, time, material, and electrode. Frequency was included in the proposed model in order to investigate possible frequency and time

interactions. Previous research has suggested that the fatigue rate may be based on the log of the number of cycles of voltage applied to a particular FE device. Multiplying frequency by time provides a total number of cycles. A lack of fit test for the five parameter model still indicated that the proposed empirical model did not fit the response being measured (Table IX).

Table IX. Five Parameter Linear Model for DP

	significant	coefficient	p-value
intercept	Y	10.8	*
$volt_{applied}$	N	.41	.29
material	Y	5.9	.00
electrode	Y	2.9	.00
frequency (Hz)	N	.42	.27
time (secs)	N	.64	.10
Sum Squares Model	1021.6	*	*
Sum Squares Total	1066.4	*	*
F-test (H_o: coeff = 0)	Y $F^* = 73.01$	F(.95;5,16) 2.54	.00
Error Terms Normal (Wilke-Shapiro)	Y		*
Does the model fit (H_o: Model fits)	N $F^* = 10.5$	F(.95;10,6) 4.06	*

To demonstrate that the proposed five-parameter model did not fit the true response, an assumption was made that the linear model did fit the data. Based on this assumption a gradient search could be conducted and the actual test responses compared

with the predicted response. The gradient search increased along the frequency, time, and voltage axes.

The coefficients of the proposed model implied that DP would increase with increased voltage and decrease with increased frequency and increased time parameters (the coefficients for frequency and time in Table IX are switched in sign due to the initial structure of the factorial design). The frequency axis varied from 1 kHz to 2.5 kHz, the time axis from 4444 seconds to 13932 seconds, and the voltage axis from $V_{80\%}$ to $V_{98\%}$. For each of the four samples, at least two measurements were taken along the gradient within the ranges given. For all samples, the proposed linear model underestimated the observed experimental values. In fact, the proposed model actually indicated that DP should be negative for 0/20/80 Pt/Pd at a point where the observed value was greater than $4\mu C/cm^2$.

2.3 Other Analysis. Since a linear model was not adequate, an attempt to model interaction terms with the available data appeared appropriate. An initial premise was made that the poling voltage and aging could be removed as parameters based on analysis to this point. By removing these columns from the matrix, however, the property of orthogonality was lost so that not all two-factor interactions could be estimated without aliasing.

The main effect parameters left in the model were applied voltage (hereafter referred to simply as voltage), material, electrode, frequency, and time. The two-factor interactions are:

voltage*time (VT); voltage*frequency (VF); voltage*material (VM); voltage*electrode (VE); time*frequency (TF); time*material (TM); time*electrode (TE); material*frequency (MF); material*electrode (ME); electrode*frequency (EF).

When an attempt was made to fit all 5 main effects and all 10 two-factor interactions, 3 of the two-factor interactions were dropped from the model, by both Statistix 3.5 and SAS, because of high correlations with other two-factor interactions. The software packages drop the second variable if two variables are highly correlated. For instance, if the proposed model was DP = VT + EF, EF would be dropped from the model if it was highly correlated with VT. If the proposed model was written DP = EF + VT, then VT would be dropped.

A regression model including voltage, material, electrode, time, and VT was proposed based on a best subset regression analysis. This model suffered from two specific deficiencies. A normal probability plot of the residuals appeared to contain outliers and the lack of fit test failed. The results are presented in Table X.

2.4 Summary of RSM Design One. Within the ranges allowed for this screening design, it was determined that aging and the poling voltage had no statistically significant effect in determining DP. Therefore, these two parameters were eliminated from consideration in future models. A decision was also made to stop fitting models for DPr, due to time constraints. Attempts

Table X. Five Parameter Model for DP with Two-Factor Interaction Term VT

	significant	coefficient	p-value
intercept	Y	10.8	*
volt	N	.59	.07
material	Y	5.8	.00
electrode	Y	2.9	.00
time	Y	.76	.03
VT	Y	.92	.01
Sum Squares Model	1035.5	*	*
Sum Squares Total	1066.4	*	*
Miscellaneous	C_p = 6.8	R^2 = .971	*
F-test (H_o:coeff = 0)	Y F^* = 107.45	F(.95;5,16) 2.85	.00
Error Terms Normal (Wilke-Shapiro)	Maybe	0.9376	*
Does the model fit (H_o: Model fits)	N F^* = 7.02	F(.95;10,6) 4.06	*

to fit first-order linear models for DP failed, as did an attempt to fit a model with the interaction term VT.

2.5 Interim Findings. The most significant effects in the first-order RSM design were the material and electrode, as determined by the individual sum of squares. The sum of squares values were not presented since this model failed the lack of fit test.

3 RSM Design Two: Main Effects and Two-Factor Interactions

Analysis directed towards investigating two-factor interactions using RSM Design Two produced several models which

passed the lack of fit test for predicting DP. DP and DPr values observed in the experiments of Design Two are again presented in separate tables for each sample as seen in Tables XI - XIV. Although models for DPr were not fitted, the value of DPr was used as a flag for identifying devices in which the difference between DP and DPr was noticeably different from other devices.

Table XI. 0/60/40 Pt/Pt

Run	DP	DPr	DPr - DP
10	26.678 29.547	14.344 34.137	-12.334 4.59
11	17.499	18.624	1.125
13	20.036	21.103	1.067
16	18.335	20.122	1.787

Table XII. 0/60/40 Pt/Pd

Run	DP	DPr	DPr - DP
9	9.542	10.754	1.212
12	13.463 14.703	15.049 16.028	1.586 1.955
14	13.348	14.847	1.499
15	13.693 12.886	15.394 14.213	1.701 1.327

An initial examination of the Tables XI - XIV indicates, as for RSM Design One, that the difference between DP and DPr appears to be the largest for 0/20/80 Pt/Pd, except for run 10 in Table XI. For 0/20/80 Pt/Pd, the value of DPr - DP ranged from

Table XIII. 0/20/80 Pt/Pt

Run	DP	DPr	DPr - DP
1	5.996 6.400	6.198 6.602	0.202 0.202
4	7.582	8.390	0.808
6	6.976	7.755	0.779
7	8.418	8.764	0.346

Table XIV. 0/20/80 Pt/Pd

Run	DP	DPr	DPr - DP
2	3.373	5.679	2.306
3	2.854 2.220	4.497 3.949	1.643 1.729
5	2.653 2.652	3.979 4.929	1.326 2.277
8	5.218	9.802	4.584

approximately 50% to 90% of the value of DP. In the worst case for the other samples, the value of DPr - DP was only 46% of the value of DP. That value occurred for run 10 of Table XI when the difference between DPr and DP equalled -12.334. If that value is considered to be an outlier, then the value of DP - DPr was never more than (4.59/29.547) * 100% = 16% of the value of DP, also found in Table XI for run 10. For the other samples the value of DPr - DP was always less than 15% of the value of DP. Again, the interpretation of these results is beyond the scope of this study.

Replicant experiments were performed for run 8 of Table XIV and run 10 of Table XI. The results are given in Table XV. The results indicate that the first measurement for DPr on run 10 may have been in error, but the measurement for DP on both runs 8 and 10 appears to have been correct.

Table XV. Additional Data Points: Checking for Outliers and Incorrect Measurements

Material	Electrode	Run	DP	DPr
0/20/80	Pt/Pd	8B	4.901	10.379
0/60/40	Pt/Pd	10C	28.686	31.555

3.1 Determination of Main Effects and Two-Factor Interactions. An attempt was made to fit a model to DP using only the main effects, but this test failed the lack of fit criteria. The next step was fitting a model which included all main effects and two-factor interaction terms, as seen in Table XVI. This model fit exactly because there were sixteen parameters and sixteen parameter settings. Not only did an exact fit involve too many variables, but a scatter plot of the standardized residual indicated curvature in the true model was not being detected by the proposed model.

3.2 Developing a Parsimonious Model. Therefore, a best subset regression analysis was run and the process of selecting a parsimonious model which fit the data began. The first six parameters to enter the model were voltage, material, electrode, VT, EF, and ME. Mallow's CP criteria at this point was 54.7,

Table XVI. Key Statistical Terms for 15 Parameter Model of DP

	significant	coefficient	p-value
intercept	Y	11.07	*
voltage	Y	1.05	.00
time (secs)	N	-.41	.86
frequency (Hz)	N	-.20	.38
material	Y	5.71	.00
electrode	Y	3.07	.00
VT	Y	-1.12	.00
VP	Y	-.62	.028
VM	Y	.64	.026
VE	N	.053	.81
TP	N	.49	.07
TM	N	-.49	.06
TE	Y	-.66	.022
MF	Y	-.77	.01
EF	Y	-.98	.00
ME	Y	1.15	.00
Sum Squares Model	1255.2	*	*
Sum Squares Total	1260.7	*	*
Miscellaneous	C_p = 16.0	R^2 = .996	*
F-test (H_o:coeff = 0)	Y F^* = 91.41	F(.95;15,6) 3.94	.00
Autocorrelation (Durbin-Watson)	N	2.9926	*
Error Terms Normal (Wilke-Shapiro)	N	resid=.78 stderr=.88	*
Does the model fit (H_o: Model fits)	N/A	*	*

whereas one would expect a good model to have a value of around 6, that being the number of parameters in the full model. Despite the high CP, value the model was evaluated for fit. When the model failed to fit the observed response DP, the next variable which would have entered the model, MF, was allowed to enter the model and a lack of fit test performed. Again the model failed to fit and the next entering variable was TE. At this point, the model indicated a good fit with eight parameters. The best subset regression model also indicated that if TE did not enter the model, then VM or TP were the next best candidates. Models using these parameters,instead of TE, were proposed but did not pass the lack of fit test. Table XVII presents the sequence of tests for fit of a particular model. Table XVIII presents a summary of the statistical tests performed with an eight parameter model using TE as the last parameter to enter the model. The equation for the model is given by.

$$DP = 11.192 + 1.1*volt + 5.8*material + 3.2*electrode - 1.2*VT - 0.8*TE - 1.1*EF + 1.3*ME - 0.9*MF$$

Next, observations of DP at points within the operating region, but at different points than the RSM design parameter settings, were compared with predicted values at the new observation points. Predicted values were within 15% of the observed value for each sample, although only one measurement was taken for each sample. Next data collected at points outside the operating region, in the direction of increasing voltage, frequency, and time, was compared with the models predictions.

Table XVII. Sequence of Lack of Fit Tests

variables in model (cumulative)	(H_o: Model Fits)	F^*	$F(1 - \alpha)$
volt material electrode VT, EF, ME	N	6.3	F(.95;9,6) 4.10
PM	N	5.19	F(.95;8,6) 4.21
TE	Y	3.95	F(.95;7,6) 4.21
VM instead of TE	N	4.81	4.21
TF instead of TE	N	4.86	4.21

These predictions region consistently underestimated the observed value as seen in Table XIX, indicating that the rate of fatigue had curvature greater than that predicted past the upper bound of the operating region.

3.3 Other Analysis. Since the data in phase one was collected in the same operating region as phase two, analysis on a combined data set was attempted. A comparison was made of the response, DP, for a given sample, at equivalent voltage, frequency, and time settings. The comparison test checked whether one set of observations consistently displayed higher values than the other data set. No such trend developed, and a mean value (μ) for each set of observations was computed. Using the data in Appendix A, Tables XXVII - XXX, approximate standard

Table XVIII. Key Statistical Terms for Eight Parameter Model

	significant	coefficient	p-value
intercept	Y	11.19	*
volt	Y	1.13	.006
material	Y	5.75	.000
electrode	Y	3.18	.000
VT	Y	-1.19	.004
TE	Y	-.78	.037
PE	Y	1.28	.002
PM	Y	-.88	.022
Sum Squares Model	1229.9	*	*
Sum Squares Total	1260.7	*	*
Miscellaneous	C_p = 29.6	R^2 = .976	
F-test (H_o:coeff = 0)	N F^* = 64.92	F(.95;8,13) 2.77	.000
Error Terms Normal (Wilke-Shapiro)	possible curvature	resid=.842 stdres=.837	*

deviations (σ) were interpolated for each sample at $V_{70\%}$ and $V_{80\%}$. Each set of data points was then checked and all observations fell within 3σ of μ.

By combining data sets, it is possible to look at more combinations of voltage, frequency, and time parameter settings for each sample. For a single RSM design data set, there exist only four combinations of voltage, frequency, and time per sample. The combined data set provides six combinations per sample. Table XX contains the results of combining the data sets. A regression analysis was performed, but the results were not significant relative to prior results.

Table XIX. Predictor Points for Eight Factor Model

	Predicted	Observed
0/60/40 Pt/Pt Center Point	21.4	20.2
0/60/40 Pt/Pd Center Point	12.5	12.5
0/20/80 Pt/Pt Center Point	7.3	7.3
0/20/80 Pt/Pd Center Point	3.5	4.0
0/60/40 Pt/Pt 1 radius from edge	6.2	21.5
0/60/40 Pt/Pd 1 radius from edge	11.2	14.0
0/20/80 Pt/Pt 1 radius from edge	-1.2	3.43
0/60/40 Pt/Pt 3 radii from edge	-12.1	10.6

3.4 Graphical Analysis: Design One and Two Data Combined.

The next step was to examine the difference in response between two samples when the parameter settings for voltage, time, and frequency were equal. For each combination of samples, a plot of the differences in response was plotted in Figures 29 - 34, with Figure 28 providing the axis orientation. The analysis of these plots was confined to simple inferences based on the change in DP when moving along an edge of the cube parallel to one of the axes. Values at the center point (CP) were also evaluated.

Examining Figure 31, several comparisons can be made about the relative behavior of 0/60/40 Pt/Pt (60/Pt) and 0/20/80 Pt/Pd

Table XX. Combined Data Sets
A: 0/60/40 Pt/Pt B: 0/60/40 Pt/Pd
C: 0/20/80 Pt/Pt D: 0/20/80 Pt/Pd
(* indicates no observation at that point)

volt	freq	time	A	B	C	D
-1	-1	-1	19.2	9.5	6.0	1.7
-1	-1	1	20.0	11.0	7.1	2.7
-1	1	-1	18.4	*	*	2.1
-1	1	1	*	14.1	8.8	*
1	-1	-1	28.3	12.9	4.3	3.4
1	-1	1	23.4	13.3	7.0	4.2
1	1	-1	*	14.2	7.3	*
1	1	1	19.5	*	*	4.5

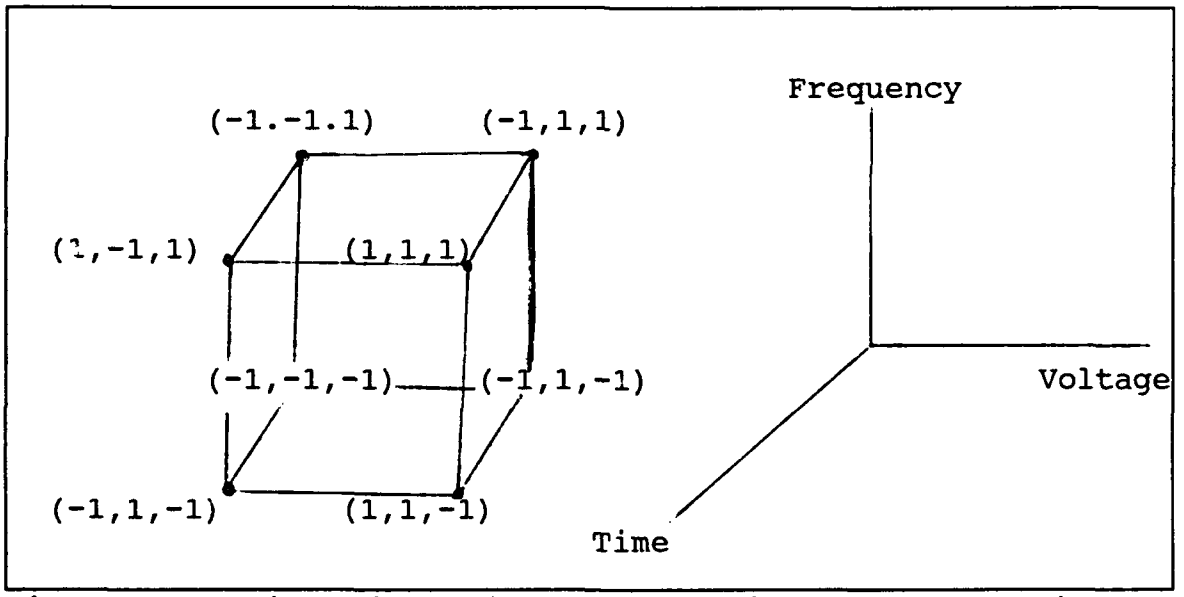

Figure 28. Axis Orientation and Coordinates of Cube in the Volt, Frequency, Time Domain

(20/Pd). It appears that the difference in DP increases when moving from $V_{70\%}$ to $V_{80\%}$. This may indicate that, time and frequency being equal, sample 20/Pd will show a higher decay rate

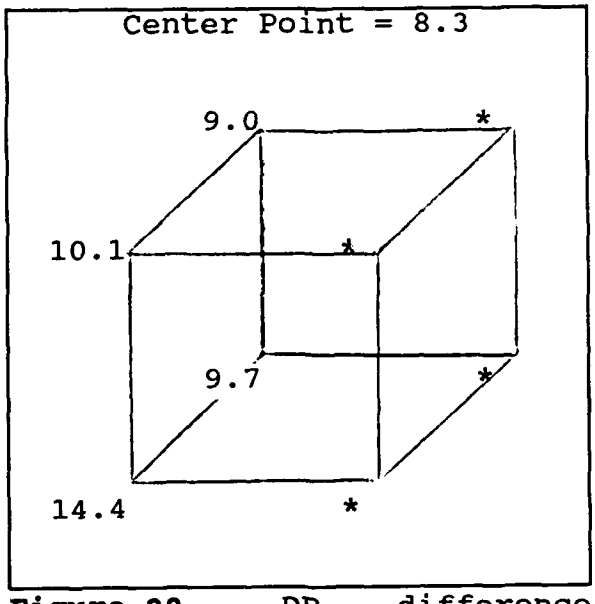

Figure 29. DP difference 0/60/40 Pt/Pt and 0/60/40 Pt/Pd (* indicates no observation)

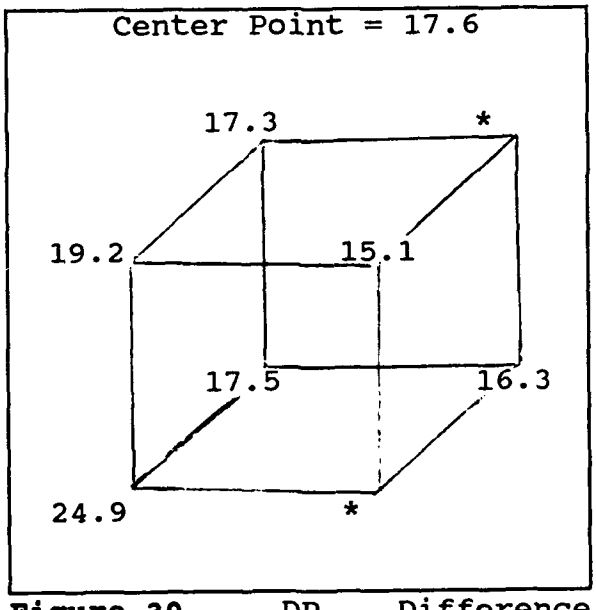

Figure 30. DP Difference 0/60/40 Pt/Pt and 0/20/80 Pt/Pd (* indicates no observation)

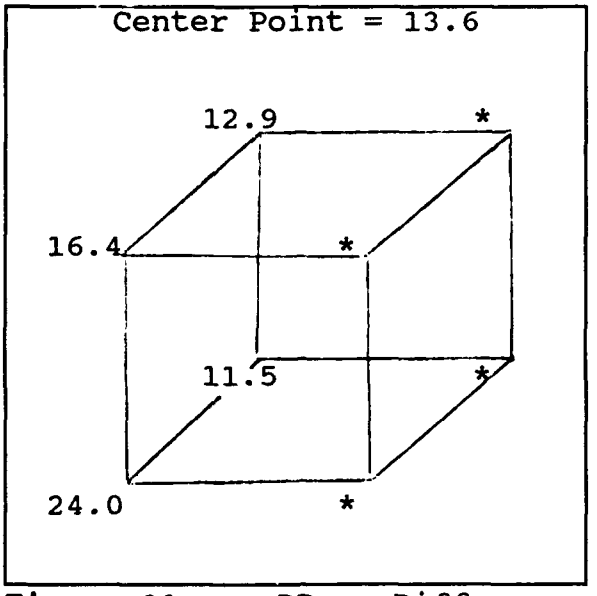

Figure 31. DP Difference 0/60/40 Pt/Pt and 0/20/80 Pt/Pt (* indicates no observation)

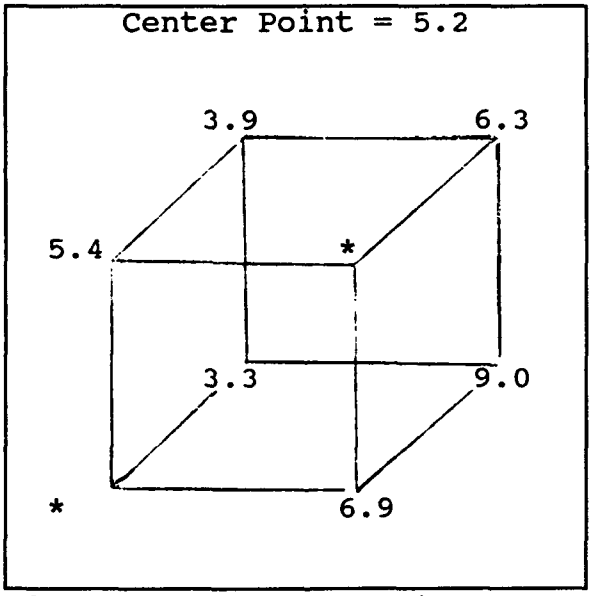

Figure 32. DP Difference 0/60/40 Pt/Pd and 0/20/80 Pt/Pt (* indicates no observation)

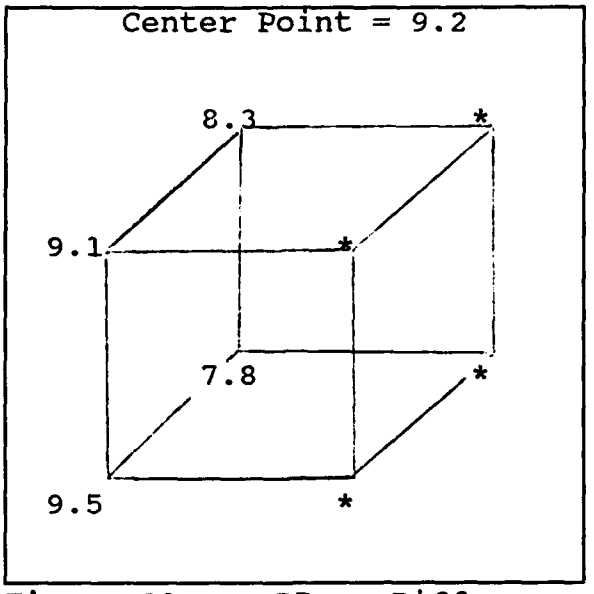

Figure 33. DP Difference 0/60/40 Pt/Pd and 0/20/80 Pt/Pd (* indicates no observation)

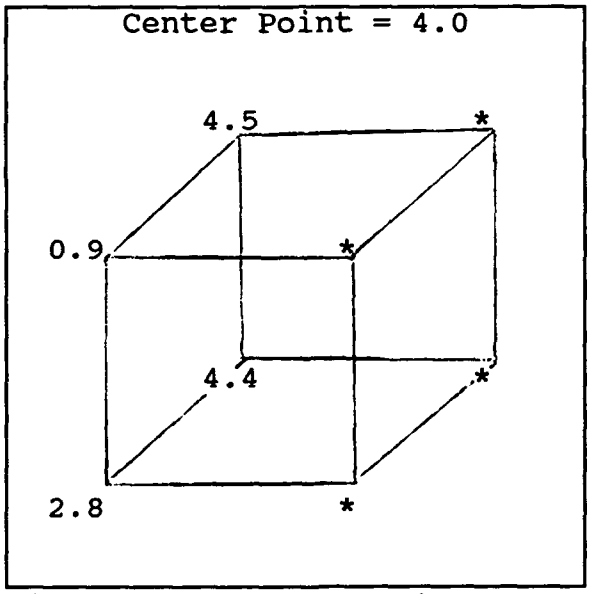

Figure 34. DP Difference 0/20/80 Pt/Pt and 0/20/80 Pt/Pt (* indicates no observation)

than 60/Pt, in the absolute sense of DP, as the operating voltage approaches $V_{80\%}$. There may be an indication that sample 60/Pt decays faster than 20/Pd as time increases, but this is difficult

to ascertain. Neither of these observations appears to be linear in nature since the absolute difference in DP, along the increasing voltage axis, decreases as time is increased. Similar observations exist when comparing sample 60/Pt with either 0/60/40 Pt/Pd (60/Pd) or 0/20/80 Pt/Pt (20/Pt), (Figures 29 and 30, respectively) except that the difference in absolute values along the time axis is pronounced.

Comparing 60/Pd with 20/Pt (Figure 32) suggests that the absolute difference in DP increases as frequency is increased. This implies that 20/Pt decays faster than 60/Pd when operating at higher frequencies. Returning to Figure 31, sample 60/Pt appears to decay faster than sample 20/Pd at higher operating frequencies. Any assessment of the linearity of these decay rates is fraught with speculation, but the changes do not appear to be linear in nature.

The (60/Pt, 20/Pd) and (60/Pd, 20/Pt) pairings are bilaterally symmetric, that is, each pairing contains both materials and both electrodes. The bilateral symmetry suggests that the change in DP, as a result of changes in frequency, can be interpreted as two competing effects. One of the effects, say electrode type, causes the difference in DP between two samples to decrease at a greater rate for a higher frequency. The other effect, in this case the material type, competes by causing the difference in DP to increase at a greater rate for a higher frequency. The data presented in the figures does not allow a

simple determination of how DP is affected by the proposed frequency*electrode and frequency*material interactions.

From this simple analysis of the samples it appears that similar mechanisms are operating among all four samples. These mechanisms appear to be nonlinear, and careful study of the figures above suggested interactions which might account for the rates of change of the difference in DP for different samples at the same parameter settings. Examination of the values of the center points with respect to the cube points in the figures above indicates no curvature in the FE response. The observations made in this section support the earlier regression analysis by confirming the nature of the interactions.

3.5 Summary of Phase Two. Although an exact model was fitted to DP, this model involved too many terms, several of which were statistically insignificant (time, frequency, VE, TF, TM) at the .05 level of significance. A parsimonious model with eight terms was then fitted (voltage, material, electrode, VT, TE, EF, ME, MF), but the error terms exhibited some nonnormality for this model. Either the empirical model or the anomalous behavior of 0/60/40 Pt/Pt (explained in a later section) may have been the source of the curvature in the error terms.

Within the operating region, the parsimonious model of eight terms displays excellent predictive powers. Outside the operating region the model loses its utility for predicting the value of DP. As the voltage, time, and frequency parameters were increased, DP was underestimated by the model.

3.6 Interim Findings.

• The type of FE material and the electrode type are the most significant factors for determining the value of DP when examining different FE samples.

• The most statistically significant interaction term is ME.

• Most research has indicated that fatigue is linear in the log of cycles, but this design indicates that the number of cycles is not statistically significant in modeling DP.

• Two interim findings not found in the literature suggest that there is an interaction of the cycling frequency with both the FE material and the electrodes. This two-factor interaction could be confounded with the three-factor interaction frequency * material * electrode.

• The statistical significance of the first-order term in voltage may be the result of an implicit dependence of the relative voltages with respect to the material/electrode combination. This implicit dependence may also be the cause of the statistical significance of the two-factor interaction term between time and voltage.

• The statistical significance of the TE interaction does not appear to provide any insight, except the obvious conclusion that at a given time the value of DP for a specific FE with one electrode combination will be different than the same FE with a different electrode combination.

4 RSM Design Three: Central Composite Design (CCD)

The CCD used sample 0/20/80 Pt/Pt for all experiments. The variables included in the design were voltage, time, and frequency. By eliminating material and electrode type as parameters it was possible to develop a model for one sample.

4.1 Graphical Analysis. The 3-D design of Figure 35 allows relatively simple analysis. For instance, movement along the voltage axis (time and frequency at "0", their centerpoint values) appears to indicate that DP will have a lower value for a higher voltage, other factors being held constant within the operating region. Similar comparisons can be made by moving along the edges of the cube parallel to the voltage axis, suggesting that no significant interactions occur with frequency or time.

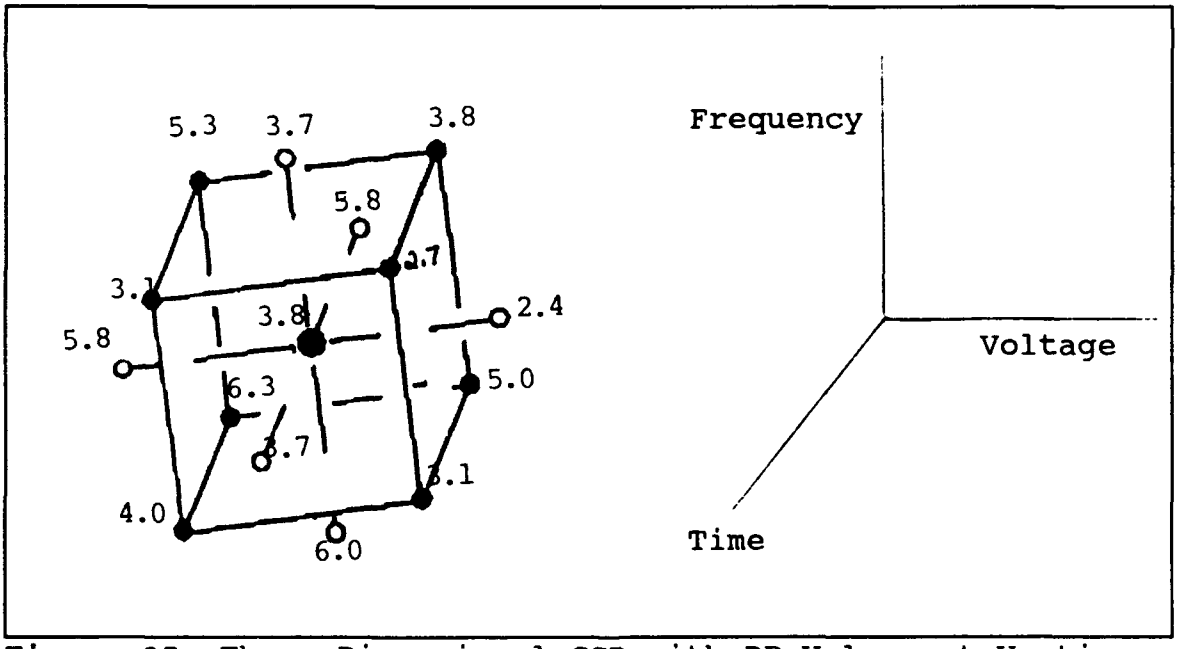

Figure 35. Three-Dimensional CCD with DP Values at Vertices

This simple analysis brought into question the values for runs 4, 8, 20 and 22. Run 4's value was either lower than

expected or run 8 was slightly higher than expected. Runs 20 and 22 both appeared to have larger values than expected. As a result of this simple analysis, further data was collected at the same parameter settings as originally used in runs 4, 8, 20, and 22. For runs 4, 8, and 22 the extra data appeared to confirm the visual impression gained through examining Figure 35. As a result the values used for modeling the above runs are the mean of the data measurements taken. The new data points and the mean value used during modeling are given in Table XXI.

Table XXI. Additional Data Points for Runs 4, 8, 20, 22

Run	New Data Points	Mean
4	3.287, 3.142	3.075
8	2.854	2.782
20	3.748	3.705
22	3.085, 3.229	3.344

4.2 Determination of Main, Two-Factor and Quadratic Effects.

The initial model contained three main effects, three two-factor interactions (VT, VF, TF), three pure quadratics, and the three-factor interaction term volt*frequency*time (VFT). From the initial testing it was determined that none of the two-factor interactions were statistically significant as shown in Table XXI. VT was highly significant in the factorial model for estimating two-factor interactions. This suggests, since time was sample independent, that the effect of the applied voltage (V_x) is linked very strongly to the differences between samples.

Therefore, the interaction term VT in the factorial model can be viewed simply as a function of the material and electrode interaction. VFT and the quadratic term volts^2 were also not statistically significant. Extensive testing was not performed on the full proposed model as development of a parsimonious model seemed more useful.

Table XXII. Key Statistical Terms for CCD Model One

	significant	coefficient	p-value
intercept	Y	3.8	*
volt	Y	-.98	.000
time (secs)	Y	-.56	.000
frequency	Y	-.57	.000
volt^2	N	-.018	.84
time^2	Y	.26	.013
frequency^2	Y	.23	.024
volt*time	N	.18	.17
volt*frequency	N	.12	.36
time*frequency	N	.046	.71
volt*time*freq	N	.097	.45
Sum Squares Model	23.9	*	*
Sum Squares Total	25.4	*	*
F-test (H_o:coeff = 0)	Y F^* = 19.36	F(.95;10,12) 2.75	.00
Error Terms Normal ((Wilke-Shapiro)	Y	.9839	*

4.3 Developing a Parsimonious Model. Best subset regression analysis indicated that voltage, time, frequency, time^2, and

frequency^2 all belonged in the model. Attempts were made to fit this model using only linear terms, or deleting one of the pure quadratics, but these attempts failed to pass the lack of fit test. Also, the model with first-order terms underestimated the values for the center points and overestimated the values for the axial points, good indicators of curvature in a model. Table XXII provides the pertinent data for a proposed quadratic model of DP with three first-order terms and two quadratic terms. The equation for the proposed model is:

$$DP = 3.83 - 1.01*volt - 0.59*time - 0.51*frequency + 0.23*time^2 + 0.28*frequency^2$$

4.4 Other Analysis. Insufficient amounts of data existed for thoroughly testing the predictive power of the parsimonious second-order model developed. Sources of test data included runs 1, 4, 6, and 7 from the previous two factorial designs. Some of these data points were taken near the boundary of the CCD operating region, and some outside that region. Two of the data points used to test the predictive power of the 8 parameter model developed in Phase Two were also available. Unfortunately, none of this data contained parameter settings which fell entirely within the operating region of the CCD. Very little information can be gleaned from those results, but the data is provided in Table XXIII.

4.5 Overview of Phase Three. A parsimonious model was developed from the CCD using two quadratic terms and three linear terms. The development of this model was enhanced by indications

Table XXIII. Key Statistical Terms for Parsimonious CCD Model

	significant	coefficient	p-value
intercept	Y	3.8	*
volt	Y	-.98	.000
time (secs)	Y	-.56	.000
frequency (Hz)	Y	-.57	.000
frequency^2	Y	.23	.016
time^2	Y	.26	.008
Sum Squares Model	23.5	*	*
Sum Squares Total	25.4	*	*
Miscellaneous	C_p = 4.7	R^2 = .923	*
F-test (H_o:coeff = 0)	Y F^* = 40.81	(F.95;5,17) 2.81	.000
Autocorrelation (Durbin-Watson)	N	1.7045	*
Error Terms Normal	Y	.9547	*
Does the model fit (H_o: Model fits)	Y F^* = 3.18	F(.95;9,8) 3.39	*

in Figure 35 that several of the data points had observed values different from those expected. Continued analysis of this figure (assuming only one factor at a time changes) indicated that DP decreased more rapidly with higher voltages, DP decreased faster with higher frequencies, and the longer the period of time a device was tested the lower the value of DP. Since the model included quadratic terms which tend to increase DP with increasing frequency and time, this indicates that some curvature in the response surface exists. Over the operating region, these quadratic terms sufficiently accounted for this curvature.

Table XXIV. Parsimonious CCD Prediction Data

Volt	Frequency	Time	Predicted	95% Interval	Actual
-1	-1.668	1	6.1	5.2, 7.0	8.4
1	-1.668	-1	5.3	4.3, 6.2	7.6
1	-1.816	1	4.4	3.4, 5.4	7.0
-1	-1.816	-1	7.4	6.4, 8.4	6.0
1.84	-1.601	2.9	4.1	2.3, 6.0	3.4
3.68	-1.461	5.86	7.18	.08, 13.5	1.7
0	-1.779	0	5.58	4.6, 6.5	7.3

4.6 Interim Findings.

• The interaction term VT was not statistically significant in the models developed from the CCD. This datum supports the conjecture that the significance of the voltage terms in earlier models was the result of an implicit dependence upon the material/electrode combination.

• A model was fitted using first-order terms in time, voltage, and frequency which all caused to DP to decrease as their values increased. Quadratic terms in time and frequency caused DP to increase as their values increased, but at a slower rate than the rate of decrease of the linear terms. This appears to be a new model, but further research is required before this finding can be extended to other ferroelectrics.

5 Anomalous Results

Several experiments performed in the course of this study produced observations which could not be addressed within the

time available. The first errant observation was a temporary increase in DP for 0/60/40 Pt/Pt between approximately 44 and 1444 seconds of the FATIGUE test. The increase is visually significant, as seen in Figure 36, and all tests performed on sample 0/60/40 Pt/Pt occurred in this region of increasing DP. In Figure 36, the applied voltage was $V_{93.4\%}$, the frequency was approximately 2 kHz, and the duration of the experiment was 11,734 seconds (about 3 hours + 15 minutes).

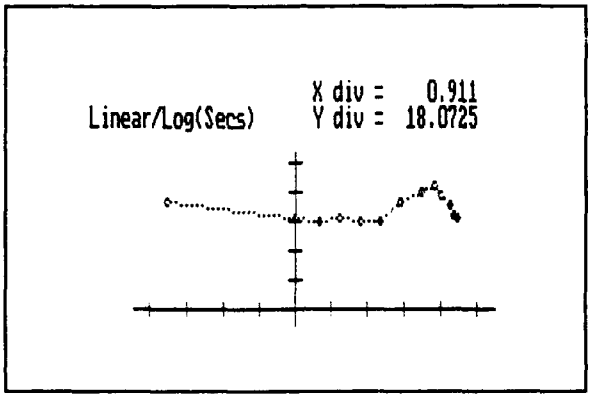

Figure 36. Anomalous DP Increase in 0/60/40 Pt/Pt

Table XXV. Sample Values of DP Relative to Duration of Test

time (secs)	DP
44	21.7
144	24.3
444	31.8
1444	27.0
2944	22.9
4444	18.4

The increase in DP has an apparent peak at 2944 seconds. The actual peak is unknown since measurements were only taken at 44, 144, 444, 1444, 2944, and 4444 seconds. By 4444 seconds the value of DP returns to a value approximately the same as that measured at 44 seconds. This peak is the center of the operating region for both factorial designs, therefore all analysis accomplished in those two designs may be influenced by this growth in DP for 0/60/40 Pt/Pt. Not all 0/60/40 Pt/Pt devices exhibited this behavior.

In six 0/60/40 Pt/Pt devices checked for increasing DP, voltage did not appear to affect the onset of a period of increasing DP. No analysis was performed to determine if voltage affected the peak value of DP achieved between 44 and 4444 seconds. No analysis was performed to determine how frequency affected the onset time of increasing DP values, nor how frequency affected the peak value.

Because none of the other samples displayed this behavior it is difficult to assess how this affected the factorial design modeling process. It is believed, however, that the earlier analyses still stand. The graphical analysis of the combined factorial data sets provided independent analysis supporting the significance of interaction terms in the final factorial model. Nor did the graphical analysis indicate curvature at the center points of the 3-D cubes. The primary reason for assuming that the DP growth pattern of 0/60/40 Pt/Pt did not affect the analysis is that the pattern began prior to, and ended close to

or after, the actual region of operations. Since RSM is predicated on fitting a model to local phenomena, the net result of DP growth was simply a phenomena to model locally.

The second anomalous result occurred in the polarization measurement P^r, defined in chapter III, Figure 15. P^r is used in calculating DPr, and in an ideal material, P^r should be zero. It was discovered that this value increased over time for 0/60/40, particularly with the Pt/Pt electrodes. For 0/20/80 the value of P^r decreased over time, indicating the material was, in a sense, approaching the characteristics of an ideal material. The change in P^r appears to have been primarily a material related phenomena, with the 0/60/40 Pt/Pt sample displaying less ideal characteristics over time. The data for P^r is not presented due to time constraints. This behavior may be tied somehow to the growth in DP discussed above.

The third anomalous result occurred while testing 0/20/80 Pt/Pd near $V_{100\%}$, at approximately 2.5 kHz, for a duration of 13932 seconds. Based on previous tests with increasing $V_{\%}$, frequency, and time it was expected that DP would have a value less than 3.0 $\mu C/cm^2$. The results of two tests, performed three weeks apart, were significantly higher than 3.0 $\mu C/cm^2$ as seen in Table XXVI. Insufficient resources did not allow this problem area to be examined. Potentially the source of these unexpected observations lies in an incorrect value of $V_{100\%}$. Since no other samples were tested at this value, it is impossible to conclude whether DP would have increased for all samples approaching $V_{100\%}$,

or if this behavior was peculiar to 0/20/80 Pt/Pd. If the estimated $V_{100\%}$ was established above the true $V_{100\%}$ for 0/20/80 Pt/Pd, the anomalous behavior occurred because the test was performed above the true $V_{100\%}$.

Table XXVI. DP Values for 0/20/80 Pt/Pd Approaching $V_{100\%}$

volt	time (secs)	frequency (Hz)	DP
75%	2944	600	3.4
80%	4444	1000	3.4
89%	9536	1750	2.6
98%	13932	2500	5.4

6 Summary

A sequence of three designs explored FE response to changes in parameters. All attempts at fitting first-order models of DP failed. In every case the linear model underestimated the actual FE response outside the operating region and overestimated the response at the center of the operating region. In the first factorial model, the variables for aging and poling voltage were determined to be insignificant within the operating region selected. Due to time constraints, it was not possible to extend the aging period beyond 24 hours. Once the decision was made to remove aging as a variable, there was no further need for a poling voltage.

The second factorial model produced an exact fit because there were sixteen parameters and sixteen parameter settings.

This model was ungainly, and a reduced model in eight parameters still had a good fit and good explanatory power. The key observation in this model was that all the interaction terms, in the parsimonious model, either explicitly or implicitly included material and electrode as part of the interaction. The two terms which did not explicitly include material or electrode, voltage and VT, are dependent upon the type of material and electrode. The absolute voltage applied to a device is a function of the relative voltage and the material/electrode combination.

Using 0/20/80 Pt/Pt, the CCD indicated that no interactions occur among the variables voltage, time, and frequency. Over the operating region of this design, DP operates in a linear fashion with respect to voltage. Although DP has linearly decreasing terms in time and frequency, there are quadratic terms which temper the rate of decrease. Outside the operating region these quadratic terms generate predictions which overestimate the observed values of DP. The fact that no VT interaction is statistically significant suggests that the previous assertions are correct regarding the implicit dependence of voltage on the sample material and electrode.

Several anomalous results were observed during data collection. The anomalous result most pertinent to the credibility of this analysis was the area where 0/60/40 Pt/Pt experienced growth in the value of DP. This bulge covered the entire operating range for the factorial experiments and probably affected the empirical models proposed to fit the observations.

This does not detract from the usefulness of the model-building process.

VII. Conclusions and Recommendations

1 Summary of Experimental Results

The first objective of this study was to examine how an initial poling voltage, aging, cycling voltage, frequency, time, ferroelectric (FE) material, and electrode material affected the fatigue rate of a ferroelectric sample. The second objective was to demonstrate the efficiency of using Response Surface Methodology (RSM) in FE studies. Five findings and six recommendations resulted from this study.

This study began by defining DP as the best measure of fatigue of a FE material. Using RSM, an iterative series of experimental designs was constructed to direct the data collection process. The conclusions and findings made in this study are valid within the operating region of the experimental designs.

The first design acted as a screening design and allowed the elimination of two variables (aging and initial poling voltage) from further modeling. This screen may have occurred because cycling a material rapidly eliminates aging effects, or because 24 hours was not enough aging time. The only purpose of the initial poling voltage was to establish an initial "0" or "1" device state, thereby making aging testable. The type of material and electrode combination were the most significant terms among the parameters remaining, but a statistically significant linear model which fit the observations could not be obtained.

The second design allowed two-factor interactions among the remaining five variables to be studied. At this point it appeared that the relationships among the four samples were nonlinear and that several interaction terms were significant. The degree of nonlinearity was difficult to ascertain since, for 0/60/40, the response DP appeared to exhibit extensive curvature within the operating region. The interaction terms reinforced the finding from the first design that the material and electrode type were the primary determinants of DP. A parsimonious model with eight terms was then fitted to the observed data. All the interaction parameters in the model included, either explicitly or implicitly, the type of material and electrodes. Plots of the error terms indicated that curvature in the proposed model was not accounted for, possibly indicating the need for quadratic terms. It is also possible that the localized curvature of the DP curves of 0/60/40 Pt/Pt, discussed under Anomalous Results in Chapter 6, may have accounted for this curvature.

The third design removed the ferroelectric material and electrode material as parameters in order to study interactions among voltage, frequency, and time using a central composite design (CCD). The tentative proposal was that the settings of voltage, time, and frequency might be affecting DP, but the effects were masked by the differences between the samples.

The CCD allowed the estimation of all main effects, two-factor interactions, the three-factor interaction, and all pure quadratics. Within the operating region, three interim findings

were made. First, no interaction terms were statistically significant. Second, DP decreased linearly with increases in voltage. Third, DP had linear decreasing terms in time and frequency, but quadratic terms in these parameters countered the decrease to some extent (DP still decreased, but not as fast).

2 Findings

Five findings resulted from this study.

2.1 Finding One: When comparing different FE samples, the fatigue rate, as measured by DP, is primarily a function of the FE material, the electrode materials, and the interaction of the FE and electrode material with each other and with other parameters.

This finding corroborates previous FE research which indicated that fatigue rates are dependent upon the type of material and electrode. A study by Bullington, discussed in Chapter 2, Section 3.1, indicated that the material and electrode interaction affected the fatigue rate of FE materials.

2.2 Finding Two: As the fatiguing voltage is increased, a decreasing linear relationship in DP is found.

This finding agrees with research by Shepherd discussed in Chapter 2, Section 4.1. This finding extended his research by testing a new material. This study did not replicate the rise in DP seen in Shepherd's results because that operating regime was below the operating region of the experimental designs. The research also extended Shepherd's work by separating the number of cycles applied to a device into separate frequency and time

components. The research in this paper presents an alternate experimental design approach which allows the experimenter to capture the results of Shepherd's work, and explore other parameters at the same time.

The anomalous results for 0/20/80 Pt/Pd at $V_{98\%}$ do not allow this hypothesis to be presented as valid above $V_{88\%}$, the last value at which this sample showed a decrease in DP. No tests were performed between $V_{88\%}$ and $V_{98\%}$ for 0/20/80 Pt/Pd.

2.3 Finding Three: DP for 0/20/80 Pt/Pt was modeled with first-order terms in voltage, frequency, and time, and quadratic terms in time and frequency. No significant interaction terms occurred between any of the parameters.

When comparing different FE samples, these terms are masked by the overwhelming effects of the FE materials and electrode materials. When examining a single material, these parameters suggest an empirical model which can be used to predict operational performance for a single FE device over a wide operating range of voltages, frequencies, and time. The form of the equation is presented below, where the coefficients are sample dependent.

$$DP = constant - a*volt - b*frequency - c*time + d*frequency^2 + e*time^2$$

This empirical model appears to be a new way of representing the fatigue rate of a particular FE sample. Finding three proposes that this equation can be applied to other FE samples, but insufficient time was available to test this hypothesis. The

proposal appears acceptable since finding one determined that the only significant difference between the fatigue rates of different samples was a function of the FE material and the electrode materials.

2.4 Finding Four: A statistically significant interaction appears to be taking place between the applied frequency and the FE material, and between the applied frequency and the electrodes.

This appears to be a new hypothesis. It is possible that these two-factor interactions are confounded with a three-factor interaction between the FE material, the electrodes, and the frequency, but insufficient observations were available to dealias the effects.

2.5 Finding Five: Response Surface Methodology is a useful tool for directing FE research efforts.

Findings one and two indicate that RSM provides a new tool for studying the hypotheses of other FE researchers. Finding three indicates that the analytical tools of RSM can lead to new proposals for explaining the decay rate of ferroelectrics. Finally, finding four demonstrates that a simple empirical model for predicting DP can be developed for a single FE sample.

3 Recommendations

Six recommendations resulted from this study.

3.1 Recommendation One: The criteria for determining $V_{100\%}$ should be investigated.

The evaluation of $V_{100\%}$ established the operating environment for this study, but several questions remain concerning the exact determination of $V_{100\%}$. Not all samples displayed the same behavior with increasing applied voltage, so selection of the correct criteria for determining $V_{100\%}$ is open to question. The evidence in Appendix A appears to support the values selected, but the anomalous results of 0/20/80 Pt/Pd at $V_{98\%}$ indicate that further research near the $V_{100\%}$ region may be required.

Additional research would fall into two categories. The first category regards the determination of $V_{100\%}$. The second category would extend this study examining the fatigue behavior of several samples as the applied voltage approached $V_{100\%}$.

3.2 Recommendation Two: Perform a study using relative values of DP, in order to evaluate relative fatigue rates of different FE samples.

This study used the absolute value of DP to measure the difference between different material and electrode combinations. It is possible that a relative ratio might provide further insights into the fatigue rate question. Data is presented in the charge program of the RT66 which allow the calculation of DP at essentially time zero. For subsequent FATIGUE programs the values of DP observed could be normalized so that the decay rates of different samples could be compared on a relative basis.

Some data was collected on initial DP values during the course of this study, but this did not appear to present a sufficient data population from which to calculate relative

values of DP. Initial values for DP could not be derived from the time = 0 measurement of the fatigue program because the software occasionally delayed the first measurement for one second. Using the value of DP at one second to establish a relative DP scale is feasible, but might distort, or mask entirely, differences between samples.

3.3 Recommendation Three: Design experiments to determine if aging affects fatigue rates when the aging period is greater than 24 hours, or when the cycling frequency is much lower than the frequencies used in this study.

The effect of aging on fatigue merits further investigation, even though the results of aging were inconsequential over a 24 hour period. One approach might be a 2^{5-1}_{V} design for testing one material's fatigue response to

- an initial poling voltage
- aging for a period of time significantly longer than 24 hours
- voltage
- frequency
- time settings

This design would allow all first-order terms and two-factor interaction terms to be estimated, and could be augmented to form a CCD.

3.4 Recommendation Four: Using a FE material other than 0/20/80 Pt/Pt, determine if a similar quadratic equation can be used to predict DP for the new material.

A FE sample other than 0/20/80 Pt/Pt should be tested using a CCD to evaluate the applicability of a quadratic equation as a general model for predicting DP in a specific material. Presumably, the coefficients of the model for the new material will change, but the form will remain the same. Until this test is performed, finding three cannot be extended to other FE materials. In conjunction with this test, canonical analysis of both models should be performed to enhance understanding of the response surface under study.

3.5 Recommendation Five: Develop an experimental design with test location as a parameter.

An experimental design with location as one of the parameters would allow the effects of environment to be modeled relatively inexpensively. FE devices are sensitive to temperature and humidity, but environmentally-controlled tests can be expensive. By performing tests at different locations, some understanding might be gained regarding the effects of humidity and temperature. This experiment would require recording temperature and humidity throughout the entire experimental time frame, including those times between experiments. Some criteria would then have to be developed for comparing the values recorded.

3.6 Recommendation Six: Design a full factorial experiment in five factors to test finding four.

Finding four proposed interactions between the applied frequency and the FE material, and between the applied frequency and the electrodes. A full factorial design involving

- voltage
- frequency
- time
- FE material
- electrode

would require only $2^5 = 32$ design points in order to estimate all interaction terms free of aliasing. If the three-factor interaction term frequency * FE material * electrode turned out to be significant, a possible explanation would be the manner in which the FE material and the electrode adhered to each other.

4 Conclusions

This study contributed to the body of knowledge in ferroelectrics and provided corroborating evidence of the findings of several other researchers. It also demonstrated how an analysis tool, RSM, can be used to develop empirical models that predict the behavior of FE samples. An empirical model involving three first-order terms and two quadratic terms was proposed as a predictor of DP in a given FE sample. Further research is required to determine if the quadratic model proposed can be extended to FE samples other than that sample whose behavior the model predicts.

APPENDIX A: Determination of $V_{100\%}$

1 Introduction

Each material used in this thesis had a different V_{max}, where V_{max} is defined, somewhat euphemistically, as the voltage at which the hysteresis loop first exhibits undesirable characteristics. This appendix describes the tools that were used to determine the initial onset of "undesirable characteristics", providing a methodology for establishing V_{max} for any material/electrode combination. It should be noted that V_{max} is not necessarily the same as $V_{saturation}$, the voltage required to drive a device to saturation, and is definitely not $V_{breakdown}$, the minimum voltage required to destroy device operating characteristics. V_{max} is being proposed as a standard of measurement for this paper which other researchers may find useful.

Equally important is the establishment of a relative voltage reference scale. The utility of a relative voltage reference scale is that different devices can be evaluated at the same relative reference points. If absolute scales are used to compare dissimilar devices, then distortions in the data may not be separable. For instance, if 4 volts is used to test two devices, with V_{max} of 5 and 10 volts respectively, it can be argued that any results are confounded by the fact the devices are being tested in different operating regimes. Therefore, this paper proposes a relative reference voltage scale that establishes an equivalency between V_{max} and $V_{100\%}$. Different

devices can then be compared at the same relative voltages in terms of a percent of V_{max} for each device. The $V_{100\%}$ values found for each device are listed in Table XXVII.

Table XXVII. $V_{100\%}$ Values for Samples

Material	Electrode	$V_{100\%}$
0/60/40	Pt/Pt	10.0
0/60/40	Pt/Pd	7.0
0/20/80	Pt/Pt	5.0
0/20/80	Pt/Pd	3.5

Along with providing a common scale for discussion purposes, the relative voltage scale proposed enhances the utility of Response Surface Methodology (RSM). Suppose an experimenter wishes to use a two-level, factorial design to examine the voltage responses of two materials, all other parameters held constant. Using an absolute voltage scale limits the experimenter to two absolute voltage values to meet the criteria for constructing a two-level design. Using a relative voltage scale still limits the design to two values, but these values contain the basis for examining four absolute voltages. To picture this, consider using $V_{70\%}$ and $V_{80\%}$ to satisfy the two-level factorial criteria. If the $V_{100\%}$ for material one is 10V and for material two it is 5V, then the actual voltages applied to material one are 7V and 8V, for material two the applied voltages are 3.5V and 4V. Within the actual factorial design $V_{70\%}$ would be coded as -1 and $V_{80\%}$ coded as 1.

The simple example above illustrates the flexibility a relative voltage scale provides. The major concern a researcher then must consider is whether a relative voltage scale actually provides information on devices operating in similar regimes. For this thesis the assumption is made that the relative voltage is a useful and applicable tool.

2 $V_{100\%}$ Determination Criteria

Three criteria were used to determine $V_{100\%}$ for each of the four samples. The first criteria was a visual examination of over a hundred hysteresis loops for each sample using the CHARGE program of the RT-66. The second criteria involved calculating mean values and variances of saturation polarization (P_s), remnant polarization (P_r), and minus remnant polarization ($-P_r$) at each of the voltages at which hysteresis loops for a sample were generated. The third criteria involved plotting P_s, P_r, and $-P_r$ versus voltage, and plotting the change in these polarizations with respect to changes in voltage setting. Details on the exact procedures are presented in the following sections.

All figures and tables for the remaining sections are presented at the end of the appendix. Figures 39-54 are hysteresis loops, Tables XXVIII-XXXI are polarization measurements, and Figures 55-62 are plots. Each of these three groupings are organized so that 0/60/40 Pt/Pt is presented first, followed by 0/60/40 Pt/Pd, 0/20/80 Pt/Pt, and 0/20/80 Pt/Pd.

This allows the reader to quickly look up values for any particular FE sample.

2.1 Test Procedure. The testing of samples, using the CHARGE program, began at 1.5V and initially proceeded in 0.5V increments. Once a preliminary operating region was determined, the starting point and increments were modified to provide more efficient testing procedures. In some cases this resulted in voltage increments of 0.25 or 0.20 near regions which appeared to display "undesirable characteristics". For each run, P_s, P_r, and $-P_r$ were recorded. Not all of the data is presented in the following pages for the sake of brevity. No data which would have altered the findings was left out of this thesis. For instance, values for E_c and $-E_c$ were obtained from several hundred experiments. Limited analysis of this data provided no insight, so it was not reported.

2.2 Visual determination of $V_{100\%}$. For each sample, the first five devices were tested to destruction. Destruction was indicated when a football shape, Figure 37, was generated (as the loop) or the CHARGE program indicated that the capacitor's DC resistance was less than 600,000 ohms. Subsequent testing did not proceed to destruction as sufficient indications of "undesirable characteristics" were evident before testing proceeded to destruction.

There are three visual indicators which were used to evaluate the loops to determine $V_{100\%}$. All three indicators are subjective and none of the samples displayed the exact

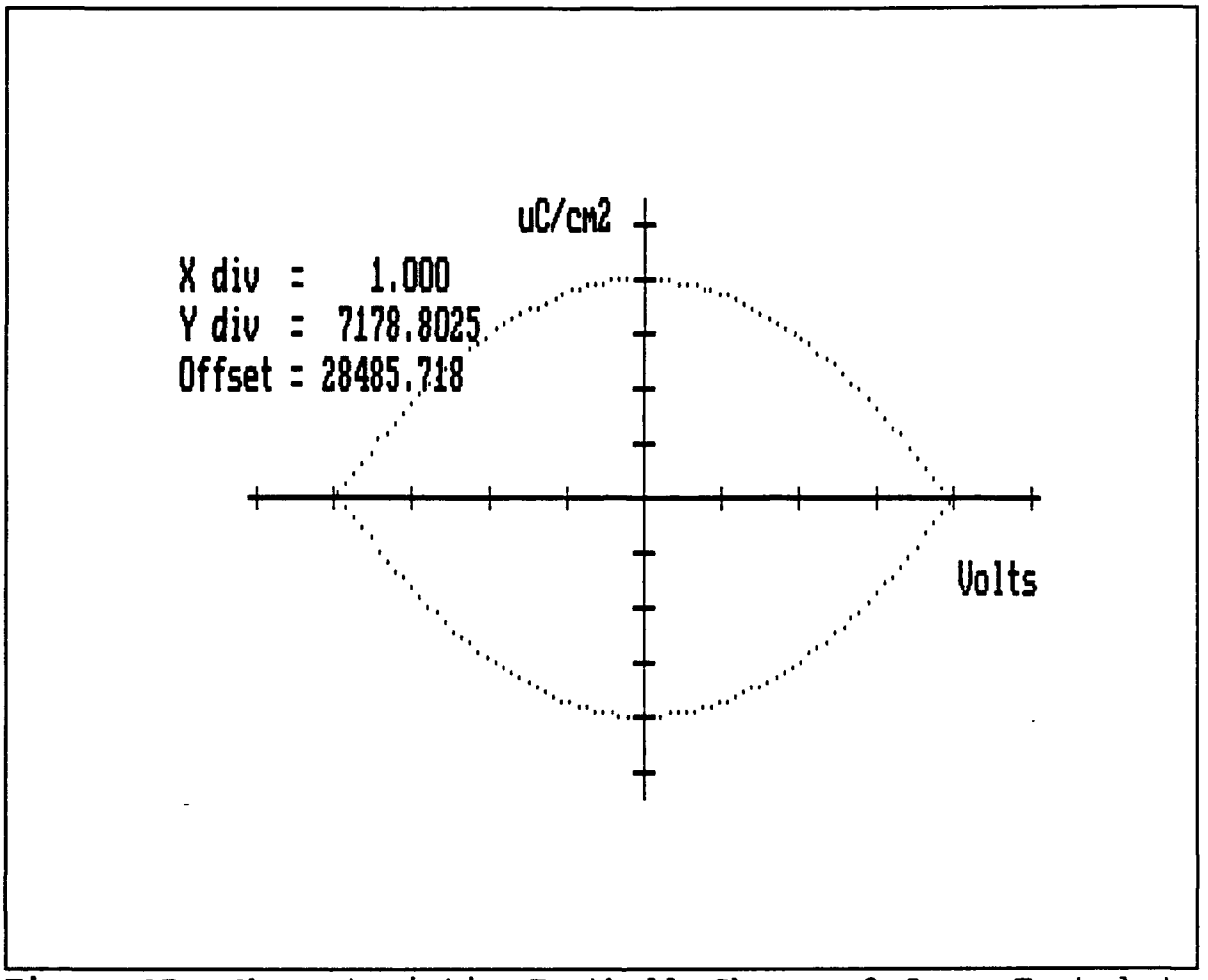

Figure 37. Characteristic Football Shape of Loop Tested to Destruction

characteristics that will be described. It was not uncommon for several of the indicators to appear at a voltage below that finally selected for $V_{100\%}$.

The first indicator is that the loop does not present as "smooth" an appearance above $V_{100\%}$, as seen in Figure 38. The second indicator is seen by examining P_s in a sequence of hysteresis loops. It becomes apparent that, particularly for voltages above $V_{100\%}$, the curve appears to hook down, or slice to the right, in order to reach the P_s data point. The same

characteristic hook also appears at the $-P_s$ data point, except it hooks up (slices to the left). A third visual indicator is to examine the loop discontinuity along the vertical axis where $-P_r$ occurs. In general the top half of the loop crosses the negative y-axis at a point above where the bottom half of the loop crosses the negative y-axis. Approaching $V_{100\%}$, this gap becomes smaller and smaller, until the direction of the gap reverses and the top half of the loop crosses the negative y-axis at a point lower than where the bottom half of the loop intersects the axis, as seen in Figure 38. The reader can gain a better appreciation of the subjective visual measures used to evaluate $V_{100\%}$ by examining Figures 39-54, sample hysteresis loops for each material.

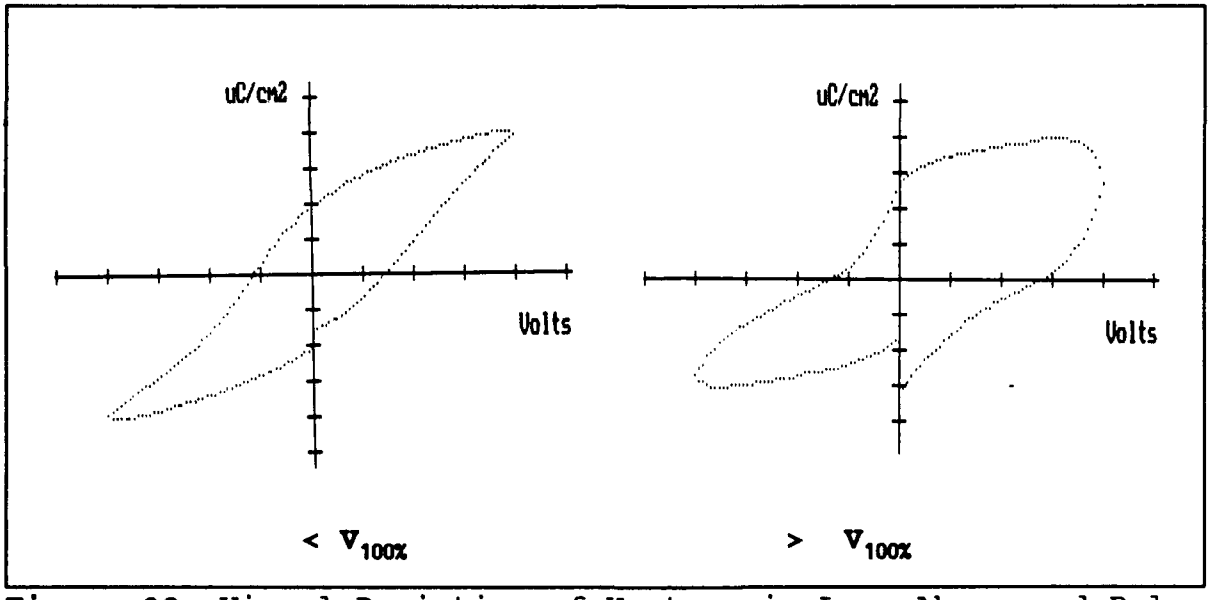

Figure 38. Visual Depiction of Hysteresis Loop Above and Below $V_{100\%}$

2.3 Mean and Variance of P_s, P_r, $-P_r$. The second method for determining $V_{100\%}$ was based on the simple concept that one might expect to find greater variance in the polarization values in a

region which exhibited "undesirable characteristics" in the hysteresis loop. Essentially this is an expectation that the variance will increase substantively above some critical applied voltage. In this case, the intent was to demonstrate that $V_{100\%}$ was the critical voltage.

Contrary to expectations, only the 0/20/80 Pt/Pd combination displayed the expected increase in variance of all three polarization values when approaching and exceeding $V_{100\%}$, as seen in Table XXXI. In fact, the variance at 3.5V was so great that an argument might be made that $V_{100\%}$ for 0/20/80 Pt/Pd should have been set lower than 3.5V. In this case, the other criteria for determining $V_{100\%}$ suggested that 3.5V was an appropriate value and testing at 3.375V suggested that 3.375V was less than $V_{100\%}$. 0/60/40 Pt/Pd exhibited little change in variance, relative to the other samples, throughout the tested applied voltage region, as shown in Table XXIX. 0/60/40 Pt/Pt demonstrated no specific trend with respect to the variance of P_s and $-P_r$. For P_r it was not clear that the variance had substantively increased until 2V above the $V_{100\%}$ established, as seen in Table XXVIII. 0/20/80 Pt/Pt demonstrated very stable variances for P_s and $-P_r$, though not as stable as for 0/60/40 Pt/Pd. The variance for P_r for 0/20/80 Pt/Pt demonstrated the expected increase in variance approaching, then exceeding, $V_{100\%}$, as shown in Table XXX.

In summary, this test is the least conclusive of the criteria for determining $V_{100\%}$. P_r is the measurement most likely to show increasing variance approaching and exceeding $V_{100\%}$. This

test should be considered as an adjunct to the other tests. However, the data on the means is used extensively in the third, and last, test for determining $V_{100\%}$.

2.4 Plotting P_s, P_r, $-P_r$ Against Applied Voltage. The concept behind this criteria for determining $V_{100\%}$ was based on the idea that P_s, P_r, and $-P_r$ would exhibit a linear relationship, with respect to applied voltage, until entering the region designated as displaying "undesirable characteristics". The basic rationale was that plots of the polarization values against applied voltage would be parallel as long as the voltage was $V_{100\%}$ or less. Plots were also made of the change in polarization with respect to (w.r.t.) the change in voltage using simple slope formulas. In evaluating the slope plots, one of the criteria developed was to treat as critical points those points where the slope of P_r w.r.t. voltage crossed the slope of P_s w.r.t. voltage. For all samples, a slope crossing occurred prior to the $V_{100\%}$ point. If the gradient of P_r became much greater than that of P_s, then the device was displaying an imminent failure mode. One of the characteristics as a device begins to fail is that P_r begins to increase faster than P_s and will actually become larger than P_s, causing severe distortions in the hysteresis loop as in Figure 38 when above $V_{100\%}$.

Plots for 0/60/40 Pt/Pt, Figures 55 and 56, and 0/20/80 Pt/Pt, Figures 59 and 60, appear to be good indicators for $V_{100\%}$. The plots for 0/60/40 Pt/Pd, Figures 57 and 58, are inconclusive, although a slope crossing does occur at a location on each side

of 7.5V ($V_{100\%}$ for 0/60/40 Pt/Pd), seen in Figure 58. Figures 61 and 62 for 0/20/80 Pt/Pd displayed a good visual correlation between $V_{100\%}$ and the point at which P_r began to develop a slope greater than that for P_s. Slope crossings for voltages greater than $V_{100\%}$ may in part be attributed to increased variability in device characteristics, but it has already been noted that 0/60/40 Pt/Pd displayed stable variance above $V_{100\%}$.

3 Limitations

Five limitations must be acknowledged in the procedures used to determine $V_{100\%}$. First, the response of a ferroelectric (FE) device is dependent upon its prior state, thus each test performed on a particular device changes the response of that device to future tests. Since each device began testing at voltages less than $V_{100\%}$, the values found after the first time a device is sampled are not the values which would have been found had the device been initially tested at each of the intermediate voltages. A related limitation, the second, is that the same sequence of voltages was not used to test each device. Both of these factors may have affected the variability of the test results.

Limitations one and two could have been eliminated had hysteresis loops been generated on a new device for each voltage examined. This would probably not have provided data any better than that actually found since the changes in a particular FE sample caused by running the CHARGE program are probably insignificant with respect to the values measured. The key

reasons for not performing each test on a new device were the limited number of devices available and the limited time available. Setup time for each test would have been prohibitive considering that over 500 tests were performed. The same sequence of tests was not performed on each device because part of the test pattern was to isolate a critical region and concentrate resources on collecting data in that critical region.

A third limitation results from the fact the samples tested were not complete wafers. When manufacturing a wafer of FE devices, there is variability in device quality based on location on the wafer, in particular when comparing devices at the edge of the wafer with devices in the center. The desired test situation would involve complete wafers in order to provide a sample data base which included devices distributed across the wafer. In fact, two of the samples included a wafer edge and two samples did not. It is impossible to assess how this limitation affected the study.

From a statistical standpoint, a fourth limitation exists in the sense that no large samples (number of data points > 30) at any particular voltage for any sample were collected. In all cases an attempt was made to collect sufficient data points in the critical regions to insure that the data was a representative distribution of device characteristics for each sample. In this instance, the results appear to justify the decision to stop collecting data because obvious trends in the data exist based on the criteria explained in evaluating $V_{100\%}$.

A fifth potential limitation is that the researcher may have unintentionally selected criteria for determining $V_{100\%}$ which reflect unconscious biases. This concern seems particularly relevant when noting that for a given material (0/60/40 or 0/20/80) the $V_{100\%}$ value for the electrode combination Pt/Pd is exactly 70% of the $V_{100\%}$ value for electrode Pt/Pt. Furthermore, for a given electrode combination (Pt/Pt or Pt/Pd) the $V_{100\%}$ value for 0/20/80 is exactly half that of 0/60/40 (see Table XXVII).

4 Summary

Three tests were suggested for determining $V_{100\%}$. The most objective method involved examining the variances of the polarization values as the applied voltage approached the proposed $V_{100\%}$ value. Unfortunately this method provided the least substantive results, although it worked well for 0/20/80 Pt/Pd. Judging $V_{100\%}$ purely on the basis of the shape of the hysteresis loops is suspicious due to the subjective nature of the procedure. Preparing plots of P_s, P_r, and $-P_r$ versus applied voltage, and plots of the change in polarization w.r.t. the change in applied voltage, corroborated the results of the other tests, when the other tests appeared appropriate.

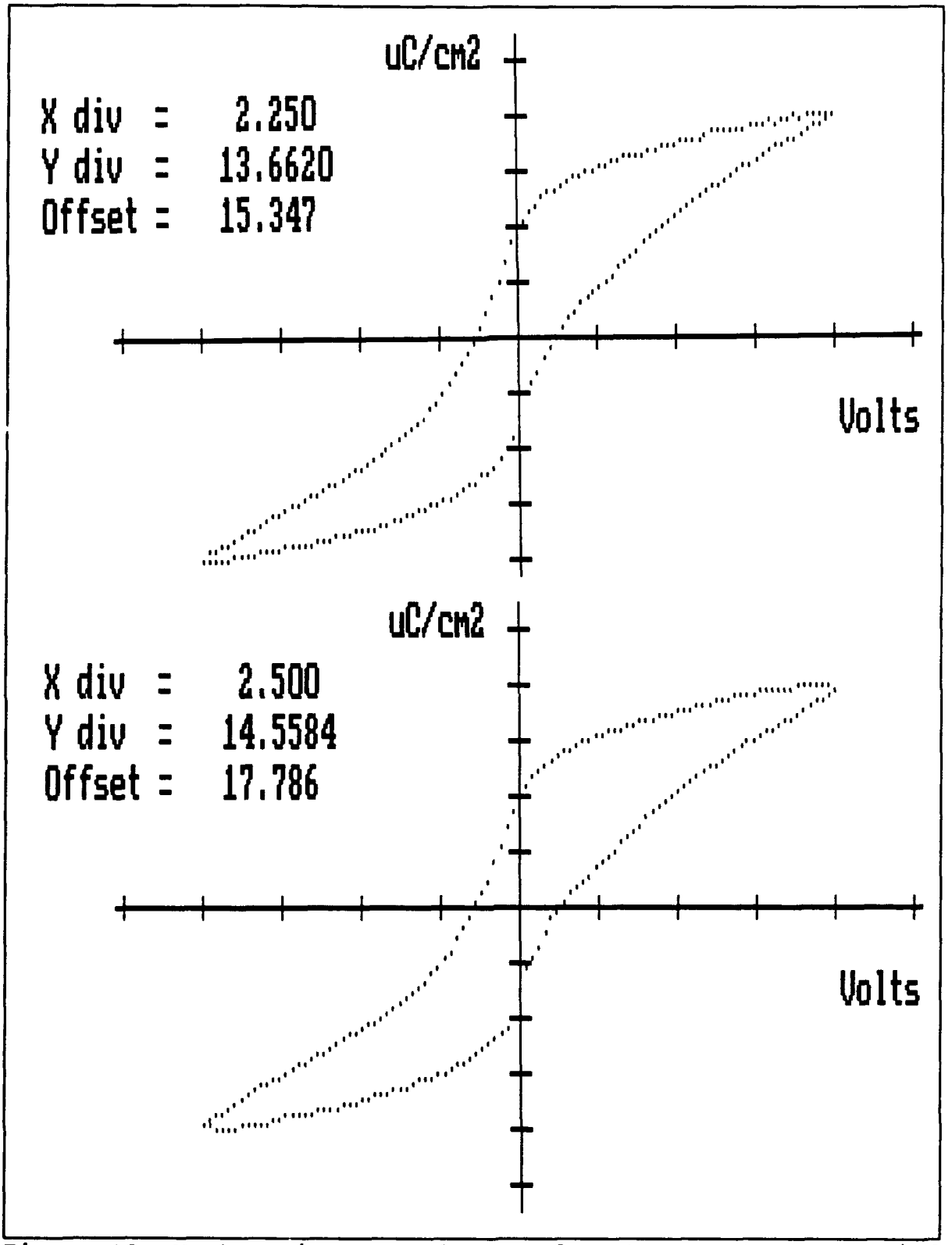

Figure 39. Hysteresis Loops for Sample 0/60/40 Pt/Pt, Applied Voltage Equal ($V_{90\%}$, $V_{100\%}$)

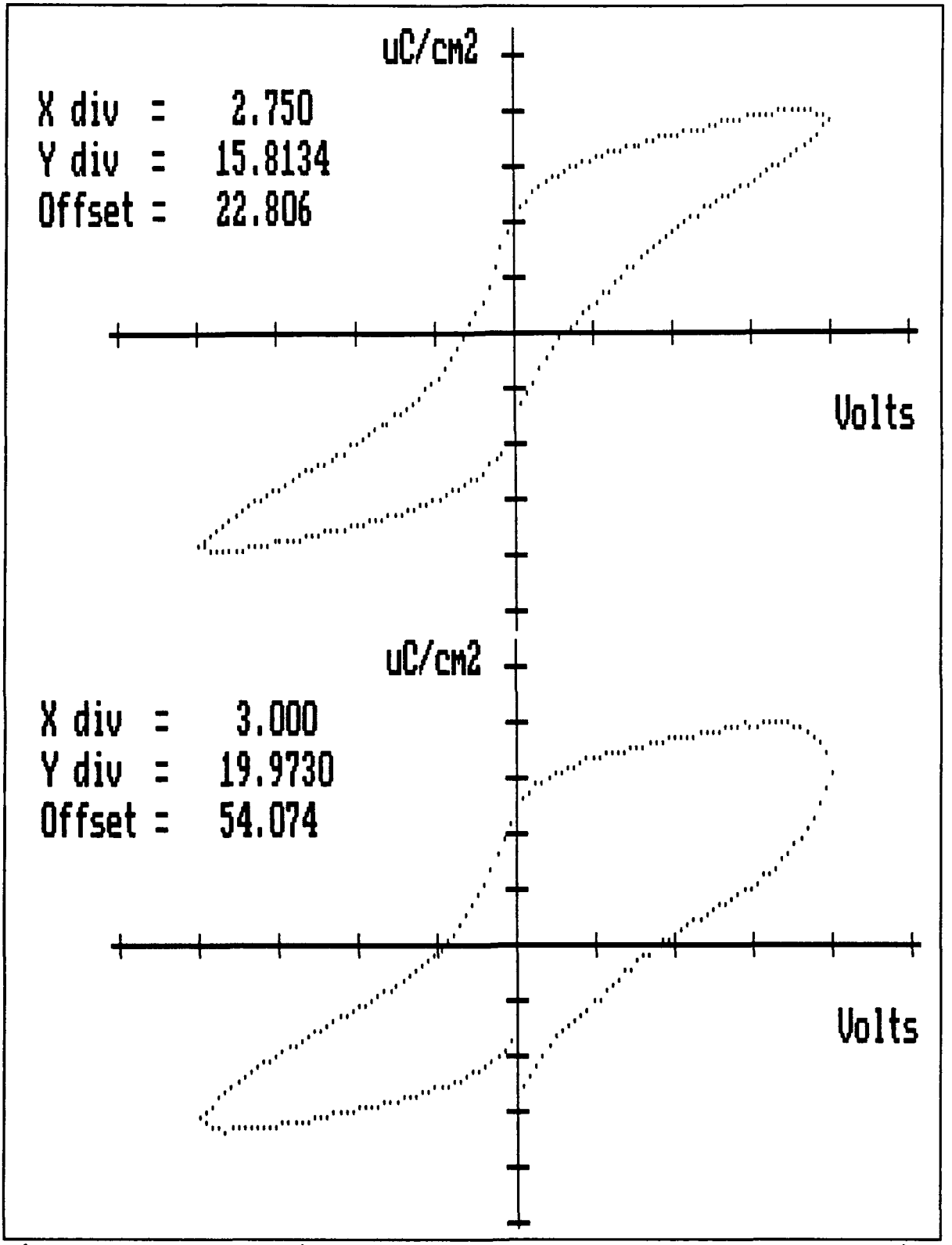

Figure 40. Hysteresis Loops for Sample 0/60/40 Pt/Pt, Applied Voltage Equal ($V_{110\%}$, $V_{120\%}$)

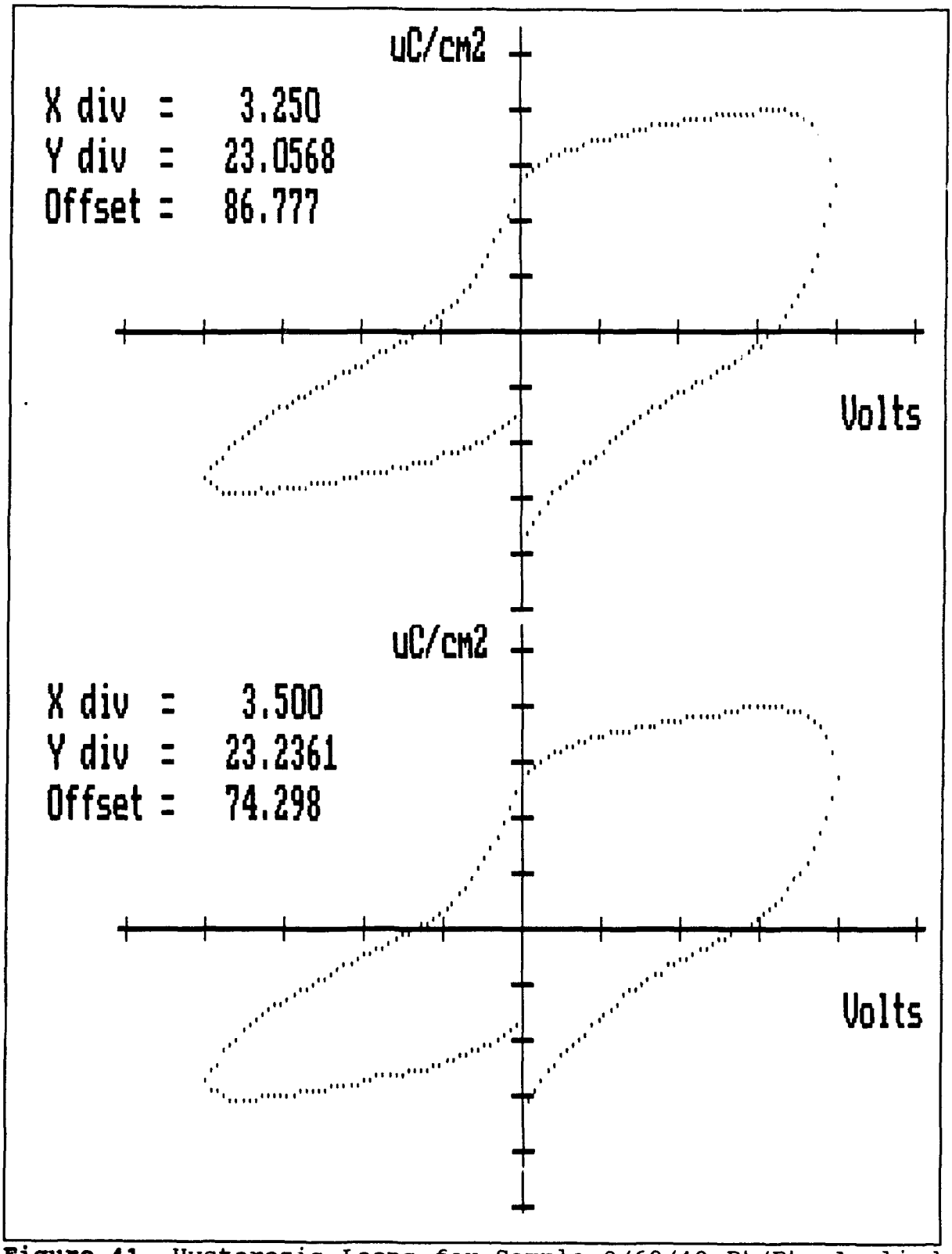

Figure 41. Hysteresis Loops for Sample 0/60/40 Pt/Pt, Applied Voltage Equal ($V_{130\%}$, $V_{140\%}$)

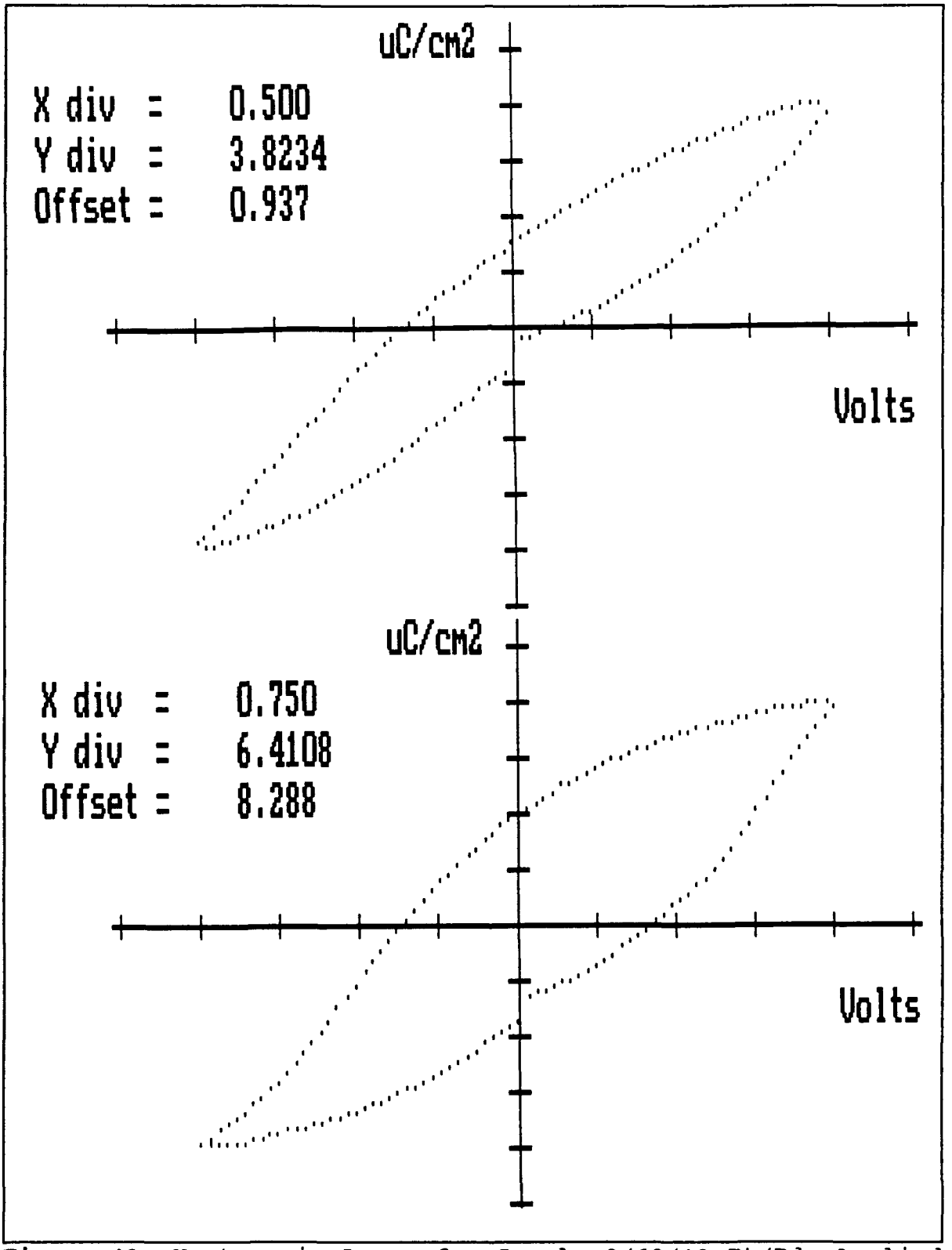

Figure 42. Hysteresis Loops for Sample 0/60/40 Pt/Pd, Applied Voltage Equal ($V_{29\%}$, $V_{43\%}$)

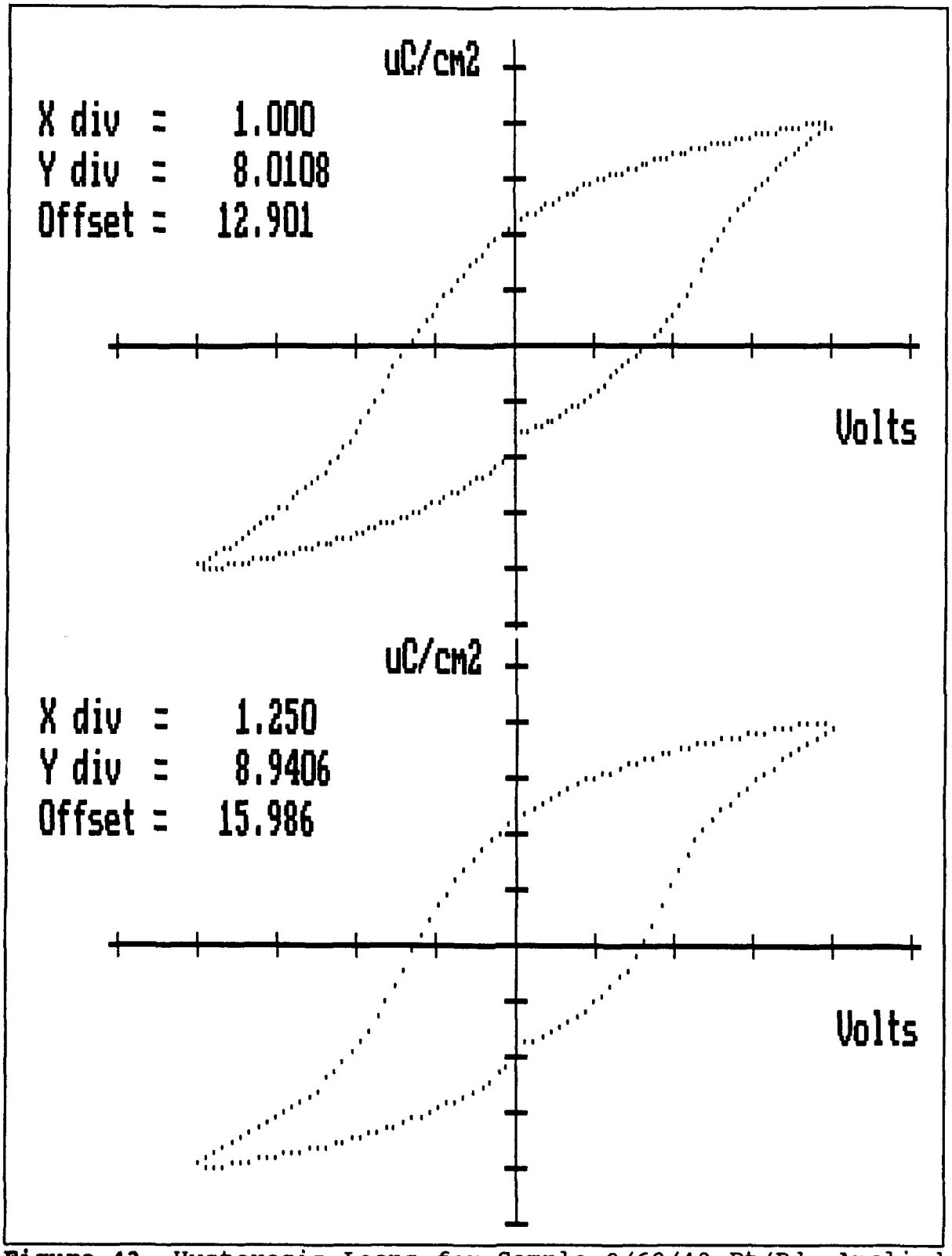

Figure 43. Hysteresis Loops for Sample 0/60/40 Pt/Pd, Applied Voltage Equal ($V_{57\%}$, $V_{71\%}$)

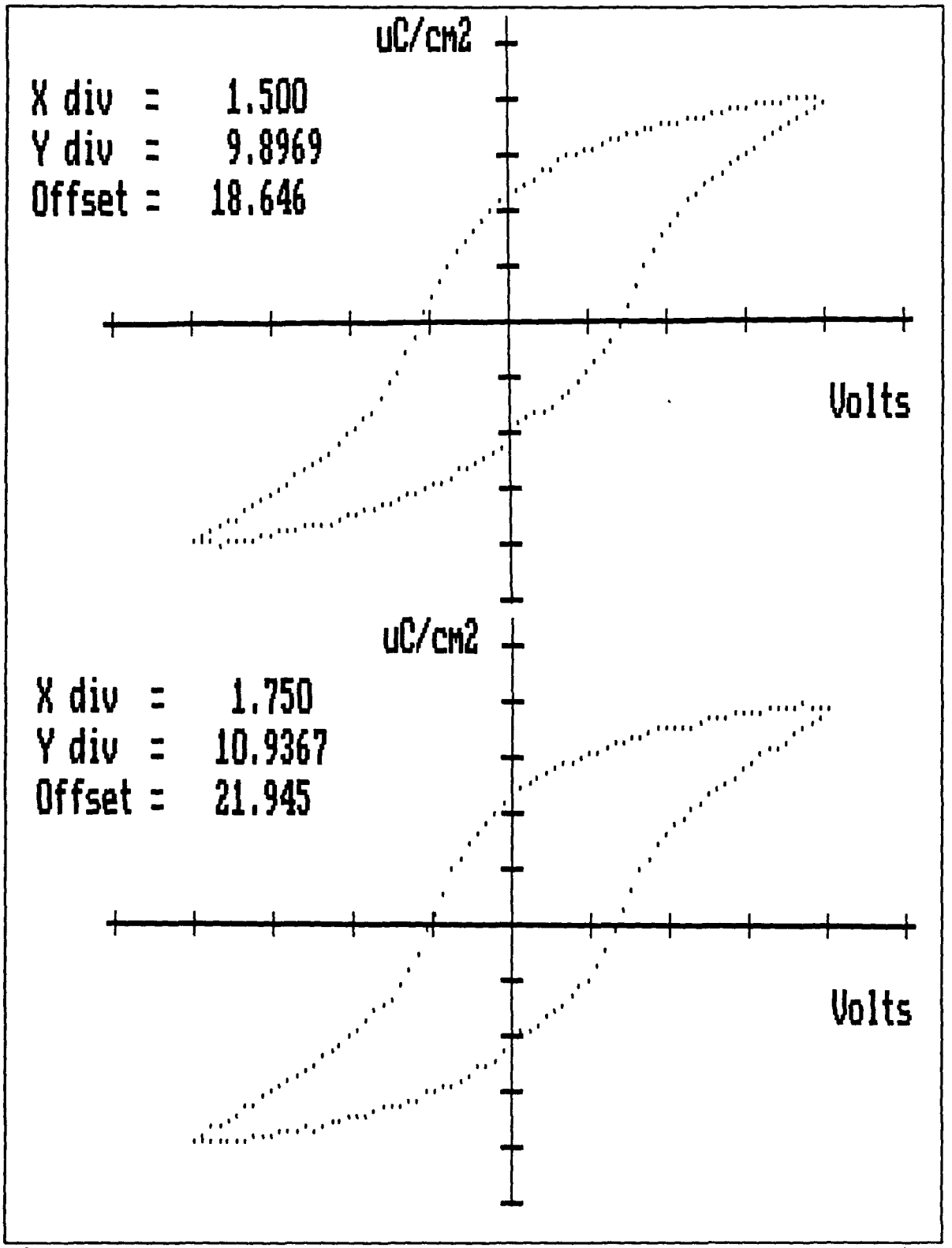

Figure 44. Hysteresis Loops for Sample 0/60/40 Pt/Pd, Applied Voltage Equal ($V_{86\%}$, $V_{100\%}$)

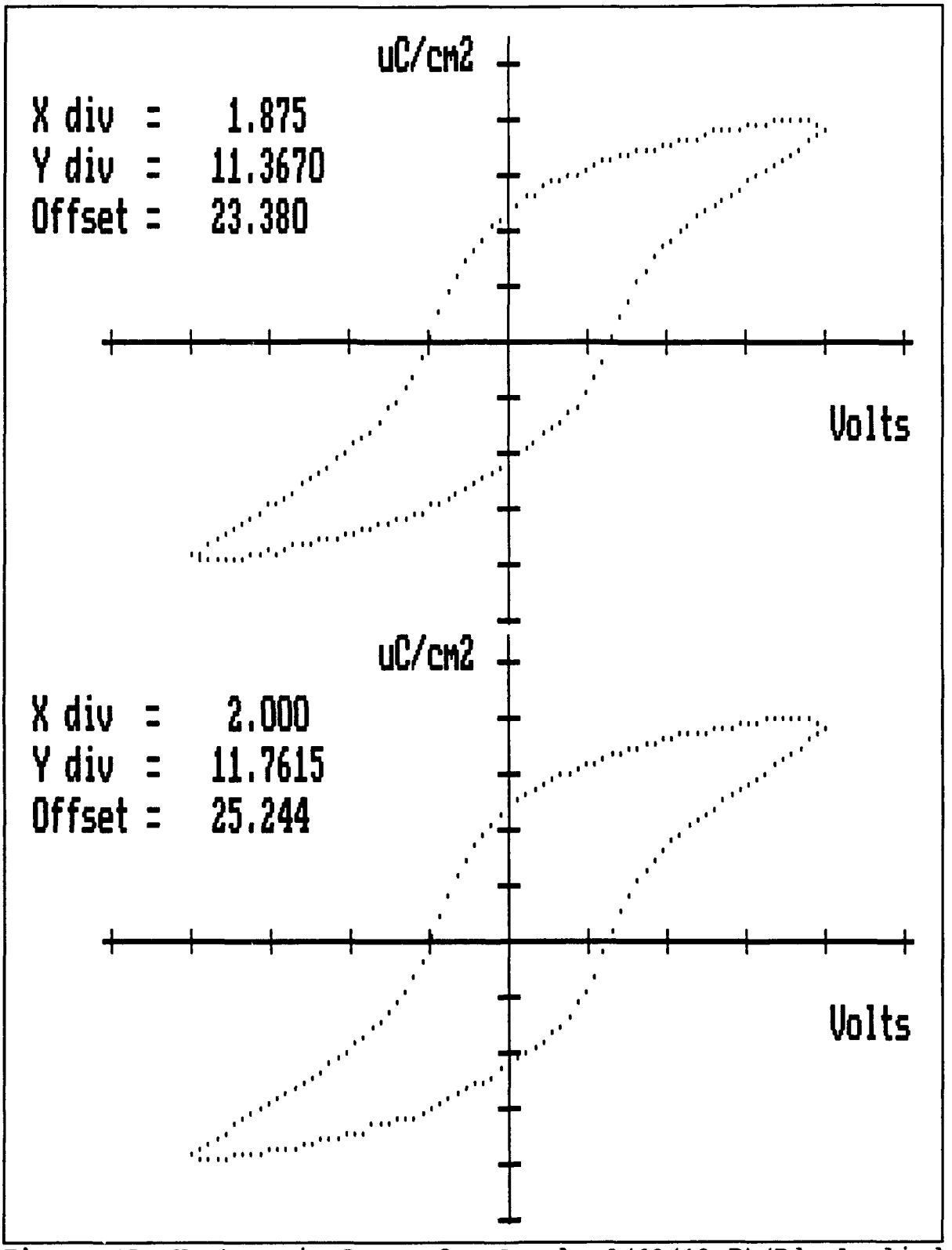

Figure 45. Hysteresis Loops for Sample 0/60/40 Pt/Pd, Applied Voltage Equal ($V_{107\%}$, $V_{114\%}$)

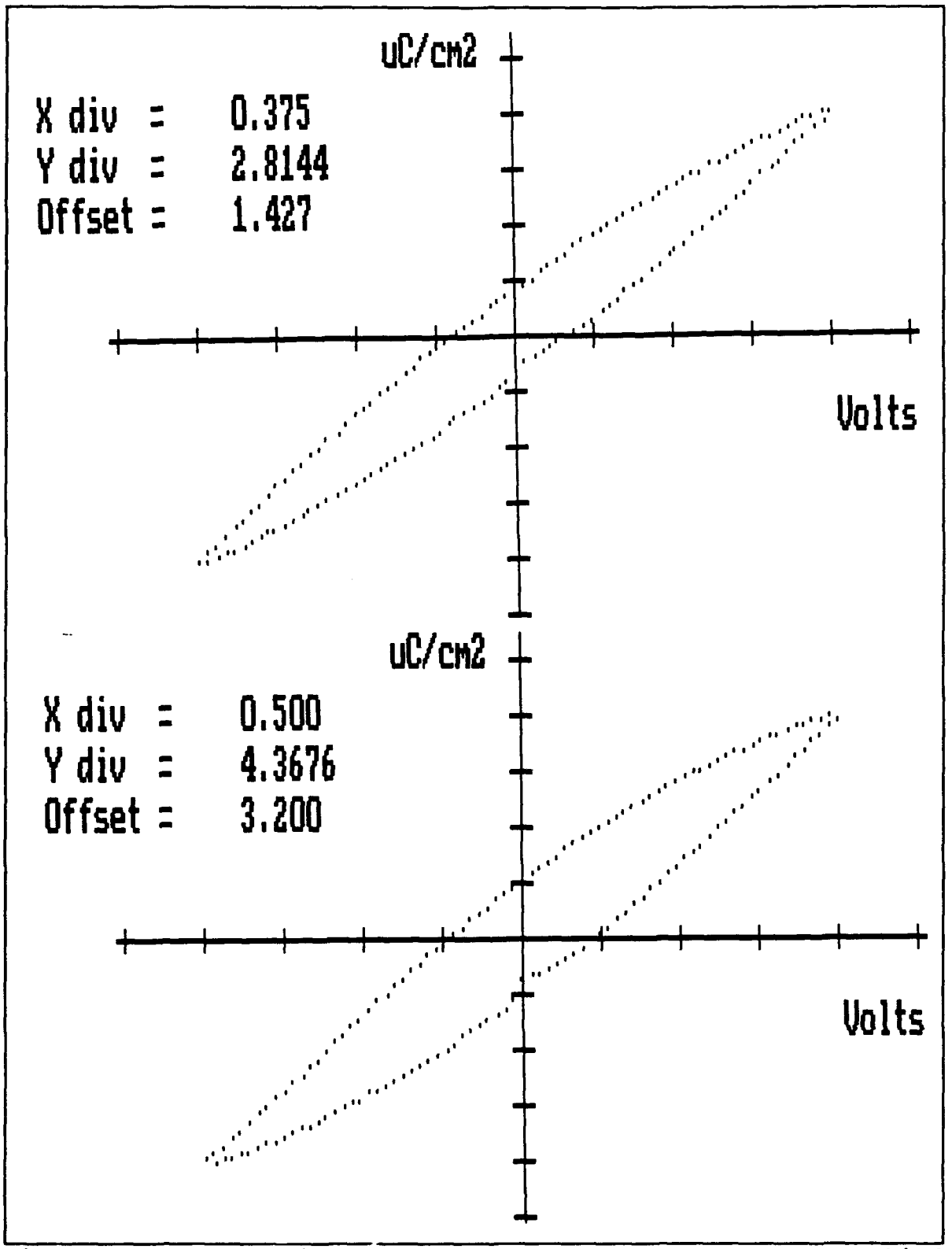

Figure 46. Hysteresis Loops for Sample 0/20/80 Pt/Pt, Applied Voltage Equal ($V_{30\%}$, $V_{40\%}$)

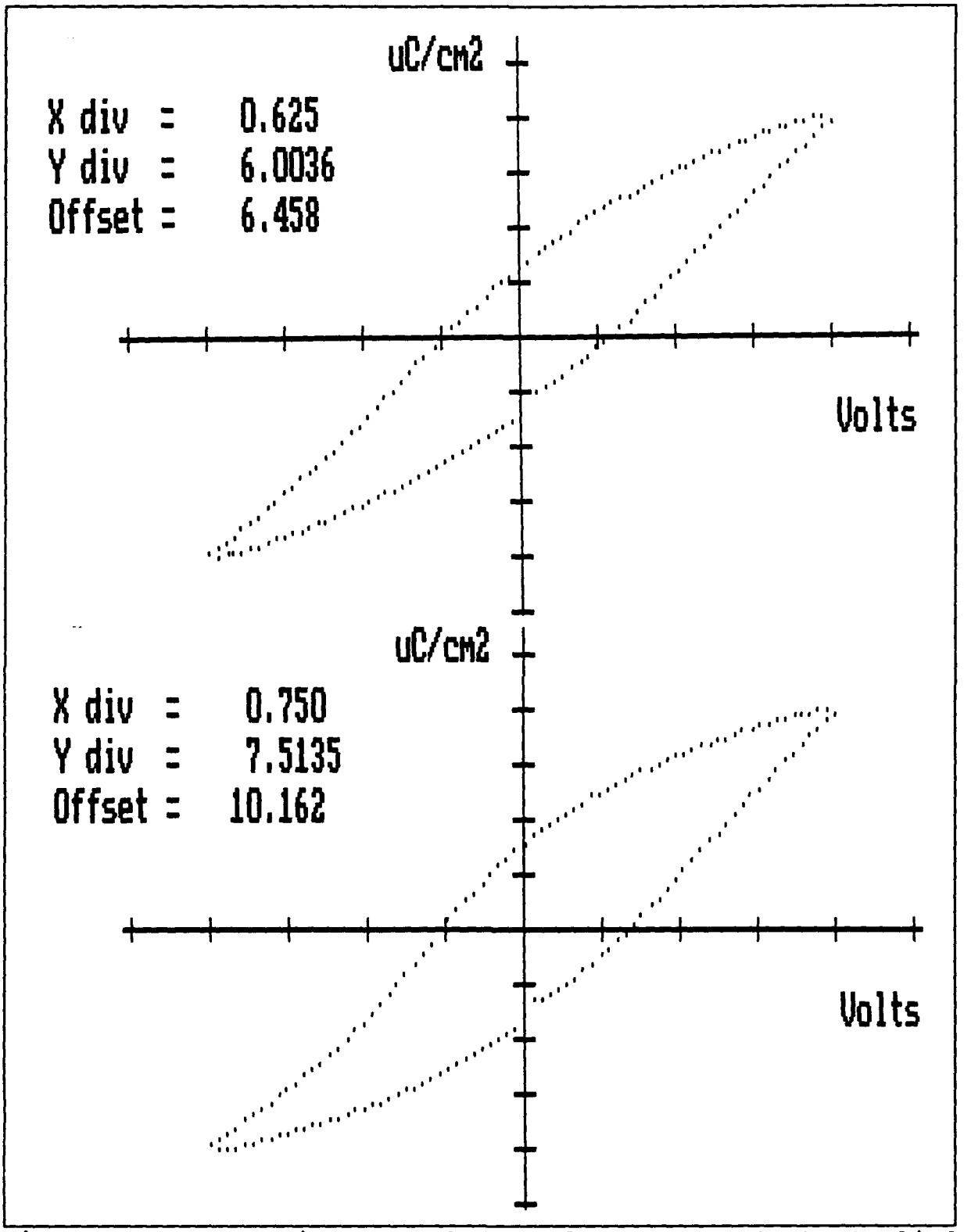

Figure 47. Hysteresis Loops for Sample 0/20/80 Pt/Pt, Applied Voltage Equal ($V_{50\%}$, $V_{60\%}$)

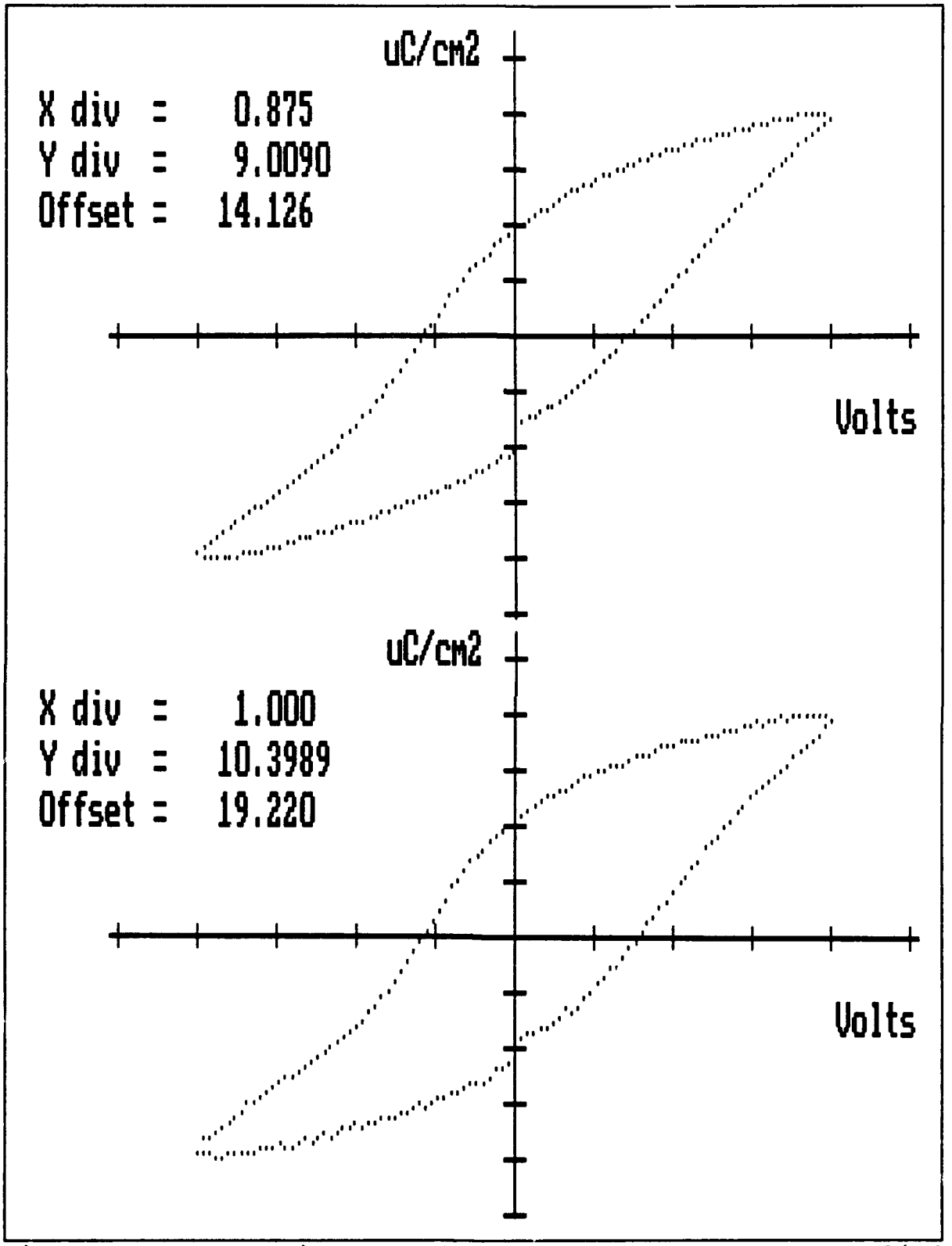

Figure 48. Hysteresis Loops for Sample 0/20/80 Pt/Pt, Applied Voltage Equal ($V_{70\%}$, $V_{80\%}$)

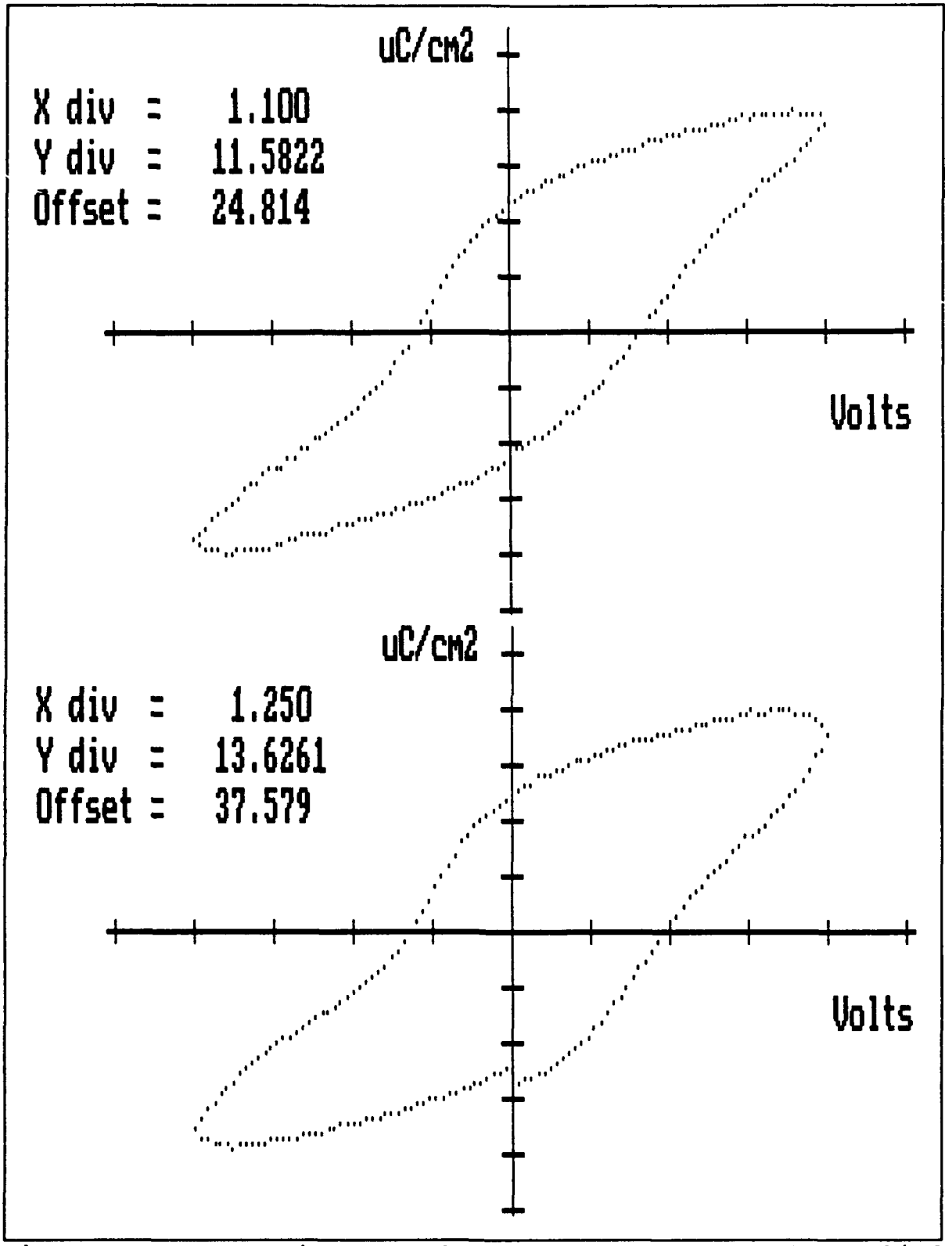

Figure 49. Hysteresis Loops for Sample 0/20/80 Pt/Pt, Applied Voltage Equal ($V_{88\%}$, $V_{100\%}$)

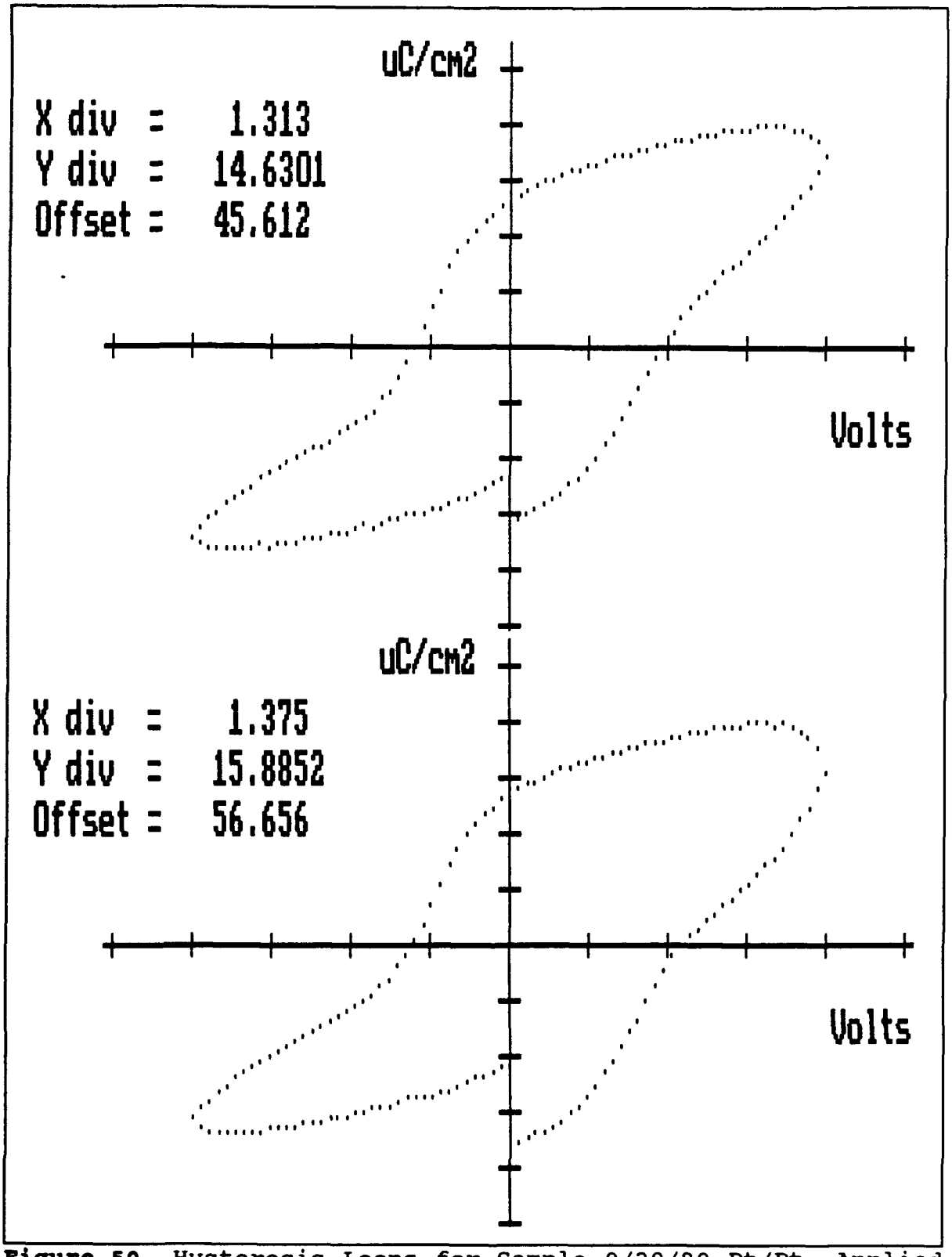

Figure 50. Hysteresis Loops for Sample 0/20/80 Pt/Pt, Applied Voltage Equal ($V_{105\%}$, $V_{110\%}$)

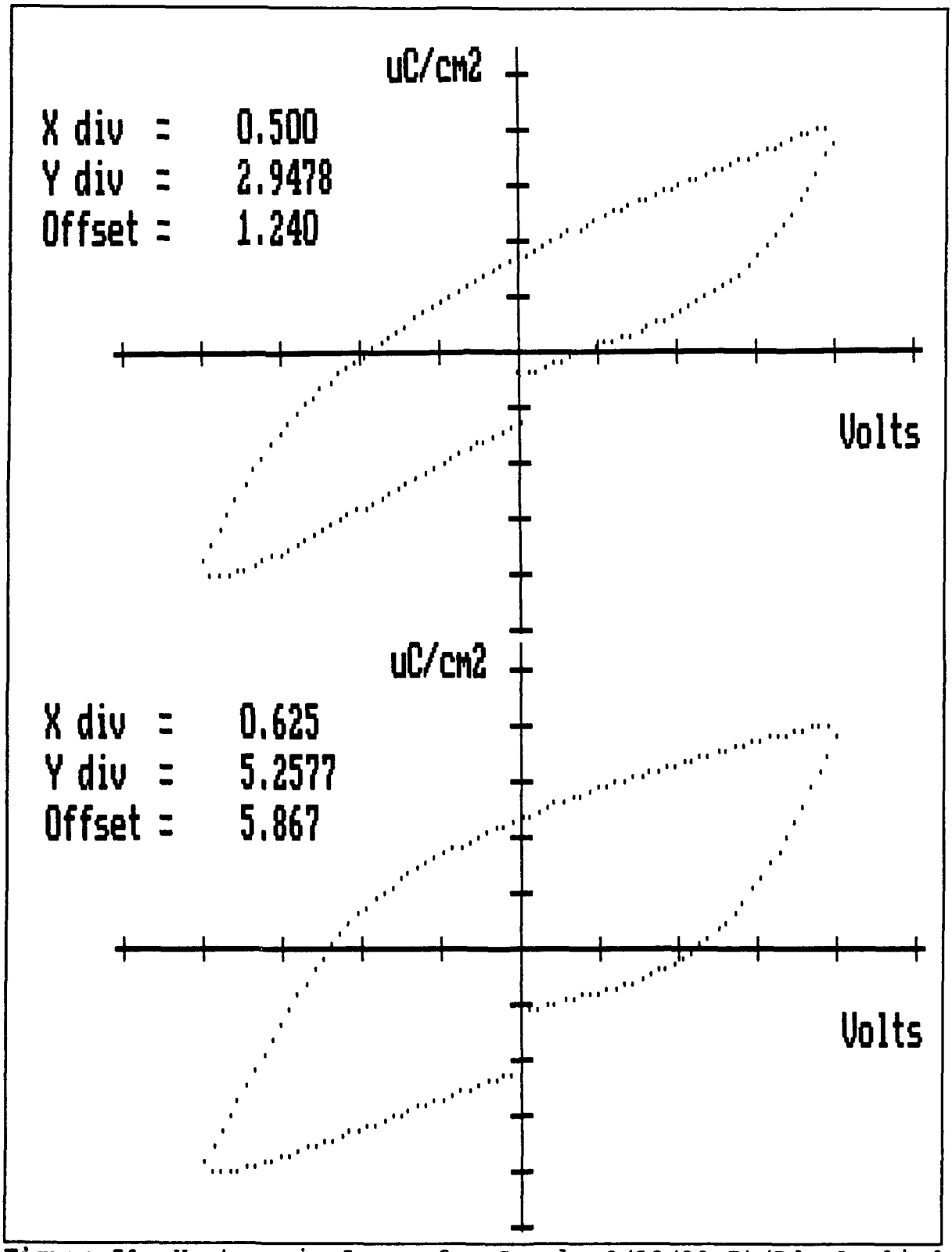

Figure 51. Hysteresis Loops for Sample 0/20/80 Pt/Pd, Applied Voltage Equal ($V_{57\%}$, $V_{71\%}$)

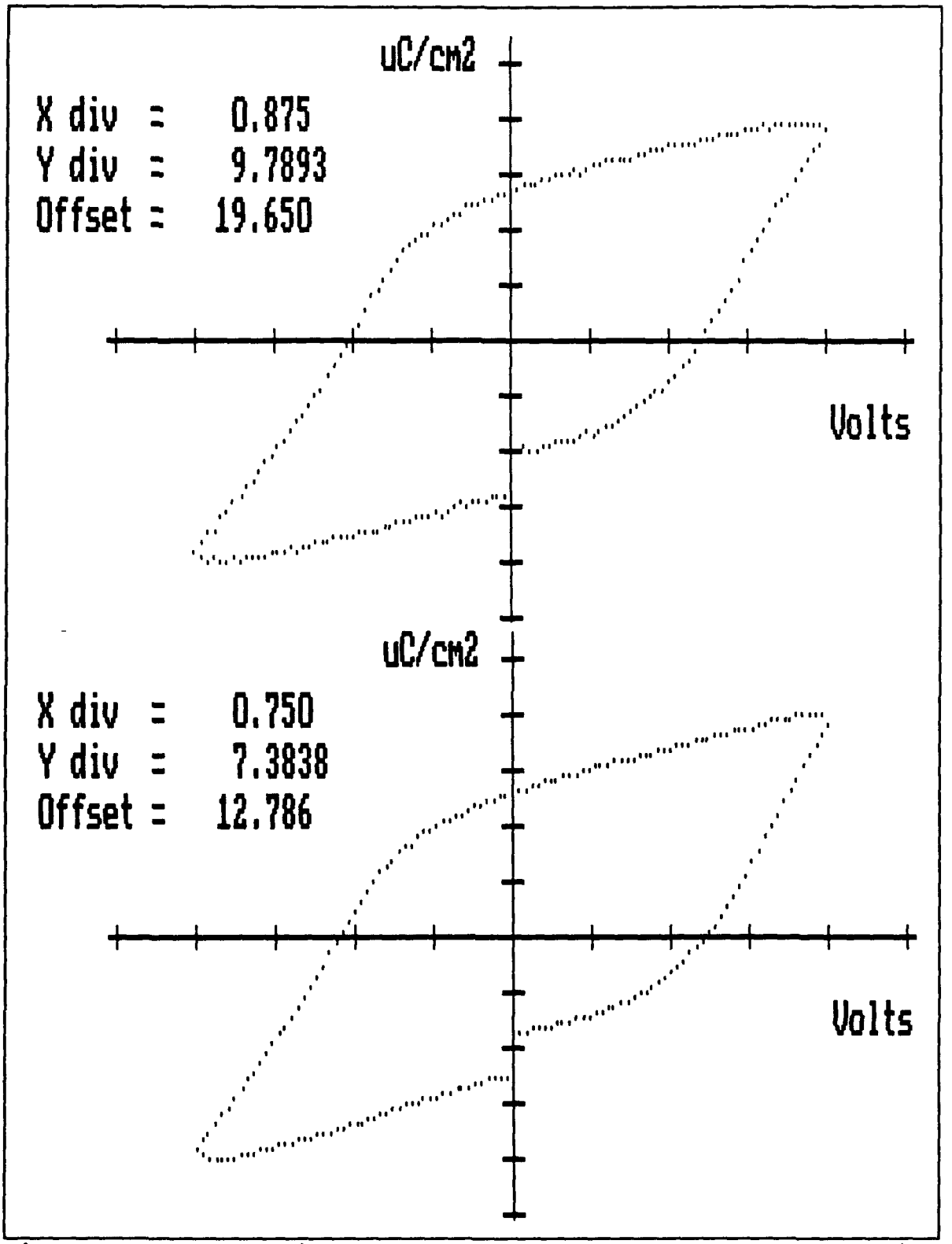

Figure 52. Hysteresis Loops for Sample 0/20/80 Pt/Pd, Applied Voltage Equal ($V_{86\%}$, $V_{100\%}$)

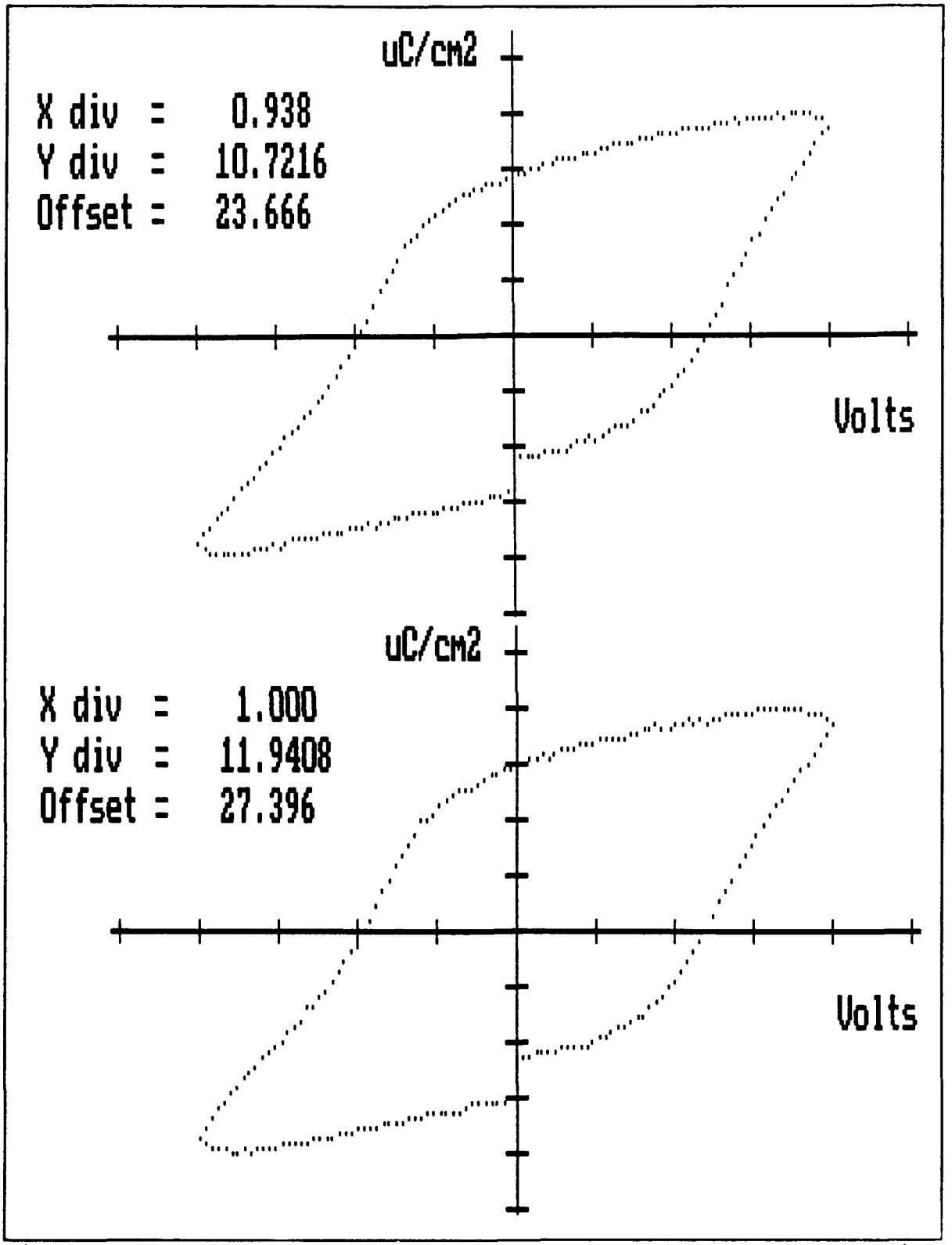

Figure 53. Hysteresis Loops for Sample 0/20/80 Pt/Pd, Applied Voltage Equal ($V_{107\%}$, $V_{114\%}$)

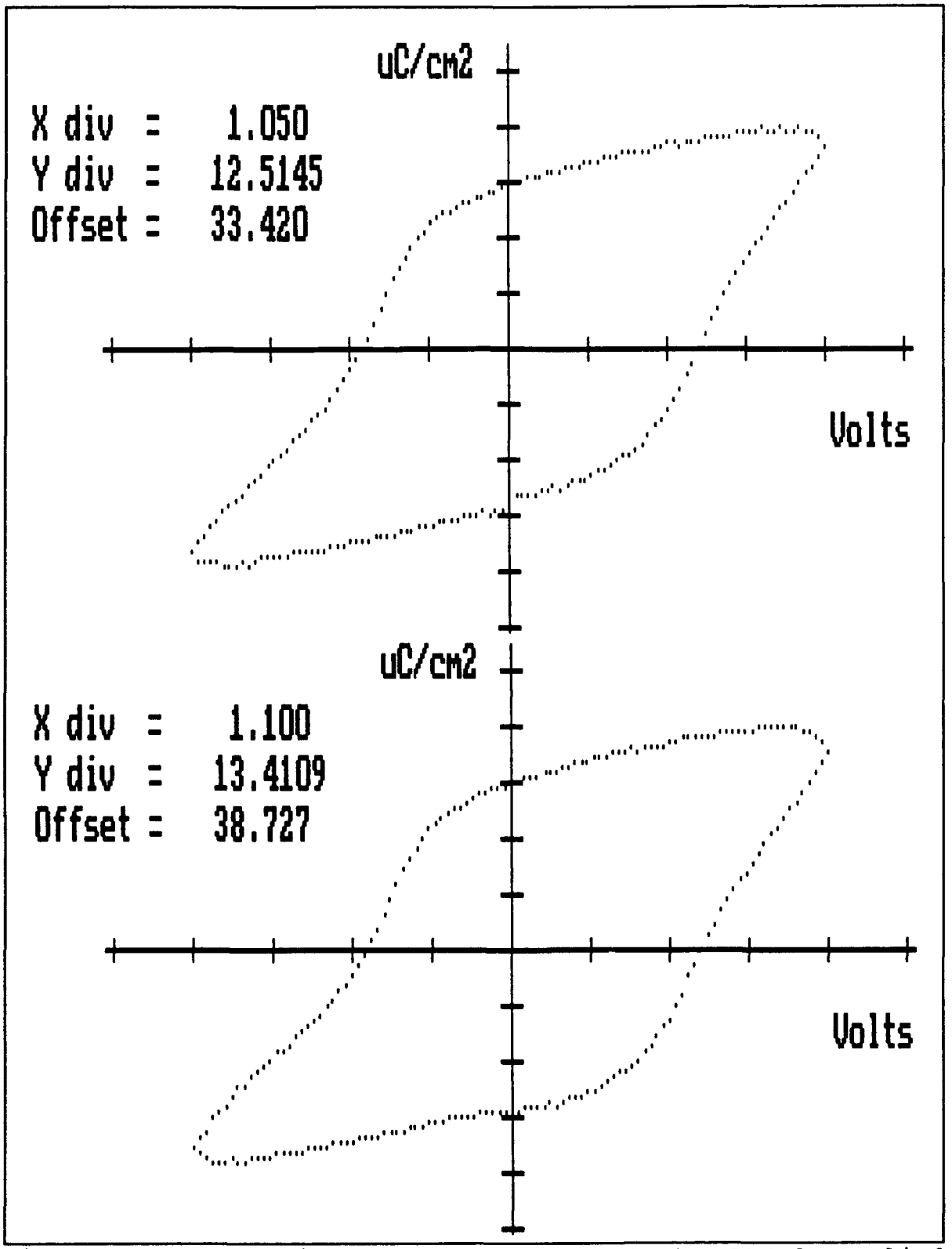

Figure 54. Hysteresis Loops for Sample 0/20/80 Pt/Pd, Applied Voltage Equal ($V_{120\%}$, $V_{126\%}$)

Volt	Number Data Points	P_s	P_s	P_r	P_r	$-P_r$	$-P_r$
		μ	σ^2	μ	σ^2	μ	σ^2
1.5	3	18.9	.2	4.4	.08	-3.4	.04
2.5	3	27.1	2.0	7.7	.2	-6.2	.08
4.0	10	36.2	.9	13.7	.4	-12.1	.8
5.0	4	40.8	1.2	17.3	.5	-15.9	.6
6.0	5	40.8	1.2	17.3	.5	-15.9	.6
7.0	9	49.4	1.2	21.8	.7	-19.9	.7
8.0	5	51.8	.3	24.3	.6	-22.7	2.4
8.5	7	57.4	4.6	29.4	3.6	-25.7	2.4
9.0	13	56.9	3.4	28.4	3.2	-25.1	1.1
9.5	9	59.8	2.4	32.1	7.0	-27.2	.5
10.0	14	60.0	2.5	32.7	4.4	-27.8	1.3
10.5	8	62.2	.9	35.9	2.2	-28.9	.3
11.0	13	62.3	2.0	37.1	3.8	-29.7	.9
12.0	8	63.3	.4	43.6	10.0	-32.3	2.0
13.0	6	64.3	2.5	51.7	23.7	-34.9	1.5

14.0	5	64.5	.6	59.9	13.1	-36.7	1.5

Table XXVIII. Polarization Measurements for Sample 0/60/40 Pt/Pt

Volt	Number Data Points	P_s	P_s	P_r	P_r	$-P_r$	$-P_r$
		μ	σ^2	μ	σ^2	μ	σ^2
2.0	6	14.5	.1	5.8	.02	-2.55	.01
2.5	6	20.9	.7	10.4	.5	-7.7	.3
3.0	8	25.5	.4	13.3	.2	-11.6	.2
3.5	8	28.4	.4	15.1	.2	-13.9	.2
4.0	8	31.2	.5	16.9	.4	-15.8	.1
4.4	7	33.5	.09	18.3	.3	-17.7	.1
5.0	9	36.8	1.2	21.0	.9	-20.0	1.1
6.0	12	43.1	3.9	25.8	4.0	-24.4	3.8
6.5	14	45.3	.9	28.2	1.6	-26.1	1.2
7.0	23	46.1	1.1	29.0	1.0	-26.4	.7
7.25	12	46.7	.7	30.0	1.7	-27.1	1.1
7.5	13	47.5	.7	31.0	1.4	-27.6	1.4
7.75	5	47.3	.7	32.36	1.4	-28.0	1.5
8.0	7	48.4	.3	33.3	.6	-28.5	.5

Table XXIX. Polarization Measurements for Sample 0/60/40 Pt/Pd

Volt	Number Data Points	P_s	P_s	P_r	P_r	$-P_r$	$-P_r$
		μ	σ^2	μ	σ^2	μ	σ^2
2.0	7	17.2	.5	5.1	.2	-4.7	2.3
3.0	10	29.5	.9	12.0	1.1	-13.8	4.0
3.5	12	34.6	.4	16.2	.9	-18.0	.8
4.0	24	39.9	1.4	21.6	2.0	-23.4	1.9
4.4	19	41.9	3.6	24.5	5.1	-25.7	2.7
4.8	16	45.0	1.4	29.4	7.1	29.2	3.3
5.0	20	45.6	1.1	30.9	4.8	29.8	1.8
5.25	14	46.9	.9	33.0	6.7	31.0	1.7
5.5	17	48.2	.8	37.2	15.9	32.7	2.9
5.75	5	48.7	1.5	43.1	24.9	34.3	21.5

Table XXX. Polarization Measurements for Sample 0/20/80 Pt/Pt

Volt	Number Data Points	P_s	P_s	P_r	P_r	$-P_r$	$-P_r$
		μ	σ^2	μ	σ^2	μ	σ^2
1.5	8	5.5	.2	1.3	.07	-.13	.003
2.0	14	10.4	.6	4.3	.5	-2.9	.3
2.5	18	19.2	3.4	11.4	2.4	-10.8	2.7
2.75	5	23.1	2.3	14.4	.3	-14.5	.9
3.0	17	27.4	1.5	18.9	2.1	-18.1	1.3
3.25	12	30.8	2.0	22.0	3.2	20.7	3.7
3.5	17	34.1	2.4	27.2	20.5	24.8	7.6
3.75	17	36.5	5.2	32.0	20.5	27.3	7.4
4.0	10	39.1	6.2	33.4	8.9	29.2	13.1
4.2	8	41.1	5.0	37.4	17.3	30.9	9.9

Table XXXI. Polarization Measurements for Sample 0/20/80 Pt/Pd

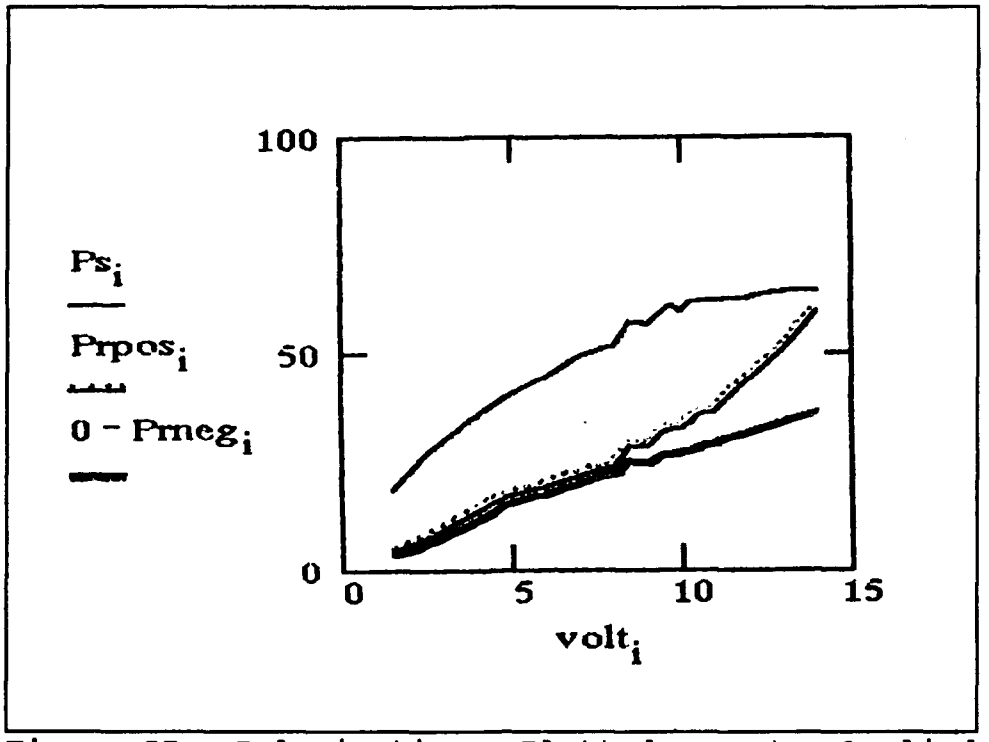

Figure 57. Polarizations Plotted w.r.t. Applied Voltage for Sample 0/60/40 Pt/Pt

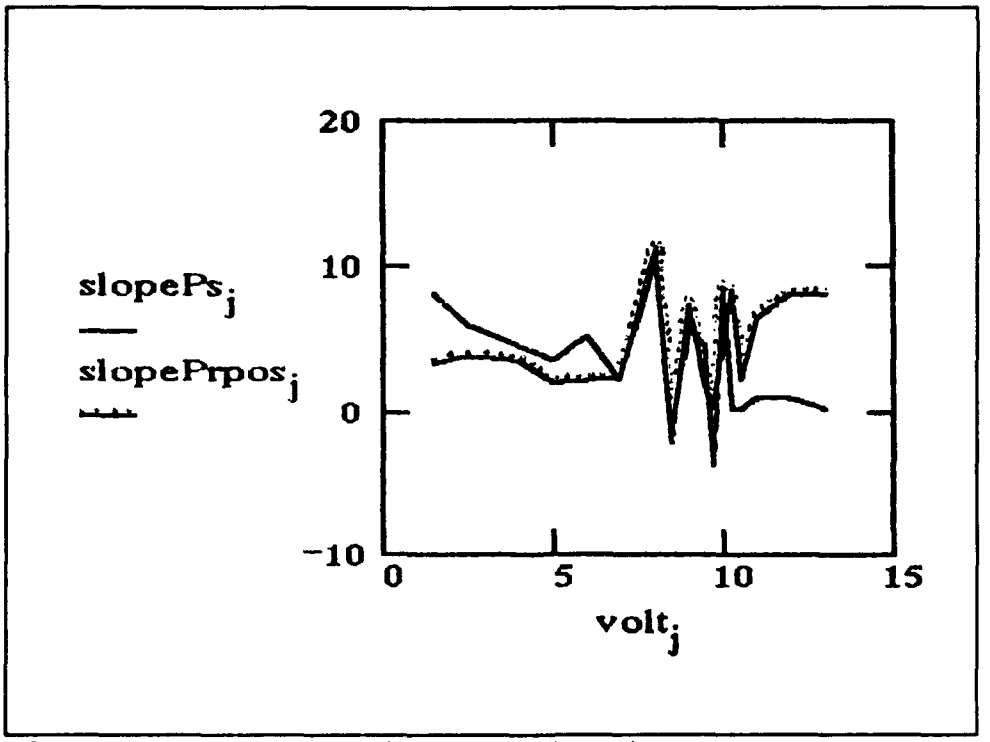

Figure 58. Change in Polarization Values w.r.t. Change in Applied Voltage for Sample 0/60/40 Pt/Pt

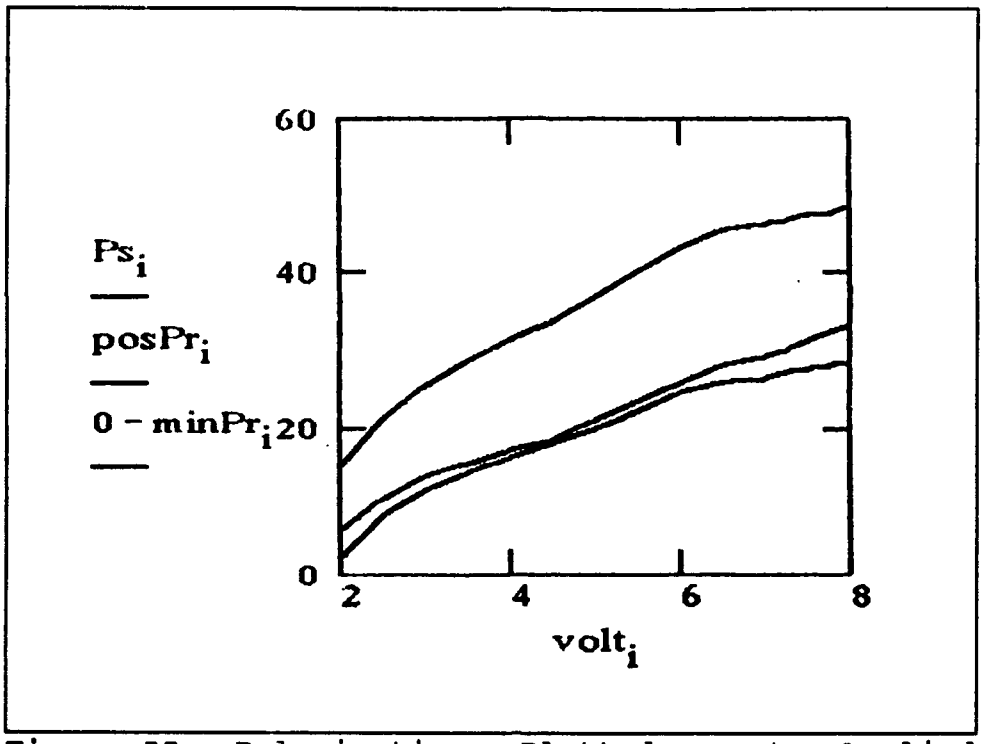

Figure 55. Polarizations Plotted w.r.t. Applied Voltage for Sample 0/60/40 Pt/Pd

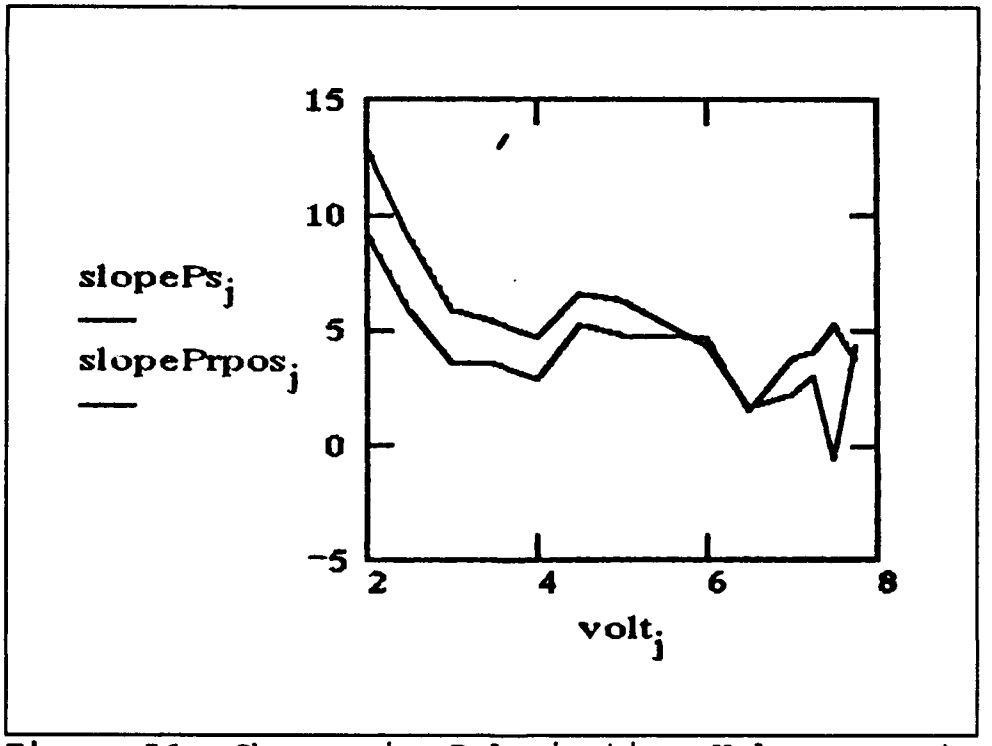

Figure 56. Change in Polarization Values w.r.t. Change in Applied Voltage for Sample 0/60/40 Pt/Pd

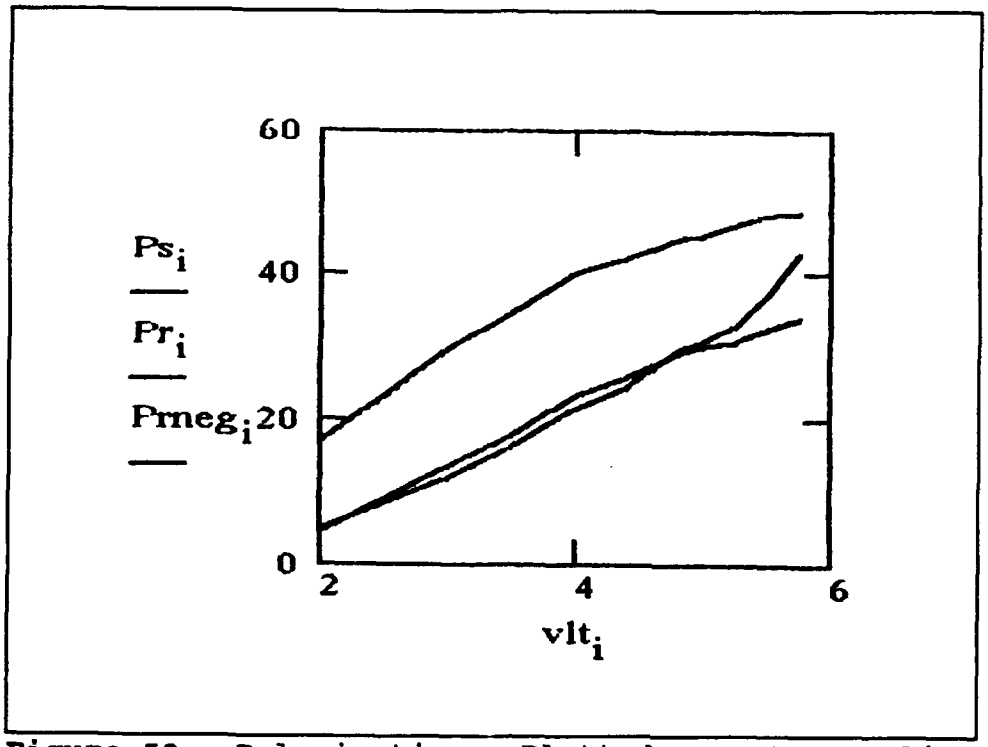

Figure 59. Polarizations Plotted w.r.t. Applied Voltage for Sample 0/20/80 Pt/Pt

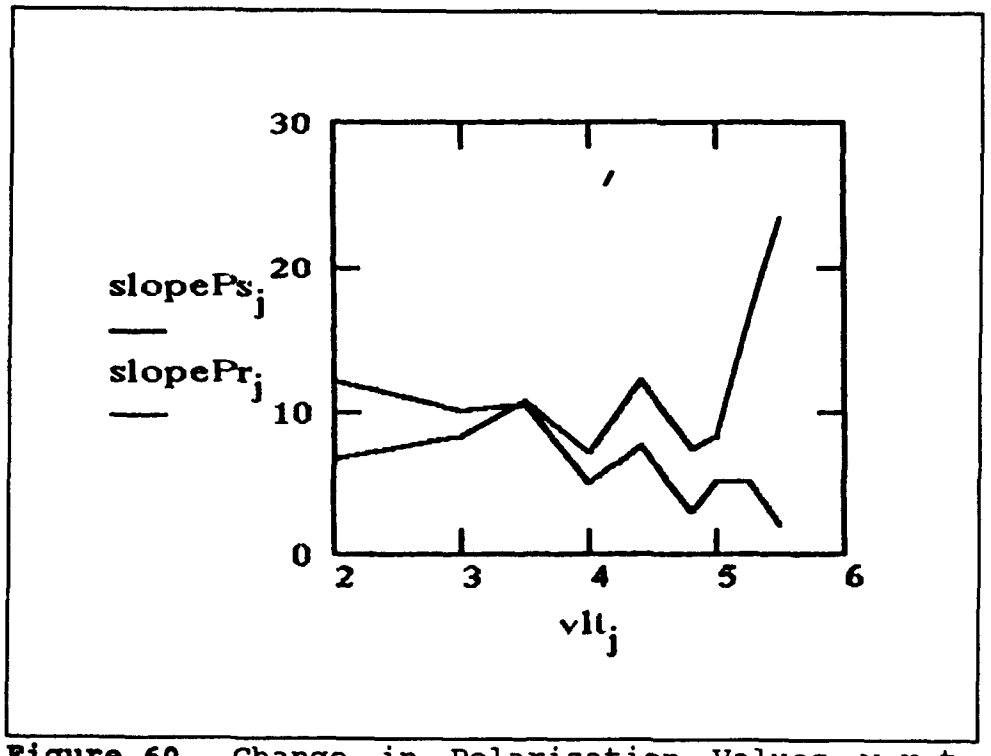

Figure 60. Change in Polarization Values w.r.t. Change in Applied Voltage for Sample 0/20/80 Pt/Pt

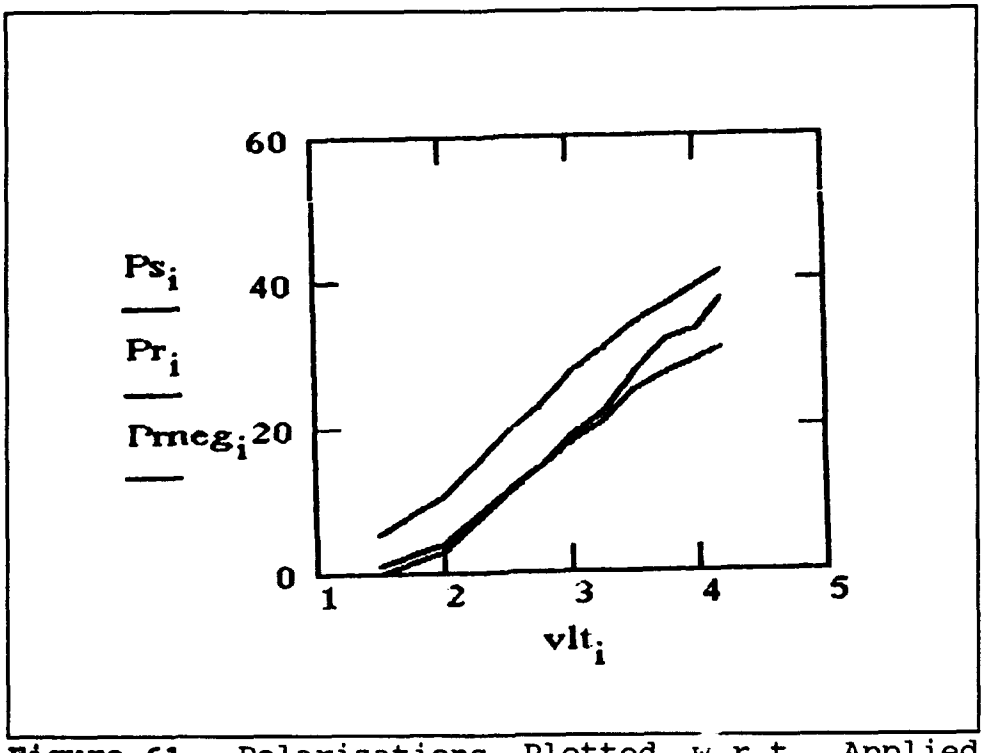

Figure 61. Polarizations Plotted w.r.t. Applied Voltage for Sample 0/20/80 Pt/Pd

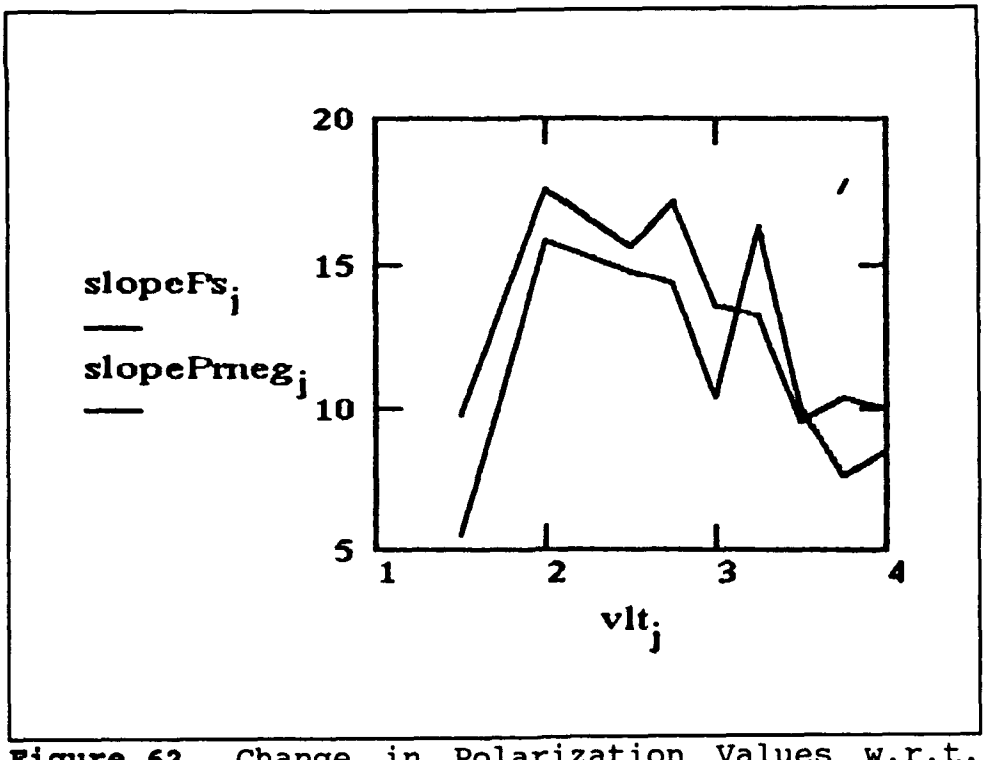

Figure 62. Change in Polarization Values w.r.t. Applied Voltage for Sample 0/20/80 Pt/Pd

Appendix B: MathCAD Template

This appendix contains a MathCAD template used to conduct a variety of statistical tests used in this study. The template begins by using least-squares regression techniques to estimate regression coefficients for a model. An ANOVA table is constructed and a general linear test performed. Several checks for outliers in the data are made, including scatter plots, and a normal probability plot of the error terms is created. Finally, a lack of fit test is performed to provide a statistical indication of how well the regression model fits the observations.

X1:voltage
X2:time
X3:frequency
X4:time squared
X5:frequency squared

ORIGIN ≡ 1

Y = READPRN(ccdb)

X = READPRN(ccda)

n = rows(X) n = 23

i = 1..rows(X)

$one_i = 1$

Note: runs 09-17 are replicants for the center points.

X = augment(one, X) Y = $Y^{<1>}$

$$X = augment\left[augment\left[augment\left[augment\left[X^{<1>}, X^{<2>}\right], X^{<3>}\right], X^{<4>}\right], X^{<5>}\right]$$

By augmenting different X matrices it is possible to investigate different design matrices. Interaction terms can also be created.

$$x1x2_i = \left[X^{<1>}\right]_i \cdot \left[X^{<2>}\right]_i$$

The interaction term could then be included in the matrix by the augment command. The small box to the right of the equation indicates the equation has been turned off for calculations.

p = cols(X) p = the number β coefficients to be estimated

p = 6

FULL MODEL df $df_{full} = n - p$ $df_{full} = 17$

For α = .05 and df.full = 17 the 2-tail tcrit is

tcrit = 2.110 Source: (5:1248)

$Fcrit = tcrit^2$

(1-tail, RIGHT)
(dfn=dfRed-dfFull;dfd=dfFull)

Fcrit = 4.45

Estimate β coefficients with b

$df_R = p - 1$ $df_R = 5$

$$b = \left[X^T \cdot X\right]^{-1} \cdot X^T \cdot Y$$

$df_{full} = 17$

$Y_{hat} = X \cdot b$

F(.95;7,13) = 2.86
(13:1134)

Yhat values are the predicted values of the least-squares model

$$b = \begin{bmatrix} 3.84 \\ -0.98 \\ -0.56 \\ -0.57 \\ 0.26 \\ 0.23 \end{bmatrix}$$

Obtain the ANOVA Table

j = 1..n $J_{i,j} = 1$ creates a matrix of ones

$SSTO = Y^T \cdot Y - \frac{1}{n} \cdot Y^T \cdot J \cdot Y$

total sum of squares for the regression model

$SSE = e^T \cdot e$

total sum of squares of the error terms

$SSR = SSTO - SSE$

total sum of squares of the regression coefficients

$MSR = \frac{SSR_1}{df_{SSR}}$

e: the residuals

$e = Y - X \cdot b$

mean(e) = $2.45 \cdot 10^{-15}$

min(e) = -0.47

max(e) = 0.59

var(e) = 0.08

$df_{SSE} = n - p$ degrees of freedom for the error terms

$df_{SSR} = p - 1$ degrees of freedom for the regression coeff.

$MSE = \frac{SSE_1}{df_{SSE}}$ a measure of the fit of the model

ANOVA TABLE

Source	SS	df	MS
Model	SSR = 23.46	p - 1 = 5	MSR = 4.69
Error	SSE = 1.95	n - p = 17	MSE = 0.11
Corrected Total SS	SSTO = 25.42		

Can now perform inferences

$SSE_{full} = SSE_1$ $SSE_{red} = SSTO_1$

$df_{full} = 17$ $df_{red} = n - 1$ $df_{red} = 22$

Ho: B0=B1=B2=B3=B4=B5=0

Check to see if terms are significantly different than zero

If Fstar <= Fcrit conclude Ho
If Fstar > Fcrit conclude Ha

$$F_{star} = \frac{\frac{SSE_{red} - SSE_{full}}{df_{red} - df_{full}}}{\frac{SSE_{full}}{df_{full}}}$$

$\frac{MSR}{MSE} = 40.81$

$F_{star} = 40.81$

$R_{sqr} = \frac{SSR_1}{SSTO_1}$

vs Fcrit(.95;5,17)=2.81

Therefore cannot conclude Ho, which is the result we sought

$R_{sqr} = 0.92$

Rsqr is a measure of the fit of a model.

****
Construct a Normal Probability Plot of Errors
****
Enter and sort raw residuals [e.i]

$SPERC := sort(e)$

$n := length(SPERC)$ $\quad n = 23$

$MSE := \frac{e^T \cdot e}{n - p}$ $\quad MSE = 0.11$

Now obtain the Expected [100 * ((i - .375)/(n + .25))] th percentiles of the standard normal

$i := 1..n \quad z := 0 \quad PERC_i := \frac{i - .375}{n + .25} \quad PPERC_i := root\left[cnorm(z) - \left[PERC_i\right], z\right] \cdot \sqrt{MSE_1}$

cnorm(z) returns the P[Z<=z] for the N(0,1) dist.

PPERC contains the expected percentiles

Construct a probability plot for residual values vs expected N(0,MSE) percentiles to determine if it is plausible to assume the residuals were draw from a N(0,MSE) population We converted the data to a N(0,1) so the line I'm about to create will always be 45 degrees. The line is just a visual aid.

$line_i := PPERC_i$

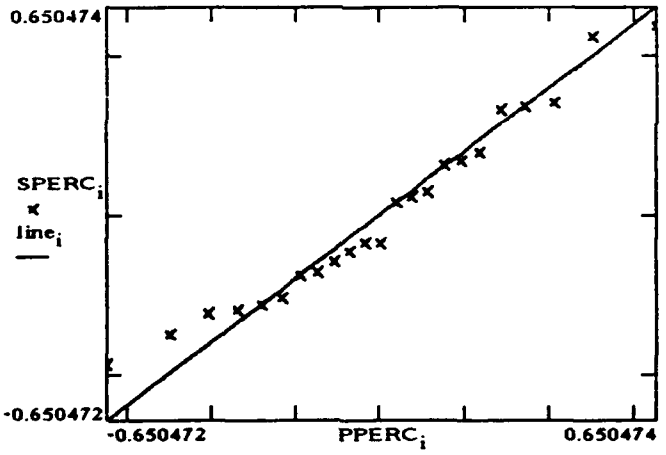

We are looking for a reasonably good straight line fit

Linear correlation of residuals [e.i] vs expected percentile

corr(SPERC, PPERC) = 0.98

This coefficient of correlation is indicative of normality in the error terms. At the $\alpha = .05$ level we expect the coefficient to be greater than 0.952

The next step is to produce scatter plots of the residuals plotted against the variables in the model. Scatter plots may provide indications of autocorrelation, outliers, or curvature which the model did not account for. For this example the results reflect the large number of central design points.

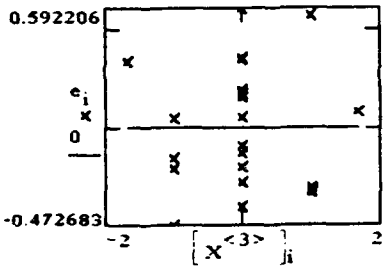

Frequency

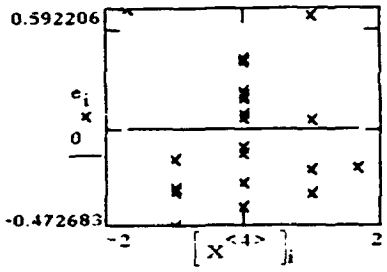

Time

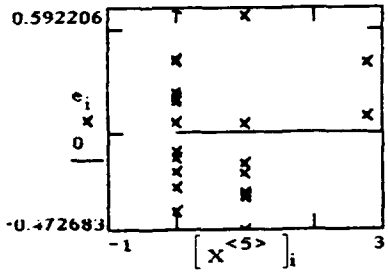

Period squared

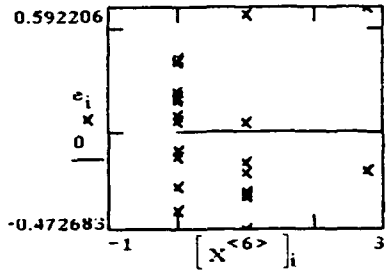

Time squared

k = 1..rows(X)

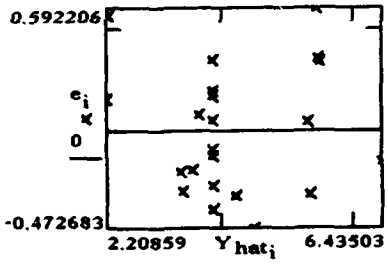

fitted values: appear to be randomly distributed

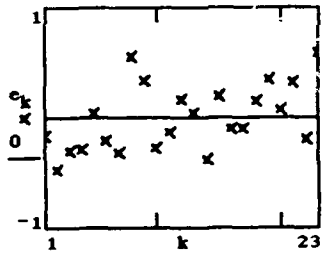

sequence of runs: It seems that the cube points (1-8) overestimate and the axial points (18-23) underestimate, but it is difficult to be certain of the effect of this

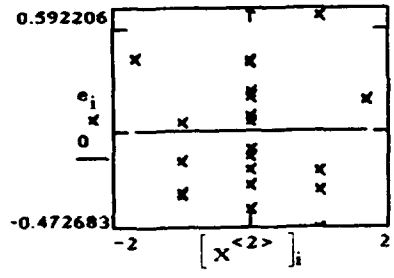

Volt

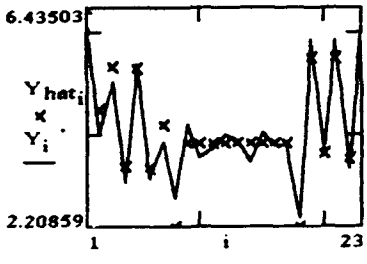

actual vs predicted: appears to be a reasonable picture

The next step is constructing a lack-of-fit test. The first step is to create a design array which has only 15 rows in the design matrix, one for each set of parameter settings. Since the only replicants occurred for the center points, a row will be used for each factorial and axial point, and the center points will be represented by a row of zeroes (Row 9).

Next, a new response matrix, z, is generated. The number of columns in z = 9, the maximum number of replicants at any parameter setting in X, that is, the center points For each row in z, the observed responses for the corresponding row in X are entered. In this instance only row 9 of the z matrix will have more than one entry.

A new vector, ny, is created which indicates how many replicants were observed for a particular X row. Readers wishing further development can refer to Neter's textbook (13).

$cols(X) = 6$

$kk := 1..cols(X)$

$XX_{1,kk} := X_{1,kk}$ $XX_{9,kk} := X_{9,kk}$

$XX_{2,kk} := X_{2,kk}$ $XX_{10,kk} := X_{18,kk}$

$XX_{3,kk} := X_{3,kk}$ $XX_{11,kk} := X_{19,kk}$

$XX_{4,kk} := X_{4,kk}$ $XX_{12,kk} := X_{20,kk}$

$XX_{5,kk} := X_{5,kk}$ $XX_{13,kk} := X_{21,kk}$

$XX_{6,kk} := X_{6,kk}$ $XX_{14,kk} := X_{22,kk}$

$XX_{7,kk} := X_{7,kk}$ $XX_{15,kk} := X_{23,kk}$

$XX_{8,kk} := X_{8,kk}$

$c := 15$

$j := 1..c$

$m := 2..9$

$z_{j,m} := 0$

$z_{9,2} := Y_{10}$

$z_{9,3} := Y_{11}$

$z_{9,4} := Y_{12}$

$z_{9,5} := Y_{13}$

$z_{9,6} := Y_{14}$

$z_{9,7} := Y_{15}$

$z_{9,8} := Y_{16}$

$z_{9,9} := Y_{17}$

$yv := z$

$z_{1,1} := Y_1$ $z_{9,1} := Y_9$

$z_{2,1} := Y_2$ $z_{10,1} := Y_{18}$

$z_{3,1} := Y_3$ $z_{11,1} := Y_{19}$

$z_{4,1} := Y_4$ $z_{12,1} := Y_{20}$

$z_{5,1} := Y_5$ $z_{13,1} := Y_{21}$

$z_{6,1} := Y_6$ $z_{14,1} := Y_{22}$

$z_{7,1} := Y_7$ $z_{15,1} := Y_{23}$

$z_{8,1} := Y_8$

$$ny := \begin{bmatrix} 1 \\ 1 \\ 1 \\ 1 \\ 1 \\ 1 \\ 1 \\ 9 \\ 1 \\ 1 \\ 1 \\ 1 \\ 1 \\ 1 \\ 1 \end{bmatrix}$$

$l := max(ny)$

$l = 9$

$yvsum_j := l \cdot mean\left(\left[z^T\right]^{<j>}\right)$

$$yvbar_j := \frac{yvsum_j}{ny_j}$$

$yvhat := XX \cdot b$

$k = 1..l$

Lack of fit test for first-order regression function

Alternatives:

Ho: $E(Y) = \beta_0 + \beta_1 \cdot x1 + \beta_2 \cdot x2 + \beta3 \cdot x3 + \beta4 \cdot x4 + \beta5 \cdot x5 + \beta6 \cdot x6 + \beta7 \cdot x7 + \beta8 \cdot x8$

Ha: $E(Y) \neq \beta_0 + \beta_1 \cdot x1 + \beta_2 \cdot x2 + \beta3 \cdot x3 + \beta4 \cdot x4 + \beta5 \cdot x5 + \beta6 \cdot x6 + \beta7 \cdot x7 + \beta8 \cdot x8$

Test statistic

$$Fstar = \left[\frac{SSLF}{c-p}\right] \cdot \left[\frac{n-c}{SSPE}\right] \quad \text{OR} \quad Fstar = \frac{MSLF}{MSPE}$$

Decision Rule

If Fstar <= F(1 - α;c - p,n - c), FAIL to reject Ho
If Fstar > F(1 - α;c - p,n - c), REJECT Ho

Now obtain the pure error sum of squares

$$SSPE = \sum_j \sum_k if\left[k \leq ny_j, \left[yv_{j,k} - yvbar_j\right]^2, 0\right]$$

SSPE = 0.43

$$MSPE = \frac{SSPE}{\left[\sum_j ny_j\right] - c}$$

MSPE = 0.05

Obtain the lack of fit component

$$SSLF = \sum_j ny_j \cdot \left[yvbar_j - yvhat_j\right]^2$$

SSLF = 1.53

$$MSLF = \frac{SSLF}{c-p}$$

MSLF = 0.17

And finally the value of the test statistic

$$Fstar = \frac{MSLF}{MSPE}$$

Fstar = 3.18

c = 15

Numerator degrees of freedom c - cols(X) = 9 F(.95;9,2) = 3.39

Denominator degrees of freedom $\sum_j ny_j - c = 8$

Since Fstar < F(.95;9,8) we conclude that this model is appropriate

$yvhat^T = (6.4 \;\; 4.5 \;\; 5.3 \;\; 3.4 \;\; 5.3 \;\; 3.3 \;\; 4.2 \;\; 2.2 \;\; 3.8 \;\; 2.2 \;\; 5.5 \;\; 3.6 \;\; 5.5 \;\; 3.5 \;\; 5.4)$

$yvbar^T = (6.3 \;\; 4 \;\; 5 \;\; 3.1 \;\; 5.3 \;\; 3.1 \;\; 3.9 \;\; 2.8 \;\; 3.8 \;\; 2.4 \;\; 5.8 \;\; 3.7 \;\; 5.8 \;\; 3.3 \;\; 6)$

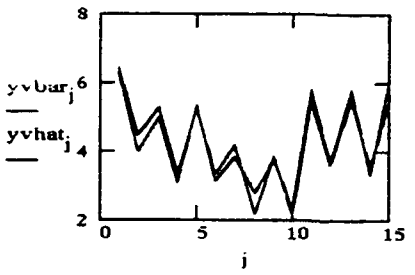

Bibliography

Response Surface Methodology

1. Box, G. E. P., "Multi-Factor Designs of First-Order", Biometrika, 49-57 (April 1952).

2. Box, G. E. P., "The Exploration and Exploitation of Response Surfaces: Some General Considerations and Examples", Biometrics, 16-60 (March 1954).

3. Box, G. E. P. and Youle, P. V., "The Exploration and Exploitation of Response Surfaces: An Example of the Link Between the Fitted Surface and the Basic Mechanism of the System", Biometrics, 287-323 (September 1955).

4. Box, G. E. P. and Hunter J. S., "Multi_Factor Experimental Designs for Exploring Response Surfaces", The Annals of Mathematical Statistics, 195-241 (March 1957).

5. Box, G. E. P. and Draper, Norman R., Empirical Model-Building and Response Surfaces. New York: John Wiley and Sons, 1987.

6. Giovannitti-Jensen, Ann and Myers, Raymod H., "Graphical Assessment of the Prediction Capability of Response Surface Designs", Technometrics, 159-171 (May 1989).

7. Grize, Y. L., "Plotting Scaled Effects From Unreplicated Orthogonal Experiments", Journal of Quality Technology, 205-212 (July 1991).

8. Hill, Hubert M., "Experimental Designs to Adjust for Time Trends", Technometrics, 67-82 (February 1960).

9. Hill, William and Hunter, William, "A Review of Response Surface Methodology: A Literature Survey", Technometrics, 571-590 (November 1966).

10. Mandel, John, "Some Thoughts on Variable Selection in Multiple Regression", Journal of Quality Technology, 2-6 (January 1989).

12. Myers, Raymond, et al., "Response Surface Methodology", Technometrics, 137-157 (May 1989).

13. Neter, John, et al., Applied Linear Statistical Models, Boston, Richard D. Irwin, Inc., 1990.

Ferroelectrics

14. Abt, Norman, "Electrical Measurement of Ferroelectric Capacitors for Non-Volatile Memory Applications", Materials Research Society Symposium Proceedings, 303-312 (April 1990).

15. Annino, A. et al., "Spray Method: Dependence of Deposition Efficiency on Substrate Temperature", Journal of Applied Physics, 141-145 (January 1991).

16. Baker, Stan, "Duo Plans DRAMatic 4-Megabit", Electronic Engineering Times, 1-2 (October 24, 1988).

17. Bloom, Michael, "A Memory to Remember", ESD: The Electronic System Design Magazine, 38-44 (October 1989).

18. Bondurant, David, "Ferroelectronic RAM Memory Family for Critical Data Storage", Colorado Microelectronics Symposium, 212-215 (March 1989).

19. Bondurant, David and Fred Gnadinger, "Ferroelectrics for Nonvolatile RAMs", IEEE Spectrum, 30-33 (July 1989).

20. Bullington, Jeff A. et al., "Optical Characterization of Fatigue and Ageing in Ferroelectric Thin-Film Capacitors", Colorado Microelectronics Symposium, 201-211 (March 1989).

21. Bursky, Dave, "Logic That Remembers Opens Novel Applications", Electronic Design, 97-99 (July 13, 1989).

22. Chen, C. J. et al., "Sol-Gel Derived Ferroelectric PZT Thin Films on Doped Silicon Substrates", Colorado Microelectronics Symposium, 185-188 (March 1989).

23. Clark, Noel A. and James F. Scott, "Studies of Structure and Switching Dynamics in Ferroelectric Crystal and Liquid Crystal Thin Films". Cornell University, Ithaca, NY, July 1989 (AD-A212 650).

24. Cole, Bernard C., "How the US is Leading the Way in Strategic Nonvolatile Technology", Electronics, 80-83 (March 1989).

25. Cole, Bernard C., "Finally, it's ferroelectric!", Electronics, 88-89 (August 1989).

26. Cormier, Denny, "ICs: Nonvolatile Ferroelectric RAMs Defy Speed Barriers", ESD: The Electronic System Design Magazine, 16-17 (May 1988).

27. Desu, Seshu B., "Size Effects in Sputtered PZT Thin Films", Materials Research Society Symposium Proceedings, 319-324 (April 1990).

28. Dey, S. K., et al., "Processing and Parameters of Sol-Gel PZT Thin-Films for Ga As Memory Applications", Colorado Microelectronics Symposium, 189-194, (March 1989).

29. Diamant, H., et al., "", The Review of Scientific Instruments, 30-33 (January 1957).

30. Evans, Joe T., "Ferroelectric Memories", ESD: The Electronic System Design Magazine, 29-35 (August 1988).

31. Evans, Joe T. et al., "Testing for Fatigue and Ageing in Ferroelectric Thin-Film Capacitors", Colorado Microelectronics Symposium, 217-224 (March 1989).

32. Evans, Joe T., private phone conversation, Vice-President, Radiant Technologies, Albuquerque, NM, September 1991.

33. Flinn, Richard A., and Trojan, Paul K., Engineering Materials and Their Applications, Boston, Houghton Mifflin Co., 1975.

34. Giancoli, Douglas C., Physics for Scientists and Engineers: with Modern Physics. Englewood Cliffs, New Jersey: Prentice Hall 1989.

35. Hayt, William H., Engineering Electromagnetics. New York: McGraw-Hill, 1981.

36. Hirano, S. et al., "Processing of Stoichiometric and Ti Doped $LiNbO_3$ Films with Preferred Orientation from Metal Alkoxides", Materials Research Society Symposium Proceedings, 13-18 (April 1990).

37. Ishizawa, N. et al., "Crystalline $BaTiO_3$ Thin Film Prepared from Ti Metal by Hydrothermal-Electrochemical Method", Materials Research Society Symposium Proceedings, 57-62 (April 1990).

38. Jingping, Xu et al., "Preparation of $Pb(Zr,Ti)O_3$ Ferroelectric Thin Films by a Pulsed Laser Ablation Technique", 1991 IEEE 41st Electronics Components and Technology Conference, 560-562 (1991).

39. Johnson, D. J. et al., "Measuring Fatigue in PZT Thin Films", Materials Research Society Symposium Proceedings, 289-295 (April 1990).

40. Josefson, Carl E., "Evaluation of Ferroelectric Materials for Memory Applications". Monterey, CA: Naval Postgraduate School. June 1990 (AD-A232 112).

41. Kostov, E. G. and Malinovsky, Vik, "Large-Scale Use of Ferroelectrics in Micro-Electronics is Reality", Proceedings of First European Conference on Polar-Dielectrics, 1659-1666 (1989 Volume 4).

42. Matsubara, S. et al., "Interface Structure and Dielectric Properties of $SrTiO_3$ Thin Film Sputter-Deposited onto Si Surfaces", Materials Research Society Symposium Proceedings, 243-254 (April 1990).

43. Messenger, George C., "Ferroelectric Memories". Marina del Ray, CA: R and D Associates. 1 November 1987 - 1 March 1988 (AD-A201 851).

44. Pugh, Robert D. et al., "Computer Simulation Study of the Effect of Defects on Switching in Ferroelectric Thin Films", Materials Research Society Symposium Proceedings, 325-330 (April 1990).

45. Pugh, Robert D., unpublished manuscript provided to the author, AFIT, July 1991.

46. Pugh, Robert D., unpublished manuscript provided to the author, AFIT, November 1991.

47. Pugh, Robert D., unpublished manuscript provided to the author, AFIT, December 1991.

48. RAMTRON Corp., "Non-Volatile Ferroelectrics", Microprocessors and Microsystems, 291-296 (May 1989).

49. Radiant Technologies, RT-66A Standardized Ferroelectric Tester, V2.0 Operating Manual, Albuquerque, NM (1990),

50. Reaney, Ian M. and David J. Barber, "Micro-Structural Characterization of Ferroelectric Thin Films in Transverse Section", Journal of the American Ceramic Society, 1635-1638 (July 1991).

51. Sawyer, C. B., Tower, C. H., "Rochelle Salt as a Dielectric", Physical Review, 269-273 (February 1930).

52. Seth, Vinay K. and Schulze, Walter A., "Fabrication and Characterization of Ferroelectric PLZT 7/65/35 Ceramic Thin Films and Fibers", Colorado Microelectronics Symposium, 175-184 (March 1989).

53. Shepherd, W. H., "Fatigue and Aging in Sol-Gel Derived PZT Thin Films", Materials Research Society Symposium Proceedings, 277-288 (April 1990).

54. Sishibashi, Yoshihiro et al., "Guest Editorial", Ferroelectrics and Related Materials Journal, xi-xiii (1989 Volume 98).

55. Sudhama, C., et al., "Sealing Properties in the Electrical and Reliability of Lead-Zirconate-Titanate (PZT) Ferroelectric Thin Film Capacitors", Materials Research Society Symposium Proceedings, 331-336 (April 1990).

56. Tsui, Y. T., et al., "New Ferroelectric Hysteresis Curve Trace Featuring Compensation and Virtual Sample Grounding", The Review of Scientific Instruments, 1423-1424 (October 1968)

57. Tuttle, Bruce A., et al., "Micro-Structure of Solution-Processed Lead Zirconate Titanate (PZT) Thin Films", Journal of the American Ceramic Society, 1455-1458 (June 1991).

58. Weast, Robert C., CRC Handbook of Chemistry and Physics (53rd Edition). Cleveland: The Chemical Rubber Company, 1972.

59. Wilson, Ron, "Process Questions Paint Cloudy Future for DRAMs", Computer Design, 36-37 (January 1, 1989).

60. Wojcik, K., "Electric Properties of $PbTiO^3$ Single Crystals Doped with Lanthanum", Ferroelectrics and Related Materials Journal, 5-12 (1989 Volume 99).

61. Xu, Y., et al., "Ferroelectric Thin Films on Silicon and Fused Silica Substrates by Sol-Gel Process", Materials Research Society Symposium Proceedings, 13-18 (April 1990).

62. Yoon, Soon-Gil and Ho-Gi Kim, "Chemical Vapor Deposition of Thin Films of Ferroelectric Lead Titanate", Ferroelectrics and Related Materials Journal, 91-98 (1989 Volume 89).

63. Yoon, Soon-Gil, "Characterization and Electrical Properties of Chemical Vapor Deposited on Ferroelectric Lead Titanate Films on Titanium", IEEE Transactions on Ultrasonics, Ferroelectronics, and Frequency Control, 333-337 (September 1990).

REPORT DOCUMENTATION PAGE

Form Approved
OMB No. 0704-0188

1. AGENCY USE ONLY *(Leave blank)*	2. REPORT DATE	3. REPORT TYPE AND DATES COVERED
	March 1992	Master's Thesis

4. TITLE AND SUBTITLE
A RESPONSE SURFACE METHODOLOGY STUDY OF FERROELECTRIC MEMORY DEVICES

5. FUNDING NUMBERS

6. AUTHOR(S)
Kevin C. Smith, Captain, USAF

7. PERFORMING ORGANIZATION NAME(S) AND ADDRESS(ES)
Air Force Institute of Technology, WPAFB OH 45433-6583

8. PERFORMING ORGANIZATION REPORT NUMBER
AFIT/GST/ENS/92M-07

9. SPONSORING / MONITORING AGENCY NAME(S) AND ADDRESS(ES)

10. SPONSORING / MONITORING AGENCY REPORT NUMBER

11. SUPPLEMENTARY NOTES

12a. DISTRIBUTION / AVAILABILITY STATEMENT
Approved for public release; distribution unlimited.

12b. DISTRIBUTION CODE

13. ABSTRACT *(Maximum 200 words)* Fatigue in ferroelectric memory devices was studied. The application of fatigue pulses to a ferroelectric sample was controlled by the RT-66 Ferroelectric Tester, a variation of the Sawyer-Tower circuit. The RT-66 also controlled data collection following the fatiguing process. Seven variables were evaluated for their potential affect on fatigue. A sequence of fatigue tests, which varied the settings of these variables, was developed using Response Surface Methodology (RSM) experimental designs. Least-squares regression models were developed once a particular RSM set of designed experiments was completed. These models were evaluated using RSM tools, and the analysis of these models allowed the iterative development of new RSM designs. Within the experimental operating region it was determined that aging did not affect fatigue, and that differences in ferroelectric materials and electrode materials were the most important factors in determining fatigue. First-order models failed to fit the data for any of the RSM designs. The final model developed had two pure quadratic terms and three first-order terms. However, this design only involved one type of ferroelectric. Further testing is necessary before the findings of this study can be extended to modeling fatigue in other ferroelectric materials.

14. SUBJECT TERMS	15. NUMBER OF PAGES
Ferroelectric Crystals, Ferroelectric Materials, Perovskites Regression Analysis, Fatigue Life, Fatigue, Ferroelectricity	183
	16. PRICE CODE

17. SECURITY CLASSIFICATION OF REPORT	18. SECURITY CLASSIFICATION OF THIS PAGE	19. SECURITY CLASSIFICATION OF ABSTRACT	20. LIMITATION OF ABSTRACT
Unclassified	Unclassified	Unclassified	UL